Microbial diversity, functionality and metabolic activity of thermal biofilms in Croatia

Kostešić, Ema

Doctoral thesis / Disertacija

2023

Degree Grantor / Ustanova koja je dodijelila akademski / stručni stupanj: **University of Zagreb, Faculty of Food Technology and Biotechnology / Sveučilište u Zagrebu, Prehrambeno-biotehnološki fakultet**

Permanent link / Trajna poveznica: https://urn.nsk.hr/urn:nbn:hr:159:752184

Rights / Prava: In copyright/Zaštićeno autorskim pravom.

Download date / Datum preuzimanja: **2024-05-11**

prehrambeno biotehnološki fakultet

Repository / Repozitorij:

Repository of the Faculty of Food Technology and Biotechnology

dabar
DIGITALNI AKADEMSKI ARHIVI I REPOZITORIJI

University of Zagreb

Faculty of Food Technology and Biotechnology

Ema Kostešić

MICROBIAL DIVERSITY, FUNCTIONALITY AND METABOLIC ACTIVITY OF THERMAL BIOFILMS IN CROATIA

DOCTORAL DISSERTATION

Zagreb, 2023

University of Zagreb

Faculty of Food Technology and Biotechnology

Ema Kostešić

MICROBIAL DIVERSITY, FUNCTIONALITY AND METABOLIC ACTIVITY OF THERMAL BIOFILMS IN CROATIA

DOCTORAL DISSERTATION

Supervisors:
PhD Sandi Orlić
PhD Janko Diminić, Associate Professor

Zagreb, 2023

Sveučilište u Zagrebu

Prehrambeno-biotehnološki fakultet

Ema Kostešić

MIKROBNA RAZNOLIKOST, FUNKCIONALNOST I METABOLIČKA AKTIVNOST TERMALNIH BIOFILMOVA U HRVATSKOJ

DOKTORSKI RAD

Mentori:
dr.sc. Sandi Orlić
dr.sc. Janko Diminić, izv. prof.

Zagreb, 2023

Information about the supervisors:

Ph.D. **Sandi Orlić**, Senior Research Associate at Ruđer Bošković Institute, Zagreb

Biography

Ph.D. Sandi Orlić was born in Pula in 1976. He obtained his bachelor's, master's and doctoral degrees at the Faculty of Agriculture, University of Zagreb, in the Department of Microbiology. In 2007, he was appointed as an assistant professor. He then completed two postdoctoral programmes, one at KU Leuven in Belgium and the other at Cavanilles Institute of Biodiversity and Evolutionary Biology, University of Valencia, Spain. Since 2010, he has been conducting research at the Ruđer Bošković Institute. He initially worked in the Centre for Marine Research and later joined the Division of Materials Chemistry, where he works today. He has completed several scientific specialisations at the Max Planck Institute for Marine Microbiology, where he is also an external collaborator in the PhD study programme. During his career, he has actively participated in several research projects and was the leader of the Croatian Science Foundation (CSF) and the Ministry of Science and Education (MSE) establishment project. Currently, he is leading a CSF project. To date, he has published 68 scientific papers and has been cited over 2,000 times.

Ph.D. **Janko Diminić**, Associate Professor at Faculty of Food Technology and Biotechnology, University of Zagreb

Biography

Ph.D. Janko Diminić was born in Zagreb in 1980. He obtained his bachelor's, master's and doctoral degrees at the Faculty of Food and Biotechnology, University of Zagreb. In 2007, he was appointed as an Assistant Professor and currently works as an Associate Professor in the Laboratory of Bioinformatics within the Department of Biochemical Engineering at the same Faculty. He has co-authored over 30 scientific papers and participated in 7 scientific research projects.

BASIC DOCUMENTATION CARD

University of Zagreb

<div align="right">

PhD thesis
</div>

Faculty of Food Technology and Biotechnology
Postgraduate study in Biotechnology and Bioprocess Engineering, Food Technology and Nutrition

UDK:
Scientific area: Biotechnical science
Scientific field: Biotechnology

MICROBIAL DIVERSITY, FUNCTIONALITY AND METABOLIC ACTIVITY OF THERMAL BIOFILMS IN CROATIA

Ema Kostešić mag. ing. cheming.

Thesis performed at Laboratory for Precipitation Processes, Division of Materials Chemistry, Ruđer Bošković Institute, Zagreb
Supervisors: Ph.D. Sandi Orlić and Ph.D. Janko Diminić, Associate Professor

Short abstract: Hot spring biofilms are stable, highly complex microbial structures that thrive under extreme conditions and exhibit metabolic flexibility, making them valuable sources of bioactive molecules with potential industrial and biotechnological applications. This study represents the first investigation of the taxonomic and genetic diversity of biofilms from thermal ecosystems in Croatia. It determines the microbial composition of biofilms and the influence of environmental parameters on these microenvironments. Through different sequencing methods and analyzes, as well as microbial labeling techniques and microscopy, functionality, metabolic activities, and contributions to biogeochemical cycles of selected geothermal biofilms are investigated. The research provides a comprehensive description of thermal biofilm communities and completes the knowledge of geothermal ecosystems in general.

TEMELJNA DOKUMENTACIJSKA KARTICA

Sveučilište u Zagrebu

Doktorski rad

Prehrambeno-biotehnološki fakultet
Sveučilišni poslijediplomski studij Biotehnologija i bioprocesno inženjerstvo, prehrambena tehnologija i nutricionizam

UDK:
Znanstveno područje: Biotehničke znanosti
Znanstveno polje: Biotehnologija

MIKROBNA RAZNOLIKOST, FUNKCIONALNOST I METABOLIČKA AKTIVNOST TERMALNIH BIOFILMOVA U HRVATSKOJ

Ema Kostešić, mag. ing. cheming.

Rad je izrađen u Laboratoriju za procese taloženja, Zavod za kemiju materijala, Institut Ruđer Bošković, Zagreb
Mentori: dr.sc. Sandi Orlić i izv.prof.dr.sc. Janko Diminić

Kratki sažetak: Biofilmovi termalnih izvora su stabilne, vrlo složene mikrobne strukture čija prilagodba na ekstremne uvjete zahtijeva metaboličku plastičnost, čineći ih vrijednim izvorima pri traženju bioaktivnih molekula od potencijalnog industrijskog i biotehnološkog značaja. Ovaj rad predstavlja prvo istraživanje taksonomske i genetičke raznolikosti biofilmova iz termalnih ekosustava u Hrvatskoj. Određen je mikrobni sastav biofilmova i utjecaj okolišnih parametara na te mikrookoliše. Različitim metodama sekvenciranja i analizama sekvenci, kao i tehnikama mikrobnog označavanja i mikroskopije, istražena je funkcionalnost, metabolička aktivnost i uloga u biogeokemijskim ciklusima odabranih geotermalnih biofilmova. Istraživanje daje sveobuhvatan opis zajednica termalnih biofilmova i upotpunjuje saznanja o geotermalnim ekosustavima općenito.

Broj stranica: 107
Broj slika: 24
Broj tablica: 10
Broj literaturnih navoda: 303
Jezik izvornika: engleski

Ključne riječi: geotermalni biofilmovi, 16S rRNA amplikoni sekvenci, BONCAT, CARD-FISH, metagenomi

Datum obrane:

Stručno povjerenstvo za obranu:
1. prof.dr.sc Jurica Žućko
2. prof.dr.sc. Blaženka Kos
3. dr.sc. Jelena Godrijan
4. prof.dr.sc. Antonio Starčević (zamjena)

MICROBIAL DIVERSITY, FUNCTIONALITY AND METABOLIC ACTIVITY OF THERMAL BIOFILMS IN CROATIA

Summary

Geothermal sources function as natural bioreactors, enabling colonization by various extremophilic microorganisms that thrive at elevated temperatures. In hot springs, biofilms are formed as a survival strategy by microbial species to adapt to fluctuating extreme conditions by aggregation and attachment through secretion of extracellular polymeric substances (EPS). This microbial metabolic adaptability can be exploited in industrial processes and for biotechnological purposes. In terms of assessing metabolic capacity and functionality using physiological methods, geothermal biofilms have several key advantages. They are accessible and stable systems with a considerable amount of biomass. Their microbial composition is relatively simple and species richness is relatively low, but at the same time they harbor a large number of metabolically diverse microorganisms. However, the intricate web of interactions within these biofilms can pose a challenge for identifying the key parameters that determine community structure and biogeochemical cycling mechanisms. Moreover, the application of physiological methods and analyses to geothermal biofilms is often limited by the EPS matrix in which the microbial cells are enclosed. EPS hinders the separation of cells and matrix components and restricts the diffusion of large molecules. Therefore, identifying an optimal combination of methods to study the composition and metabolism of these microenvironments remains of paramount importance.

Due to favorable geological conditions, there are many thermal phenomena in the northern and northeastern parts of Croatia, most of which are both poorly explored and host biofilm communities. To investigate the composition of these microbial communities and the factors influencing them, seasonal sampling of biofilms and physicochemical analyses of the corresponding geothermal waters were conducted at 12 sampling sites in autumn 2019, spring 2020 and autumn 2020. After taxonomic screening, biofilms from Bizovac and Tuhelj sources were selected for further incubation experiments under different ecologically relevant conditions and substrates. In total, environmental DNA was isolated from 61 samples and the 16S rRNA V4 region was amplified and sequenced to capture the diversity of prokaryotes. The sequenced 16S rRNA amplicons were bioinformatically processed and classified using the SILVA database. Results were statistically processed and visualized using R software and interpreted along with physicochemical parameters. It was found that the temperature and the origin of the sample had the greatest influence on the microbial composition of the thermal

biofilms. Moreover, except for the samples from the Bizovac source, all biofilms studied were dominated by the phylum Cyanobacteria, while Pseudomonadota and Chloroflexota also accounted for a larger proportion of all biofilm samples. To investigate the metabolic activities of phototrophs, chemolithotrophs, and chemoorganotrophs, biofilms from Bizovac and Tuhelj source collected in spring 2021 were incubated for several days in sodium acetate, pyruvate, thiosulfate, glucose and in the presence of light. The BONCAT method was performed to characterize the changes in biofilm activity under the indicated substrates and conditions. Subsequently, the CARD-FISH method was applied to the same samples using fluorescently labeled oligonucleotide probes (EUBI-III mix, Gamma42a, CFX1223) to determine the taxonomic identity of the targeted microbial groups. The results of the BONCAT and CARD-FISH methods were visualized microscopically, the obtained images were subjected to biovolume analysis, and the combination of quantitative analysis and 16S rRNA amplicon sequencing provided a detailed description of the active biofilm populations. In biofilms from both sources, the addition of acetate suppressed the metabolic activity of the Gammaproteobacteria class, the presence of light did not have much effect on the Chloroflexota phylum, while the entire bacterial population showed the highest metabolic activity when incubated with glucose and thiosulfate for 48 h. Biofilms from the same sources were resampled in autumn 2021 and incubated for several days in sodium acetate, pyruvate, thiosulfate, tetrathionate and potassium thiocyanate, after which changes in biofilm activity were characterized at single-cell resolution. Active biofilm fractions detected by the BONCAT method were sorted by fluorescence-activated cell sorting (FACS), DNA was extracted and the 16S rRNA V4 region was amplified and sequenced to determine changes in community composition in response to incubation conditions. The addition of thiosulfate again resulted in the highest metabolic activity in biofilms from both sources, and the addition of all sulfur substrates resulted in changes in prokaryote abundance. To assign a function to the genes and establish a link between metabolic activity and capacity, total DNA sequencing of the initial biofilm samples for metagenomic analysis was also performed. Detailed analysis of genes involved in carbon, nitrogen and sulfur cycling was performed. Complete metabolic pathways of all major biogeochemical cycles were detected in both biofilms, including the SoX system for the disproportionation of thiosulfate as well as the possibility of metal, selenate, and arsenate reduction.

In this research, the taxonomic and genetic diversity of biofilms from thermal ecosystems in Croatia was investigated for the first time. Since the function and productivity of microbial

biofilms are directly related to the diversity and composition of the community, understanding the main processes that regulate the microbial communities of thermal biofilms enables the prediction of their functioning, the characterization of their metabolism and metabolic activity and, consequently, their biotechnological significance.

MIKROBNA RAZNOLIKOST, FUNKCIONALNOST I METABOLIČKA AKTIVNOST TERMALNIH BIOFILMOVA U HRVATSKOJ

Sažetak

Geotermalni izvori funkcioniraju kao prirodni bioreaktori i omogućavaju kolonizaciju raznih ekstremofilnih mikroorganizama koji uspijevaju preživjeti na visokim temperaturama. Biofilmovi unutar termalnih izvora formiraju se kao strategija preživljavanja različitih mikrobnih vrsta kako bi se prilagodile fluktuirajućim ekstremnim uvjetima, pri čemu se agregiraju i pričvršćuju lučenjem ekstracelularnih polimernih supstanci (EPS). Ova mikrobna metabolička prilagodljivost može se iskoristiti u industrijskim procesima i u biotehnološke svrhe. Prilikom procjene metaboličkog kapaciteta i funkcionalnosti fiziološkim metodama, geotermalni biofilmovi posjeduju nekoliko ključnih prednosti. Oni su pristupačni i stabilni sustavi sa značajnom količinom biomase. Njihov mikrobni sastav je relativno jednostavan a bogatstvo vrsta relativno malo, ali istodobno, sadrže veliki broj metabolički raznolikih mikroorganizama. Međutim, složena interakcijska mreža unutar biofilmova otežava i razumijevanje utjecaja glavnih čimbenika na uočene strukture zajednice i mehanizme biogeokemijskog ciklusa. Također, primjena fizioloških metoda i analiza na geotermalne biofilmove često je ograničena EPS matricom unutar koje su mikrobne stanice zatvorene. EPS otežava odvajanje stanica i matričnih komponenti te limitira difuziju velikih molekula. Pronalaženje odgovarajuće kombinacije metoda za proučavanje sastava i metabolizma ovih mikrookoliša od iznimne je važnosti.

Zbog povoljnih geoloških uvjeta, u sjevernom i sjeveroistočnom dijelu Hrvatske postoji veliki broj termalnih fenomena, od kojih je većina slabo istražena te u kojima se nalaze zajednice biofilmova. Sezonska uzorkovanja biofilmova i mjerenje fizikalno-kemijskih parametara odgovarajuće geotermalne vode provedena su tijekom jeseni 2019., proljeća 2020 i jeseni 2020. na 12 lokacija kako bi se istražio sastav ovih mikrobnih zajednica i čimbenici koji na njih utječu. Zatim, biofilmovi iz izvora Bizovac i Tuhelj odabrani su za daljnje pokuse inkubacija u različitim ekološki relevantnim uvjetima i supstratima. Sumarno, izolirana je okolišna DNK iz 61 uzorka, 16S rRNA V4 regija je amplificirana i sekvencionirana kako bi se obuhvatila raznolikost prokariota. Sekvencirani 16S rRNA amplikoni su bioinformatički obrađeni i klasificirani pomoću SILVA baze podataka. Rezultati su statistički obrađeni i vizualizirani primjenom R software-a te interpretirani zajedno s fizikalno-kemijskim parametrima. Utvrđeno je da temperatura i porijeklo uzorka (mjesto uzorkovanja) imaju najveći utjecaj na mikrobni

sastav termalnih biofilmova. Također, izuzev biofilmova iz Bizovca, u svim istraživanim biofilmovima dominiralo je koljeno Cyanobacteria, dok su Pseudomonadota i Chloroflexota koljena bila značajno zastupljena u svim uzorcima biofilmova. Kako bi se istražila metabolička aktivnost fototrofa, kemolitotrofa i kemoorganotrofa, biofilmovi iz izvora Bizovac i Tuhelj prikupljeni su u proljeće 2021. nakon čega je provedena višednevna inkubacija u natrijevom acetatu, piruvatu, tiosulfatu, glukozi i uz prisustvo svjetla. Zatim je provedena BONCAT metoda kako bi se okarakterizirala promjena aktivnosti biofilmova u navedenim supstratima i uvjetima. Na istim uzorcima primijenjena je i CARD-FISH metoda korištenjem fluorescentno označenih oligonukleotidnih probi (EUBI-III mix, Gamma42a, CFX1223) kako bi se odredio taksonomski identitet ciljanih mikrobnih skupina. Rezultati BONCAT i CARD-FISH metoda vizualizirani su mikroskopski, na ostvarenim slikama provedena je analiza biovolumena, te je kombinacijom kvantitativne analize i 16S rRNA sekvenciranjem dan detaljan opis aktivnih populacija u biofilmovima. U oba biofilma, dodatak acetata doveo je do smanjene metaboličke aktivnosti Gammaproteobacteria razreda, prisutnost svjetla nije imala učinak na Chloroflexota koljeno, dok je cjelokupna bakterijska populacija pokazala najveću metaboličku aktivnost prilikom 48 h inkubacije s glukozom i tiosulfatom. Biofilmovi iz istih izvora ponovo su uzorkovani u jesen 2021. i inkubirani nekoliko dana u natrijevom acetatu, piruvatu, tiosulfatu, tetrationatu i kalijevom tiocijanatu, nakon čega su promjene u aktivnosti biofilmova okarakterizirane na rezoluciji jedne stanice. Aktivne frakcije biofilmova detektirane BONCAT metodom sortirane su fluorescentno aktiviranim sortiranjem stanica (FACS), nakon čega je ekstrahirana DNK te 16S rRNA V4 regija amplificirana i sekvencionirana kako bi se odredile promjene u sastavu zajednice zbog različitih uvjeta inkubacija. Dodatak tiosulfata ponovno je rezultirao najvećom metaboličkom aktivnošću u oba biofilma, a dodatak svih sumpornih supstrata rezultirao je promjenama u prokariotskoj raznolikosti. Kako bi se genima dodijelila funkcija i uspostavila veza između metaboličke aktivnosti i metaboličkog kapaciteta, na inicijalnim uzorcima prije inkubacija također je provedeno sekvenciranje ukupne DNK. Provedena je detaljna analiza gena uključenih u cikluse ugljika, dušika i sumpora. Potpuni metabolički putevi svih glavnih biogeokemijskih ciklusa su otkriveni u oba biofilma, uključujući SoX sustav za disproporcioniranje tiosulfata kao i mogućnost redukcije metala, selenata i arsenata.

U ovom istraživanju po prvi put je istražena taksonomska i genetička raznolikost biofilmova iz termalnih ekosustava u Hrvatskoj. Kako su funkcija i produktivnost mikrobnih zajednica izravno povezani s raznolikošću i sastavom zajednice, razumijevanje glavnih procesa koji

utječu na mikrobne zajednice termalnih biofilmova omogućuje predviđanje njihovog funkcioniranja, identifikaciju njihovog metabolizma i metaboličke aktivnosti te, posljedično, njihov biotehnološki značaj.

Ključne riječi: geotermalni biofilmovi**,** 16S rRNA amplikoni sekvenci, BONCAT, CARD-FISH, metagenomi

CONTENT

1. INTRODUCTION

Biofilms represent complex structures of microorganisms and extracellular matrix that interact with the surrounding environment. They are considered one of the most widespread and successful forms of life that thrive in a variety of environments (Stoodley et al., 2002; Hall-Stoodley et al., 2004), including hot springs and wells. The biofilm state provides microorganisms in extreme environments with numerous ecological and physiological advantages, such as protection under stressful conditions (e.g., nutrient deprivation, extreme temperature and pH), metabolite exchange and horizontal gene transfer (Stewart and Franklin, 2008; Burmølle et al., 2014; Srinivasan et al., 2021). Despite the growing literature on the microbial composition of hot spring biofilms, phylogenetic identification does not provide any details on the metabolism of the identified microorganisms (Azeredo et al., 2017; Costa et al., 2017). Data on the ecology and ecophysiology of biofilms in hot springs and wells remain scarce despite the availability of numerous research methods. This study had several main objectives:

1. To investigate the diversity of microbial biofilms and the influence of physicochemical parameters in hot springs and wells during different seasons.
2. To analyse the changes in diversity and activity of prokaryotic communities in selected biofilms subjected to multiple incubation series with ecologically relevant substrates and conditions.
3. To investigate the functionality of the biofilms chosen based on differences in temperature and community composition.

To achieve these objectives, the following hypotheses were formulated:

1. Microbial community composition in thermal biofilms remains stable across seasons and is mainly influenced by temperature.
2. Metabolic activity of thermal biofilms from Bizovac and Tuhelj sources increases during incubation with organic molecules and sulfur substrates.
3. Microbial communities in thermal biofilms from Bizovac and Tuhelj sources possess genes of biotechnological importance.

This research is the first comprehensive investigation of thermal biofilm communities in Croatia and provides insights into their biodiversity, functional properties, and factors influencing them. The results provide a fundamental understanding of the metabolism of microbial thermal biofilms and enable further in-depth investigations.

2. LITERATURE OVERVIEW

2.1. Geothermal environments

Geothermal aquifers are permeable layers of fluid-bearing rock in which heat from the Earth's interior is stored (Limberger et al., 2018). Heat and pervious rock strata enable density-driven convection of groundwater, and depending on the heat source, various dissolved chemical constituents in the fluids are either released from the magma by degassing and/or are the result of rock interactions in the deep groundwater (Arnórsson et al., 2006). Thus, the high permeability enables continuous circulation of heat and fluids with dissolved chemical species that exit to surface through thermal springs and wells (Figure 1), cool, and form temperature, chemical, and redox gradients (Podar et al., 2020). Consequently, thermal springs function as autonomous bioreactors that allow the colonization of diverse, specially adapted microbial communities dominated by thermophilic and hyperthermophilic archaea and bacteria able to survive in a temperature range of 50-120 ºC (Debnath et al., 2019; Des Marais and Walter, 2019). These unique properties have led some authors to refer to hot springs as "tropical rainforests" of microbial communities (Debnath et al., 2019) and to postulate the origin of life hypothesis (Damer and Deamer, 2015; Damer and Deamer, 2020) or the possibility of extraterrestrial life (Lederberg and Sagan, 1962; Des Marais and Walter, 2019), in which fluctuating hot springs play a central role.
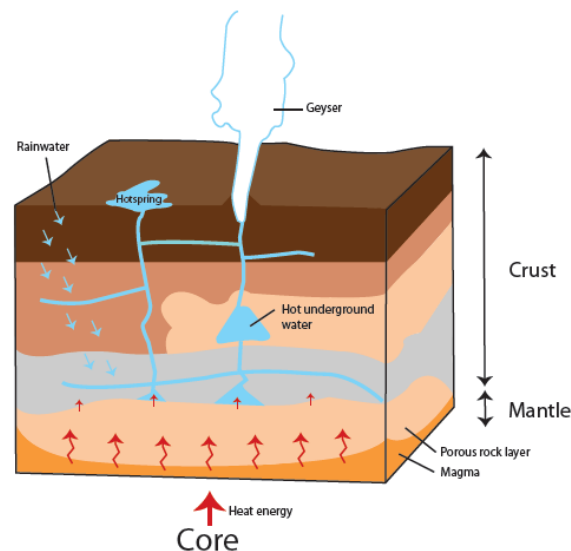
Figure 1. Formation of hot spring (URL1).

Thermal springs are geographically widespread and occur in numerous regions worldwide, including New Zealand (Power et al., 2018), the United States (Spear et al., 2006; Boomer et

al., 2009), Chile (Alcamán-Arias et al., 2018), Japan (Martinez et al., 2019), India (Sahay et al., 2017) and Malaysia (Hidayat et al., 2017). They have been extensively researched, especially for their notable medicinal properties. Hot springs have been used for healing and regeneration since ancient times. In Greece and Japan, for example, there is a long cultural tradition of using hot springs for the purpose of sanitation and treatment of various conditions such as skin diseases, stomach ailments, and rheumatic complaints (Serbulea and Payyappallimana, 2012; Gianfaldoni et al., 2017). Geothermal sources, due to their temperature and chemical composition, are considered both a therapeutic factor and a source of energy for heating and cooling systems (Ćuković Ignjatović et al., 2021; Vondra et al., 2023). As an environmentally friendly socioeconomic resource, geothermal energy can be used directly in balneology or agriculture, while indirect use is possible through geothermal power plants for electricity generation or through space heating and cooling by heat pumps (Vondra et al., 2023). Apart from the exploited health benefits, physiochemical and thermal properties, ecological studies of microbial communities in terrestrial hot springs have reshaped the view of microbial diversity, composition, structure, and functioning (Ward et al., 1998). Although cultivation methods are essential for objective analysis of populations in natural communities, their limitations cannot be denied (Brock, 1987; Ward et al., 1992; Boughner and Singh, 2016). Molecular methods, such as 16S rRNA gene sequencing, have allowed observation of the occurrence patterns of individual populations on which microbial community structure is based (Ward et al., 1998). The microbial communities of terrestrial hot springs were among the first to be studied using this technology (Stahl et al., 1985; Ward et al., 1990), revealing the impressive diversity of uncultured microbial populations in nature.

2.1.1. Hot springs and wells in Croatia

Thermal waters are defined as discharges with temperatures higher than the average temperature in the surrounding area (Marković et al., 2012; Tamburello et al., 2022). The northern and northeastern regions of Croatia are characterized by favourable geological conditions such as a high average geothermal gradient (49 °C/km), surface heat flow (76 mW/m^2), and a shallow Mohorovičić discontinuity, which leads to the occurrence of numerous thermal phenomena with large geothermal potential (Marković et al., 2012; Marković et al., 2022). According to (Novak, 1968; Ivanišević; 2008), these thermal waters are classified (among others) based on temperature, gasses and ionic content (Table 1).

Table 1. Classification of thermomineral waters in Croatia (Novak, 1968; Ivanišević, 2008).

Characteristic	Value	Name
Total mineralisation	> 1 g/L	mineral
Ions in traces		
Fe	> 10 mg/L	iron
I	> 1 mg/L	iodine
As	> 0.7 mg/L	arsenic
F	> 2 g/L	fluorine
Gases		
CO_2	> 1 g/L	carbon dioxide
S, H_2S	> 1 mg/L	sulfur
Temperature		
< 20 °C		cold
20 – 34 °C		hypothermic
34-38 °C		isothermic
> 38 °C		hyperthermic
Dominant ions		
Cl (Na, Ca, Mg)	> 20 mval %	chloride (sodium, calcium, magnesium)
HCO_3 (Na, Ca, Mg)	> 20 mval %	hydrogen carbonate (sodium, calcium, magnesium)
CO_3	> 20 mval %	carbonate (very rare)
SO_4 (Na, Ca, Mg, Fe, Al)	> 20 mval %	sulfate (sodium, calcium, magnesium, iron, aluminium)
Cl (Na)	> 240 mval %	salt

Most thermal sources in Croatia are used for balneological, recreational and medicinal purposes, while Bizovačke Toplice, for example, are used for multiple, cascading purposes, including energy utilization (Dekanič, 2008; Kolbah et al., 2009; Bačan, 2012). Bizovac is located in the Slavonia region and contains several springs of mineral, Na-HCO_3-Cl, hyperthermal water, which led to the establishment of health resort and rehabilitation clinic. Other sites in the Slavonia region include sulfur, Ca-Mg-HCO_3 Đakovačka Breznica with several cold water springs and one thermal spring, and Daruvar (Daruvarske toplice) with several Ca-Mg-HCO_3, hyperthermal and mineral peloid springs used for medical purposes since Roman times. Thermal findings, used as health resorts since ancient times, are also found in the Banovina region, such as the Ca-Mg-HCO_3-SO_4, hyperthermal waters and the peat of Topusko (Topusko Toplice). Thermal findings in Hrvatsko zagorje include Krapinske toplice (several

springs of Ca-Mg-HCO₃, hyperthermal water) and Varaždinske toplice (several springs of mineral, sulfur, Ca-Mg-HCO₃-Cl, hypothermal water and peloid) with established special clinics for medical rehabilitation, as well as Šemnica and Tuhelj (Tuheljske toplice) with Ca-Mg-HCO₃, hypothermal waters and peloid. In the Prigorje region, Kreča Ves near Sveti Ivan Zelina is a finding site of Na-HCO₃, hyperthermal water, while in the Pokuplje region, a mineral water spring Janino Vrelo, classified as Ca-HCO₃, CO₂ cold water, is used for drinking water.

There is a different legislative framework depending on whether thermal aquifers are used for balneological, medicinal and commercial purposes such as bottling and marketing, or for electricity and heat production (Marković et al., 2022). In both cases, current regulations only require daily reporting of pumped water and thermal wastewater volumes, with no requirement for monthly or annual monitoring of chemical parameters and groundwater levels/yields (Marković et al., 2022). Consequently, there is a lack of systematic data on these vital aspects for exploited geothermal sites. Moreover, their ecological aspect and biodiversity are largely unexplored (Mitrović et al., 2022; Kostešić et al., 2023). All previously mentioned geothermal sites contain extremophilic microbial biofilms (Kostešić et al., 2023) and therefore offer a valuable opportunity to uncover their immense potential.

2.2. Thermal biofilms

Microorganisms inhabit different microenvironments in thermal springs such as sediments, water columns, stromatolites, microbial mats and biofilms (Schuler et al., 2017). Biofilms are defined as associations of microbial cells, either of a single or multiple species, that have formed a community in an aggregated manner, attaching themselves to each other or to a surface by secreting extracellular polymeric substances (EPS, Ward et al., 1989; Donlan and Costerton, 2002; Prieto-Barajas et al., 2018). These types of biological organization are formed as a microbial strategy to enhance survival and adapt to fluctuating extreme conditions, and can range from simple, monospecific biofilms to several meter thick complex microbial mats (Donlan and Costerton, 2002; Msarah et al., 2018; Prieto-Barajas et al., 2018).

There is an extensive literature describing the development of biofilms and the different stages of their formation (Costerton, 1995; Costerton et al., 1995; Marić and Vraneš, 2007; Msarah et al., 2018; Prieto-Barajas et al., 2018; Kour et al., 2019; Rana et al., 2019). The formation process (Figure 2) is complex and consists of different phases including reversible and irreversible attachment, development of microcolonies, establishment of a mature, three-dimensional biofilm and dispersion of bacterial cells to initiate the formation of a new biofilm

(Msarah et al., 2018; Prieto-Barajas et al., 2018; Kour et al., 2019). Development begins with surface acclimation, during which organic and inorganic substances accumulate, altering surface properties and making it more favorable for microbial colonization (Zheng et al., 2021). The process is mediated by Brownian motion and gravitational forces, with both surface and microbial cell properties as key parameters (Kour et al., 2019). Microorganisms adhere to the surface through weak Van der Waals interactions and some of them detach within a few minutes, a phase referred as reversible adsorption (Donlan and Costerton, 2002; Marić and Vraneš; 2007). Those that remain undergo a series of morphological changes that lead to permanent, irreversible binding through stronger hydrophobic-hydrophilic interactions, making them tolerant to shear forces and similar conditions. (Kour et al., 2019; Rana et al., 2019; Krsmanovic et al., 2021). Being in a stable position with other cells, they form homogeneous and mixed microcolonies (Costerton et al., 1995). A prerequisite for microcolony formation is motility facilitated by fimbriae, differencing motility facilitated by flagella essential for the cell attachment to surface (Marić and Vraneš; 2007). As microcolonies form, cells commence the production of an EPS matrix that accounts for 90 % of the biofilm mass and consists of hexose, pentose, pyruvate, cellular components of lysed cells and non-cellular components (e.g., minerals), which, in addition to aggregation and protection, simultaneously enables inter-species substrate exchange and elimination of undesirable products from the matrix (Costerton, 1995; Kour et al., 2019; Rana et al., 2019). Different species respond to specific microenvironmental conditions with different growth patterns, and gradually a structurally more complex mature biofilm develops (Costerton et al., 1995). In the mature biofilm, microorganisms characteristic for all developmental stages exists simultaneously and form mushroom like clumps to allow efficient nutrient flow (Marić and Vraneš, 2007). When exposed to pressure, friction, or rapid water flow, the rigid structure of the biofilm begins to disintegrate, and cells, either individually or in clusters, begin to float in search of new niches (de los Ríos et al., 2007; Krsmanovic et al., 2021).

Biofilm grows naturally wherever there is a source of nutrients, heat and moisture, making thermal springs an ideal environment for its formation. Extreme temperatures and pH have been identified as the primary factors limiting microbial diversity in thermal spring biofilms (Msarah et al., 2018; Prieto-Barajas et al., 2018; Li and Ma, 2019), although other environmental factors, such as light quality (Nishida et al., 2018) and spring geochemistry (D'Imperio et al., 2007; Hamilton et al., 2019; Houghton et al., 2019), also have a strong influence on community composition.
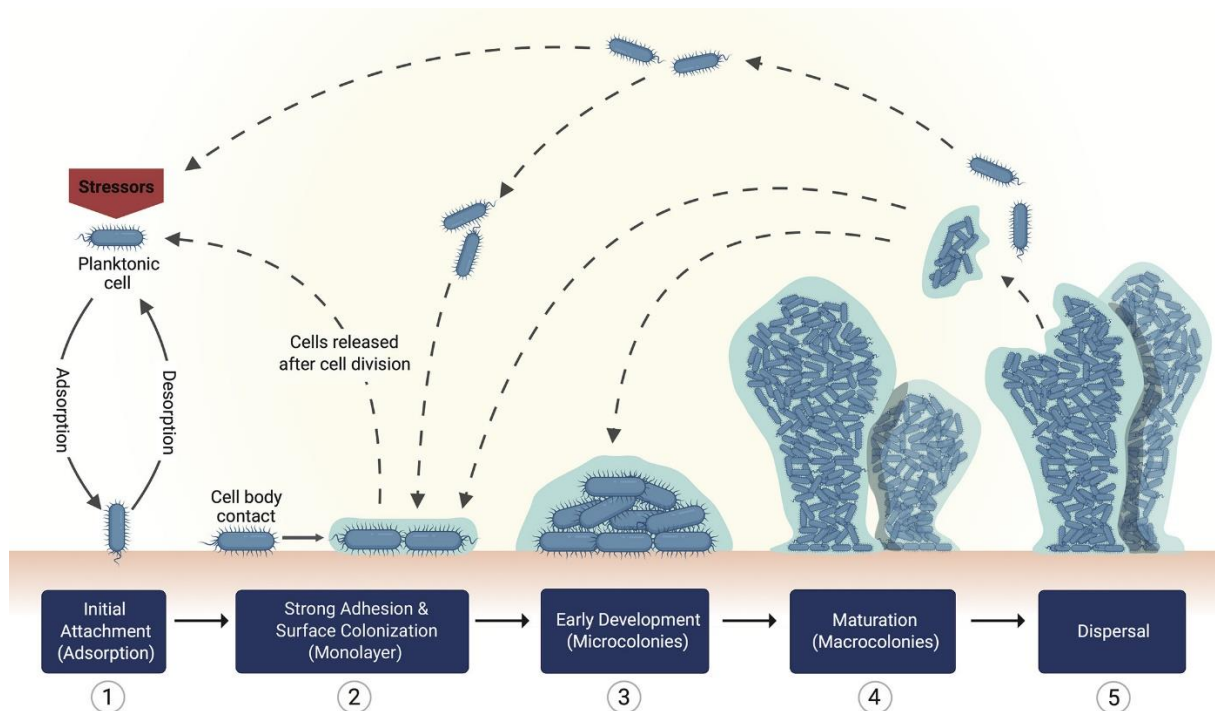
Figure 2. Schematic representation for bacterial species biofilm formation on a solid surface (Guzmán-Soto et al., 2021).

The process of ecological succession is carried out by cyanobacteria to colonize and modify the microenvironment for subsequent colonization by specialized bacteria (Boomer et al., 2009). As biogeochemical cycles and biochemical processes are linked within the biofilm (Figure 3), photosynthesis, nitrogen fixation, denitrification, sulfate reduction, metal reduction, and methanogenesis are enabled (Paerl and Pinckney, 1996; Paerl et al., 2000; Woebken et al., 2015). Therefore, the wide metabolic diversity of microorganisms coexisting in a biofilm (Figure 3) consists of primary producers that perform photosynthesis, anoxygenic photosynthetic bacteria represented mainly by green non-sulfur bacteria, green sulfur bacteria, purple bacteria, aerobic heterotrophs and anaerobes, sulfur oxidizing (SOB) and sulfate reducing (SRB) bacteria, and methanogenic archaea (Baumgartner et al., 2006; Severin et al., 2010; Klatt et al., 2016). In terms of taxonomy, the most represented phyla in thermal biofilms are Cyanobacteria, Chloroflexota, Chlorobiota, Pseudomonadota, Bacteroidota, and Deinococcota, while Planctomycetota, Bacillota, Acidobacteriota, Verrucomicrobiota, Actinomycetota, Synergistota and Armatimonadota are less abundant (Portillo et al., 2009; Huang et al., 2011; Coman et al., 2013; Mackenzie et al., 2013).
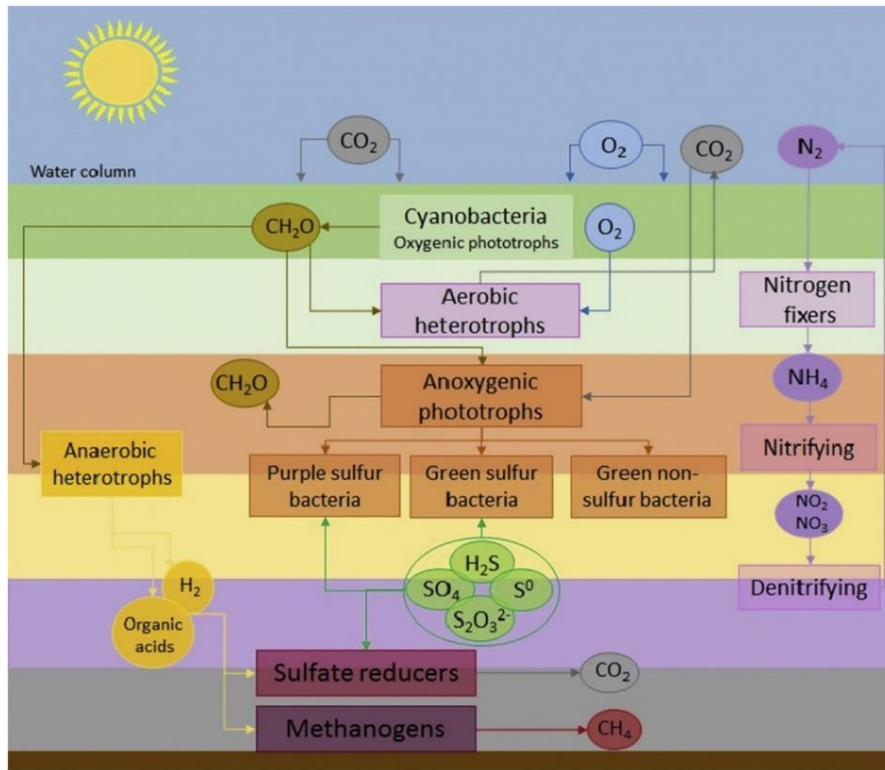
Figure 3. Metabolic structure of photosynthetic biofilm (Prieto-Barajas et al., 2018).

Described as temporally and spatially heterogeneous (Donlan and Costerton, 2002), biofilms exhibit the coexistence of diverse phenotypes, cross-feeding interactions, and defense mechanisms, resulting in a microbial community structure that is distinctly different from those found in water from the same thermal source (e.g., Urbieta et al., 2015). Therefore, the exploration of these ecological niches requires the utilization of various specialized tools and molecular methods.

2.2.1. Sequencing methods for studying thermal biofilms

Research focused on understanding the structure, function, and contributions of individual microbial species to natural biological systems and their dynamics is hampered by the lack of a coherent definition of prokaryotic 'species' (Gevers et al., 2005; Achtman and Wagner, 2008), the enormous diversity of microorganisms, many of which are currently uncultivable (Locey and Lennon, 2016), and the cognition of horizontal gene transfer (Acar Kirit et al., 2022). In general, microbial identification methods are divided into phenotypic techniques based on metabolic profiling and genotypic techniques based on profiling of genetic material (Emerson et al., 2008). Phenotypic methods provide more direct information about functionality and metabolic activity, while genotypic methods are independent of the physiological state of the

microorganisms and the cultivation conditions (Emerson et al., 2008; Franco-Duarte et al., 2019; Berg et al., 2020). Genotypic methods are further divided into fingerprint-based techniques, which are more reliable for distinguishing species and strains, and sequence-based techniques such as 16S rRNA gene analysis, which are more effective at establishing broader phylogenetic relationships (Vandamme et al., 1996). However, this division of methods is historical. Different techniques complement each other and are now more often combined to achieve a polyphasic approach that overcomes the limitations in identifying the structure and diversity of mixed microbial communities (Gillis et al., 2001).

2.2.1.1. 16S rRNA gene amplicon sequencing

Nucleic acid-based methods allow the discovery of genetic material by amplifying targeted parts of a species-specific gene region using synthetic oligonucleotides (Monis and Giglio, 2006; Hollister et al., 2015; Duman et al., 2022). Generally, three functional gene regions of ribosomal RNA - 5S, 16S/18S, and 23S rRNA - are used for identification (Ludwig and Schleifer, 1994; Gürtler and Stanisich, 1996; Jiang et al., 2019), with analysis of the 16S rRNA gene being the most commonly used method for classification of prokaryotes (Clarridge, 2004; Janda and Abbott, 2007; Kim et al., 2012). The 16S rRNA gene is a highly conserved component of the transcription machinery (Cox et al., 2013), making it well suited as a target gene for DNA sequencing of samples containing thousands of different species. Key to the success of 16S rRNA sequencing is its applicability to entire bacterial and archaeal domains (Woese, 1987; Janda and Abbott, 2007; Krieg et al., 2015; Jiang et al., 2019):

- The 16S rRNA gene is universally present in all prokaryotes in which it has the same function.
- The 16S rRNA gene consists of a (partially) conserved region that allows universal amplification, and variable/hypervariable regions that enable discrimination between different microorganisms.
- The common appropriate length of the sequence (1500 bp) allows relatively simple sequencing (e.g., Sanger sequencing) and provides sufficient information for identification of prokaryotes down to the genus level and determination of their phylogenetic position.

However, the 16S rRNA gene sequencing approach suffers from variable gene copy number (Stoddard et al., 2015; Louca et al., 2018; Starke et al., 2021) and primer efficiency (Albertsen et al., 2015; Brown et al., 2015), while metabolic functions are exclusively predictive in nature,

derived from previous taxonomic knowledge (Morrissey et al., 2016). Sequence analysis of a smaller region compared to the whole genome, combined with the higher mutation rate in this region and its approximately 99 % similarity among closely related species, leads to the conclusion that genetic analyses based solely on the 16S rRNA gene amplicon sequencing are less specific in microbial identification (Janda and Abbott, 2007; Petti et al., 2008; Adams and Thompson, 2011).

2.2.1.2. Metagenomic sequencing

Shotgun sequencing and pyrosequencing techniques have enabled the mapping of entire genomes (Cardenas and Tiedje, 2008; Singh et al., 2009; Vieites et al., 2009), and metagenomics has emerged as a powerful tool for studying the structural, evolutionary, and metabolic properties of complex microbial communities (Schmeisser et al., 2003; Tyson et al., 2003; Venter et al., 2004; Tringe et al., 2005; López-López et al., 2013; Biller et al., 2018; Keller-Costa et al., 2022). Genome sequencing involves several essential steps, including quality control, sequence assembly, sequence binning, taxonomic profiling, gene prediction, and function annotation (Zhang et al., 2021). Quality control processes, such as removing low-quality reads and filtering out contaminants, ensure the reliability and accuracy of sequencing data, while sequence assembly reconstructs the complete genome by piecing together fragmented sequencing reads (Mende et al., 2013; Schmieder et al., 2011). Sequence binning helps classify sequences into different genomes, and taxonomic profiling helps determine the origin of sequences with respect to taxonomy (Truong et al., 2015). Gene prediction focuses on identifying and annotating genes within the genome (Hyatt et al., 2010), while function annotation, as the name implies, assigns potential functions to these genes (Huson et al., 2016). Each of these steps brings different advantages and disadvantages and contributes to the overall complexity of genome analysis. For effective data analysis, continuous improvement of existing databases and analysis software is critical to increase the accuracy and efficiency of the analysis process (Yang et al., 2021; Zhang et al., 2021). In the context of metagenome-assembled genomes (MAGs) analysis, ensuring high-quality drafts is of paramount importance. This includes specific criteria such as maintaining gene integrity above 90 %, limiting contamination to below 5 %, and including essential genes such as 16S and 23S rRNA genes, and other highly conserved genes in the assembly set (Bowers et al., 2017). These criteria serve as a benchmark to gain more robust insights from metagenomic data. By comparing gene or protein sequences in a particular functional database and assigning a gene or protein to a specific function, information about a particular metabolic pathway can be obtained (Yang et al., 2021; Zhang et

al., 2021; Zeller and Huson, 2022). In this way, metagenomics technology has identified microbial species overlooked by other approaches and discovered many genes, including antibiotic resistance genes (ARGs, Riesenfeld et al., 2004; Yong et al., 2009), polyketide synthase-encoding genes (Ginolhac et al., 2004) and biocatalyst genes (Voget et al., 2003; Uchiyama et al., 2005; Tirawongsaroj et al., 2008). This has been particularly true for extremophiles, their target genes or active products, whose cultivation and extraction are limited by their living conditions. An example is the discovery of a novel thermophilic bacterium, *Candidatus* Kryptonia, from a hot spring (Eloe-Fadrosh et al., 2016). The bacterium could not be detected due to SSU rRNA primer biases but was identified by metagenome sequencing and single-cell sequencing (Eloe-Fadrosh et al., 2016). However, metagenomes can contain free DNA and DNA from dead microbes, which can lead to misinterpretation (Quince et al., 2017), while microorganisms with low abundance can be overlooked during analysis (Hazen et al., 2013). Also, identified genes are not necessarily active and a substantial number of newly identified open reading frames (ORFs, portion of a DNA sequence between start and stop codons) lack homology to well-characterized genes awaiting functional assignment (Zhang et al., 2021). Due to the imperfection of the microbial database (Smith et al., 2022), many sequencing data cannot be analyzed, both in terms of species annotation and functional analysis. Therefore, for a comprehensive understanding of the composition and genomic potential of hot spring biofilms (and other natural microbial communities), sequencing data should be complemented with additional approaches, such as fluorescent in situ hybridization (FISH) to assess community composition, single-cell approaches, and, when possible, phenotypic characterization techniques.

2.2.2 Ecophysiological methods for studying thermal biofilms

Biofilms in hot springs have been the subject of numerous in-depth studies, but interest in their exploration continues to grow. They are accessible, stable, high biomass systems that have enormous biotechnological potential (Dobretsov et al., 2011; Tripathi et al., 2016; Strazzulli et al., 2017). Their composition is usually simple enough to be evaluated by traditional methods such as microscopy (Ward and Cohan, 2015). However, because they form at redox interfaces with well-defined environmental gradients, they harbor a variety of metabolically diverse microorganisms (e.g., Swingley et al., 2012; Schubotz et al., 2013; Venturi et al., 2022). Although a substantial proportion of biofilm-dwelling microorganisms can be isolated in pure cultures, the activities in pure cultures do not reflect *in situ* activities and interactions within the biofilm community (Møller et al., 1998). Despite the comparatively low species richness

(Weiland-Bräuer, 2021), complex microbial interaction networks form in hot spring biofilms, hindering the comprehension of the drivers behind the observed community structure and biogeochemical cycling mechanisms. Although the number of studies on the genomic landscape of hot spring biofilms continues to increase, the use of post-genomic methods to study the ecophysiology of microbiomes, such as metagenomics, does not provide single-cell resolution (Du and Behrens, 2021). Also, despite the diverse suit of available methods to study the ecology and ecophysiology of microbial biofilm communities, such data are scarce for biofilms in hot springs.

To track microbial metabolic activity, incorporation of radio or stable isotope- labeled substrates or analogous substrates into microbial biomass is a widespread practice in microbial ecology (Braissant et al., 2022). Such substrate tracking approaches have been used in assessing the activities of mixed biofilm communities (e.g., Schuler et al., 2017). The same principle has also been used to link specific metabolic activities to certain groups of (micro)organisms within hot spring biofilms (e.g., using lipid biomarkers, Schubotz et al., 2013; Schubotz et al., 2015) or to connect substrate utilization to an individual cell via single-cell approaches (Wagner, 2009; Hatzenpichler et al., 2020; Alcolombri et al., 2022). Microbial cells that form hot springs (and other) biofilms are enveloped in an EPS matrix that restricts the diffusion of large molecules and complicates the separation of cells and matrix components often required for downstream analyses, leading to the challenging application of some physiology-targeted single-cell methods (Azeredo et al., 2017). Nevertheless, there are numerous studies investigating biofilm communities at single-cell resolution (e.g., Kindaichi et al., 2004; Hatzenpichler et al., 2014; Musat et al., 2016). Therefore, it is unexpected that single-cell ecophysiological methods have hardly been applied to geothermal biofilms: only a few microautoradiography (MAR) experiments performed on photosynthetic biofilms from various hot springs in Yellowstone have been published to date (Brock, 1969; Brock and Brock, 1969; Bauld and Brock, 1973; Doemel and Brock, 1977). MAR visualizes the incorporation of radiolabeled isotopes into microbial cells and can be combined with FISH to identify active microorganisms, but it requires time consuming sample processing as well as specialized laboratory equipment and radioactive waste management (Leizeaga et al., 2017; Braissant et al., 2020; Hatzenpichler et al., 2020). Another technique, nanoscale secondary ion mass spectrometry (nanoSIMS), enables visualization of stable isotope incorporation, circumventing the waste and safety issues associated with radioisotopes, but low throughput and the requirement for sophisticated instrumentation have limited its practical application (Braissant

et al., 2020; Hatzenpichler et al., 2020; Leizeaga et al., 2017). Furthermore, nanoSIMS only examines the surface of the sample, and although tomography is possible (Renslow et al., 2016; Nuñez et al., 2018), it is not practical for biofilms. Notably, both MAR and nanoSIMS are destructive methods that preclude further downstream analyses, such as genome sequencing or culturing (Hatzenpichler et al., 2020).

2.2.2.1. Bioorthogonal noncanonical amino acid tagging

Bioorthogonal noncanonical amino acid tagging (BONCAT), which can be used to visualize a large diversity of translationally active cells and can reveal under which conditions cells and cell populations are active (Samo et al., 2014; Hatzenpichler et al., 2016), has fewer drawbacks than other currently available single-cell methods. Albeit being a relatively novel method, it has been successfully applied to several types of environmental samples, including biofilms (Samo et al., 2014; Hatzenpichler et al., 2014; Babin et al., 2017; Leizeaga et al., 2017; Lindivat et al., 2020).

As shown in Figure 4 A, BONCAT is based on the incorporation of alkyne containing l-methionine analogue l-homopropargylglycine (HPG), whereupon newly synthesized proteins can be detected using azide-alkyne CLICK chemistry (Hatzenpichler and Orphan, 2015). Due to its structural similarity, HPG is incorporated into the growing polypeptide chains during translation instead of methionine (Saleh et al., 2019). The cells are then treated with a labeling reagent containing an azide functional group (dye). This reagent reacts specifically with the terminal alkyne group of HPG through a bioorthogonal azide-alkyne CLICK chemical reaction (Figure 4 A), leading to the formation of a stable covalent bond between the azide group of the dye and the terminal alkyne group of HPG (Bird et al., 2021). The CLICK reaction is highly specific and occurs under mild conditions (Nwe and Brechbiel, 2009), allowing efficient and selective labeling of HPG-containing proteins. However, the CLICK reaction requires a catalyst to proceed at a reasonable rate under physiological conditions. Copper ions are known to be particularly valuable catalysts for facilitating azide-alkyne cycloaddition (Bird et al., 2021; Nwe and Brechbiel, 2009; Hein and Fokin, 2010). Copper facilitates the formation of a reactive species known as the copper(I)-acetylide complex, which then reacts with the azide group in a 1,3-dipolar cycloaddition, leading to the formation of a triazole bond (Figure 4 A). To maintain the Cu (I) state and prevent precipitation and oxidation of copper ions, tris-hydroxypropyltriazolylmethylamine (THPTA) is introduced as a copper chelating agent, while sodium ascorbate is used as a reducing agent (Hein and Fokin, 2010). Since aldehydes can be generated as byproducts of cellular metabolism or chemical reactions, aminoguanidine

hydrochloride is used in the CLICK reaction to prevent the nonspecific reaction of aldehydes with fluorescently labeled azides and to suppress the generation of false positive signals (Hein and Fokin, 2010; Izquierdo and Delgado, 2018). This approach ensures that the CLICK reaction occurs exactly where it is intended and leads to accurate and reliable results of the BONCAT method. The introduction of a noncanonical amino acid and a biorthogonal labeling reagent integrates unique chemical functionalities into proteins synthesized by microbial cells that are not present in the natural microbial proteome (Saleh et al., 2019). In summary, only proteins synthesized during the BONCAT experiment are selectively labeled, without disrupting natural biological processes in active cells (Ma and Yates, 2018). These labeled proteins can then be detected and visualized using fluorescence microscopy.
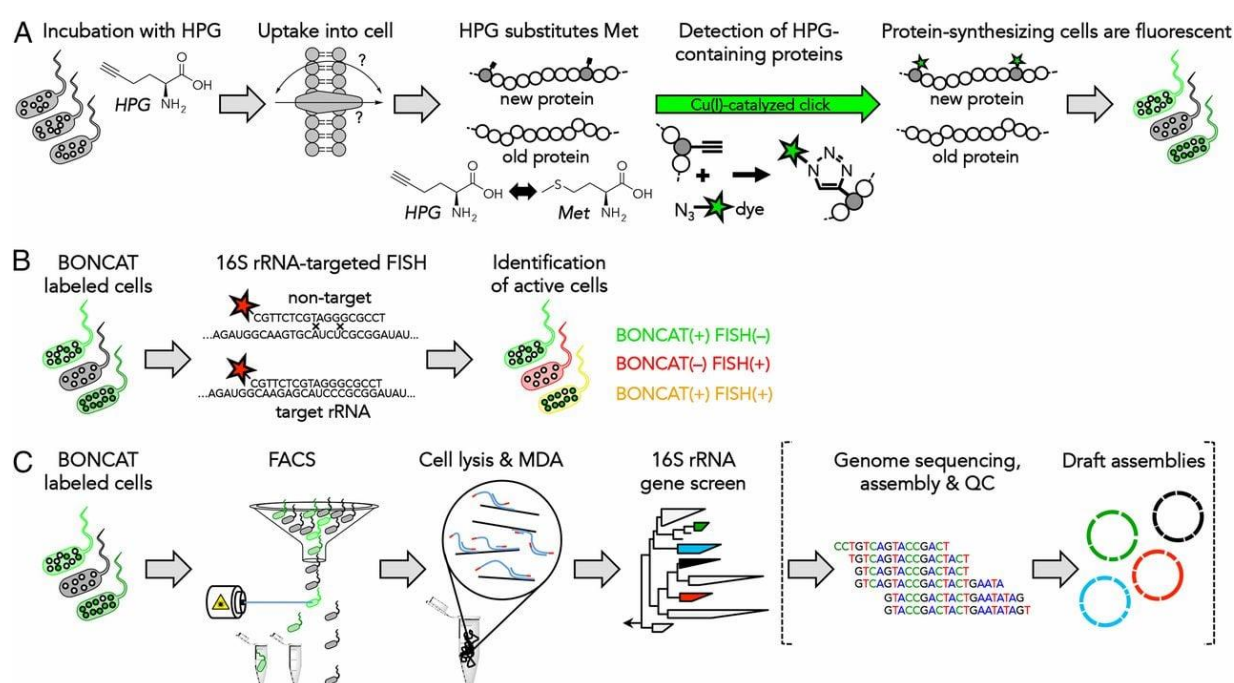
Figure 4. Concept for the visualization, identification, and sorting of translationally active cells (Hatzenpichler et al., 2016).

BONCAT requires a simple infrastructure available to most laboratories, and it is a rapid and nondestructive method compatible with many other approaches such as (meta)genomics, (meta)proteomics, nanoSIMS, FACS (Figure 4 C), and FISH (Landgraf et al., 2015; Braissant et al., 2020; Hatzenpichler et al., 2020; Lindivat et al., 2020; Reichart et al., 2020; Steward et al., 2020).

2.2.2.2. Fluorescence in situ hybridization and catalyzed reporter deposition

FISH has become one of the most routinely used molecular techniques in environmental microbiology for the detection, identification, and enumeration of environmental microorganisms bypassing the need for cultivation (Kubota, 2013). In this technique, fluorescently labeled DNA or RNA probes are bound to specific target sequences of microbial DNA in the sample (Shakoori, 2017). To improve detection of microorganisms, the tyramide signal is amplified using a technique known as catalyzed reporter deposition (CARD – FISH, Kubota, 2013). In CARD-FISH, the short DNA or RNA sequences are conjugated with the enzyme horseradish peroxidase (HRP probes). Their selection is based on prior taxonomic screening of the environmental sample to detect the presence of the targeted microbial groups and it represents a crucial step in the implementation of the method (Kubota, 2013). Prior to hybridization, the cells must be fixed, and the cell wall must be permeabilized (Amidzadeh et al., 2014). Fixation of the cells is usually performed with ethanol or paraformaldehyde to preserve the cell structure. Paraformaldehyde is a cross-linking fixative that creates covalent bonds between cell components ("freezing" the cells in their current state) to preserve cell morphology and structure and prevent loss of cells during washing and staining (Rocha et al., 2018). Permeabilization of the cell wall refers to the process of creating temporary openings or pores in the cell membrane to allow penetration of a probe and binding to a target nucleic acid sequence (Bidnenko et al., 1998; Amidzadeh et al., 2014). Enzymes such as lysozyme and achromopeptidase are particularly useful for permeabilization of bacterial cells with a rigid cell wall (Amidzadeh et al., 2014). After permeabilization, the sample is immersed in hybridization buffer to bind the HRP probes to the complementary nucleic acid sequences of the target microorganisms (Figure 4 B). The CARD step involves a catalyzed chemical reaction that amplifies the fluorescent signal generated by the binding of the tyramide-fluorophore conjugate (dye) and the HRP probe (Bobrow and Moen, 2001; Ferrari et al., 2006). HRP acts as a catalyst and leads to multiple deposition of tyramide, resulting in a stronger fluorescent signal, even for the low abundant microorganisms in the sample (Bobrow and Moen, 2001; Ferrari et al., 2006). The results are visualized using fluorescence microscopy. The analysis of the results can be qualitative or quantitative, depending on the specific experimental hypothesis and the implementation of the method.

Several challenges such as limited sensitivity, probe permeability, and hybridization efficiency have been encountered (Amann et al., 1995), nevertheless, various strategies have been developed to overcome these limitations (reviewed in Wagner et al., 2003; Amann and Fuchs,

2008; Wagner and Haider, 2012). The combination of BONCAT with CARD-FISH (Figure 4 B) allows direct linkage of the microbial identity and activity by fluorescence microscopy (Hatzenpichler et al., 2014), which can be applied to hot spring biofilms.

2.2.2.3. Fluorescence activated cell sorting

The identity and activity linkage of microbial biofilms in hot springs can be acquired at single-cell resolution through combination of BONCAT and flow cytometry. Compared to microscopic detection and counting analysis, flow cytometry offers enhanced reliability and reproducibility by reducing the potential for operator-induced bias, providing faster results at lower operational costs, and enabling significantly higher sample throughput (Lindivat et al., 2020). More importantly, flow cytometry enables the application of fluorescence activated cell sorting (FACS). This approach is based on light scattering and fluorescence emission from fluorescently labeled cells as they pass through a laser beam and allows sorting of specific microbial subpopulations of interest (Lindivat et al., 2020; Reichart et al., 2020; Du and Behrens, 2021). By integrating BONCAT with FACS (Figure 4 C), viable, active, or inactive cells can be sorted based on the fluorescence of CLICKED proteins. The sorted samples can then be subjected to sequencing and analysis (BONCAT-FACS-seq), allowing identification of metabolically active community members (Reichart et al., 2020; Du and Behrens; 2021; Trexler et al., 2023). There are numerous applications of this approach. Because activity shifts indicate microbial preferences for specific growth conditions in response to substrate changes or altered physicochemical conditions, the results of BONCAT-FACS-seq studies could aid in the development of cultivation media for specific enrichment of uncultured microbes (Reichart et al., 2020). In addition, this rapid and robust approach provides information on the physiological properties of uncultured microorganisms by replicating their *in situ* conditions as closely as possible within experimental limitations (Reichart et al., 2020; Trexler et al., 2023). Lastly, BONCAT-FACS-seq allows monitoring of microbial activity and contributes to the characterization of microbial functional potential (Lindivat et al., 2020; Du and Behrens, 2021).

Although often constrained by biofilm properties, the investigation of hot spring biofilms relies on a diverse array of techniques, ranging from advanced imaging methods for visualizing their structure to molecular approaches for understanding their metabolic activities. As these techniques continue to evolve, detection of potential applications of thermal biofilms functionality is growing.

2.2.3. Biotechnological potential of thermal biofilms

The ability to discover new chemical substances from microbial sources relies on the uniqueness of their habitat. Environments that are unexplored, taxonomically distant from the human microbiome, and exist under extreme conditions often exhibit all three characteristics simultaneously (Tanner et al., 2017). Exploration of the extreme biosphere in search of new bioactive compounds is based on the premise that harsh abiotic conditions favor the selection of microorganisms that possess unique chemistry, adaptive mechanisms, and variations in the structure, flexibility, charge, and hydrophobicity of their enzymes (Mahajan et al., 2017). In adapting to high temperature, microorganisms contain higher content of polyamines, can adjust the ratio of saturated to unsaturated lipids in their cell membranes to maintain fluidity, possess ability to reduce the length of surface loops, and evolve proteins that can function effectively by increased ion pair content and formation of higher order oligomers (Siliakus et al., 2017). In addition to elevated temperature, hot springs are often characterized by other extreme conditions, such as low pH, high salinity, and elevated metal concentration. Therefore, adaptation to the extreme conditions in hot springs requires genomic plasticity and metabolic flexibility of microorganisms, making thermal biofilms promising candidates for the discovery of bioactive molecules of industrial and biotechnological interest (DeCastro et al., 2016; Strazzulli et al., 2017). A well-known example is the discovery and isolation of the species *Thermus acquaticus* from hot spring biofilms in Yellowstone (Brock and Freeze, 1969) and its heat-resistant enzyme implementation in the polymerase chain reaction (Chien et al., 1976), which rapidly increased interest in studying the microbial diversity and functionality of these microenvironments. Applications of thermal biofilms in different fields are listed in Table 2.

Biofilms in hot springs have shown potential for bioremediation of xenobiotic and organic contaminants (Shukla and Singh, 2020). Microorganisms found in hot spring biofilms have enzymatic capabilities to degrade recalcitrant organic compounds, including alkanes, aromatic and polycyclic aromatic hydrocarbons (PAHs), which can be used to remove organic and petroleum pollutants from contaminated environments (Cui et al., 2012). Their ability of phenol degradation and dye decolorization could be employed in effective removal of these recalcitrant contaminants from industrial wastewater (Barathi et al., 2022; Cui et al., 2012; Shukla and Singh, 2020). The presence of genes associated with isoquinoline degradation detected in the strain *Lampropedia cohaerens* from biofilms of arsenite thermal springs in the Himalayas indicated its potential application in bioremediation of oil-polluted sites (Tripathi et al., 2016). Thermal biofilms are also capable of efficiently removing heavy metals through biosorption,

precipitation, and microbial reduction (Jardine, 2022; Najar et al., 2022). Through ammonia-oxidizing, denitrifying and sulfate-reducing capabilities (Lee et al., 2014; Zhang et al., 2019), thermal biofilms could be used as natural biofilters that metabolize and reduce excess nutrients, helping to mitigate eutrophication and improve water quality in receiving environments.

Table 2. List of potential applications of biofilms from hot spring.

Industries and biotechnology areas	Applications	References
Bioremediation	Degradation of pollutants and xenobiotic compounds in contaminated environments	Cui et al., 2012
Waste Treatment and Resource Recovery	Anaerobic digestion, composting and wastewater treatment processes that contribute to resource recovery and environmental sustainability	Tripathi et al., 2016
Enzyme production	Sources of extremophilic enzymes with unique properties that have applications in biocatalysis and various industries	Dumorné et al., 2017
Biofuel and Renewable Energy production	Production of biogas, ethanol, butanol and hydrogen by anaerobic digestion, fermentation, and microbial fuel cells	Narihiro et al., 2019
(Bio)pharmaceutical Industries	Production of bioactive compounds with pharmaceutical applications, such as antimicrobial agents, enzymes, and secondary metabolites	Dobretsov et al., 2011
Bioplastic and Biomaterials	Ability to synthesize biopolymers such as polyhydroxyalkanoates (PHAs)	Kourmentza et al., 2017
Mining and Mineral Recovery	Biomineralization, contribution to the recovery of metals and minerals from mining sites, efficiency improvement of metal extraction processes	Kochar et al., 2022
Food and Beverage Industries	Used in the production of fermented foods and beverages such as cheese and wine	Salas-Jara et al., 2016
Agriculture and Plant Growth Promotion	Improvement of crop productivity and nutrient uptake in agricultural systems	Haque et al., 2020
Environmental Monitoring and Research	Indicators of environmental conditions, impact on nutrient and biogeochemical cycling, climate change research	Guerrieri et al., 2022

Hot spring biofilms are also a rich source of extremophilic enzymes like protease, cellulase, amylase, and lipase, with unique properties such as excellent stability and activity at elevated temperatures and tolerance to extreme pH (Debnath et al., 2019). Thermophilic cellulases are used in bioremediation, biofuel, and textile industries for efficient degradation of cellulose, which enables the production of bioethanol and biobased fibers (Debnath et al., 2019; Dumorné et al., 2017; Khadka et al., 2022). Amylases from thermal spring biofilms can be used in the starch and food industries for saccharification and production of glucose syrups, brewing, and in detergents formulation for starch stains removal (Gupta et al., 2003). Thermophilic proteases are also suitable for detergent formulation, leather, and food processing (Gupta et al., 2002). Thermolysin, a metalloproteinase enzyme derived from thermophilic bacteria, including those found in hot spring biofilms, is used for protein hydrolysis, peptide synthesis, and meat tenderization (Cheng et al., 2021; Vermelho et al., 2013). Thermophilic lipases can also be used in food processing and for detergent formulation, as well as in biodiesel production (Ali et al., 2023; Rabbani et al., 2013; Vermelho et al., 2013). In addition to the mentioned heat-stable enzymes used in various food processing applications, hot spring biofilms produce extracellular polysaccharides such as xanthan gum and pullulan, which can be used as thickeners, stabilizers, and gelling agents in food formulations (Waoo et al., 2023). Thermal biofilms are also suitable candidates for the development of probiotic products (Salas-Jara et al., 2016), their antimicrobial compounds, bacteriocins and antimicrobial peptides, could serve as natural food preservatives (Rai et al., 2016), while pigments such as carotenoids and melanins could be used as natural food colorants and antioxidants (Di Salvo et al., 2023).

The ability of microorganisms in hot spring biofilms to produce hydrocarbons enables the synthesis of renewable biofuels with comparable properties to petroleum fuels. Their cellulolytic, fermentative, and hydrogen-producing capabilities allow the conversion of lignocellulosic biomass into bioethanol, biobutanol, and hydrogen at elevated temperatures (Salim et al., 2015; Sekoai et al., 2022). Furthermore, thermophilic biofilms could also be employed in the conversion of organic waste into methane-rich biogas through anaerobic digestion (Narihiro et al., 2019). Also, they possess lipolytic capabilities that enable the enzymatic conversion of lipids into fatty acid methyl ester (FAME), a feedstock for biodiesel production (Sahoo et al., 2017), and have been used in microbial fuel cells where they serve as bioanodes or biocatalysts for the conversion of organic material into electricity (Santoro et al., 2017).

In addition to biofuel and energy production, hot spring biofilms have also been explored as a source of novel bioactive compounds with pharmaceutical potential (Mahajan et al., 2017). A study of biofilms from hot springs in Oman showed that these microbial communities produce antimicrobial compounds under natural conditions (Dobretsov et al., 2011). Geobacillin, an antibiotic compound produced by the thermophilic bacterium found in hot spring biofilms, exhibits antimicrobial activity against a variety of bacteria and has potential applications in the treatment of infectious diseases (Zebrowska et al., 2022). In addition to antimicrobial activity, other unique secondary metabolites, such as anticancer and antiviral compounds, could also serve as valuable drug leads. Bioactive compounds from thermal biofilms such as terpenoids and polyketides have also shown promising pharmacological activities and therapeutic potential (Nandagopal et al., 2021).

Due to the ability to accumulate polyhydroxyalkanoates (PHAs), the use of hot spring biofilms in the production of biodegradable bioplastics is another investigated application (Kourmentza et al., 2017). Moreover, since they can induce precipitation of (bio)minerals like calcium carbonate (Li et al., 2015) and cellulose with high crystallinity and mechanical strength (Cheng et al., 2009; Nguyen and Nguyen, 2022), they can be used for the synthesis of biomaterials with specific properties and improved functionality. In addition to inducing precipitation, hot spring biofilms possess acid-tolerant, sulfur-oxidizing, metal-binding, and metal-resistant genes and enzymatic activities. As a result, they are excellent candidates for various applications in the mining and mineral extraction industries (Kochar et al., 2022), including the recovery of precious metals such as gold and silver and rare earth elements (REEs), bioleaching of sulfide minerals, biomineralization, bioremediation of heavy metal-contaminated environments and acid mine drainage (Castro et al., 2021; Ibáñez et al., 2023; Kochar et al., 2022; Wheaton et al., 2015).

Lastly, biofilms produce growth-promoting substances, including phytohormones (e.g., auxins, cytokinins), siderophores, and solubilizing enzymes that could enhance plant growth, nutrient uptake, and stress tolerance in agricultural systems (Haque et al., 2020; Mehta et al., 2016). Through nitrogen-fixing and phosphate-solubilizing abilities, they could be applied in the production of biofertilizers and bioinoculants (Chaudhary et al., 2022; Seenivasagan and Babalola, 2021).

Extensive amount of literature on hot spring bioprospecting supports the notion that thermal biofilms are important and unexplored sources of new compounds with unique properties and exploitation in various industries.

3. EXPERIMENTAL METHODS AND MATERIALS

3.1. Sample collection, environmental measurements and DNA extraction

Parts of chapter 3 (3.1. - 3.3.) are published in (Kostešić et al., 2023).

3.1.1. Biofilm sampling and *in situ* measurements of physicochemical parameters of geothermal waters

Seasonal sampling of biofilms was conducted in autumn 2019, spring 2020, and autumn 2020 from 12 springs and wells at 10 geothermally active sites in northern and northeastern Croatia (Figure 5 a). Additional biofilms from Bizovac well and Tuhelj spring were collected in spring 2021 for screening of activity patterns. Biofilms from the same sampling sites were resampled in autumn 2021 for a single-cell resolution activity experiment and metagenomic analysis. Depending on the presence and location of biofilms (Figure 5 b - e), samples were collected using a sterile spatula and forceps at a depth range from the air-water interface to 0.5 m water depth. The biofilm samples were stored in sterile 50-mL tubes and submerged in the corresponding geothermal water. If multiple biofilms of distinct colors were present at a site (e.g., Figure 5 b), they were sampled separately. Similarly, multilayered biofilms were separated according to the color of the layer and processed separately.

After sampling, electrical conductivity (EC), dissolved oxygen (O_2) concentration, pH, and temperature of geothermal spring waters were measured *in situ* using a WTW multiparameter probe (WTW, Germany). Sampling of biofilms and *in situ* measurements of physicochemical parameters in the geothermal spring waters were conducted as close to the spring source as possible, and the measured parameters reflect the geochemistry experienced by the sampled biofilms. Hydrogen sulfide (H_2S) concentrations in geothermal waters were determined using Reagent sulfide 1 and Reagent sulfide 2 following the USEPA Methylene Blue Method with a HACH DR3900 spectrometer, as described in DR manual 1 (URL2). If necessary, the samples were diluted for the measurement of H_2S concentration.
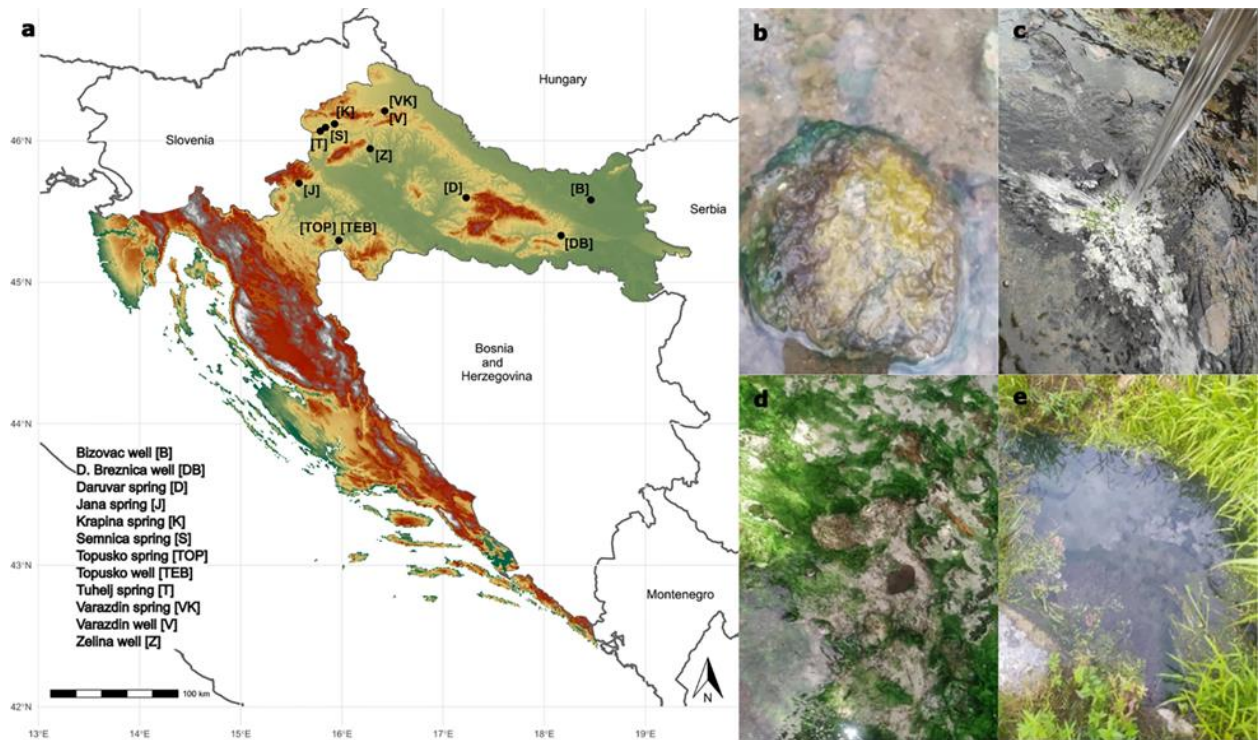
Figure 5. a Locations of thermal sites. b Close-up of different colored biofilms formed in the Topusko spring. c Biofilms in D. Breznica well. d Close-up of green and white biofilms in Tuhelj spring. e Tuhelj spring.

3.3.2. Chemical analysis of geothermal waters and DNA extraction of biofilm samples

For further chemical analysis in the laboratory, water samples were collected in 50-mL tubes and 500-mL plastic bottles and brought to the laboratory within a few hours of collection. Chemical analyses were performed at the Croatian Geological Institute. Concentrations of cations (sodium, potassium, calcium, ammonium, and magnesium) and anions (chloride, nitrate, and sulfate), alkalinity, SiO_2 concentrations, and dissolved organic (DOC) and inorganic (DIC) carbon concentrations were determined the same evening after returning from the field site. Concentrations of cations and anions were measured by an ion chromatographic method using the Dionex ICS-6000 DC instrument (Thermo Fisher Scientific Inc., Waltham, Massachusetts). Alkalinity was measured by a titration method using 1.6 N H_2SO_4 and phenolphthalein and bromocresol green methyl red indicators, while SiO_2 concentrations were determined by a colorimetric method using a HACH DR3900 spectrophotometer (Danaher, Loveland, Colorado). DOC and DIC measurements were performed with a HACH QbD1200 liquid carbon analyzer (Danaher, Loveland, Colorado).

After excess water was removed from the collected biofilms by decanting and pipetting, 0.5 g of each biofilm sample was weighed into bead-beating tubes for DNA extraction. According to the manufacturer's guidelines, total genomic DNA was extracted using the DNeasy PowerSoil Kit (Qiagen GmbH Hilden, Germany).

3.2. 16S rRNA gene amplicon sequencing and analysis of sampled biofilms

The hypervariable V4 region of the 16S rRNA gene was amplified using primer pairs 515F (5'-GTG YCA GCMGCC GCG GTAA -3, Parada et al., 2016) and 806R (5'- GGA CTA CNVGGG TWT CTAAT -3, Apprill et al., 2015). Samples were then barcoded, purified, normalised, and prepared for sequencing as described (Pjevac et al., 2021). Sequencing was performed in pair-end mode (v3 chemistry, 2×300 bp) on an Illumina MiSeq instrument (Illumina, Inc., San Diego, California) at the Joint Microbiome Facility of the Medical University of Vienna and the University of Vienna (project IDs JMF-2005-3, JMF-2007-4, JMF-2103-13, JMF-2110-16). Amplicon pools were extracted from raw sequencing data using standard FASTQ workflow parameters (BaseSpace; Illumina) and then filtered for PhiX contamination using BBDuk from the BBtools packages (Bushnell, 2014; Callahan et al., 2016a). Demultiplexing was performed using the Python package demultiplex (URL3), allowing one mismatch per barcode and two mismatches for linker and primer sequences. FASTQ reads were trimmed at 220 and 150 nt, respectively, with an error of 2 allowed for forward and reverse reads. Amplicon sequence variants (ASVs) were inferred in pooled mode in the DADA2 R package version 1.20.0 (R 4.1.1, Callahan et al., 2016a; Callahan et al., 2016b) using default settings. ASVs were further classified using the SILVA reference database (SILVA release 138, 2019) with the SINA classifier, version 1.6.1 (Pruesse et al., 2012).

Prior to downstream analysis, ASVs classified as eukaryotes, mitochondria, or chloroplasts, as well as unclassified ASVs were removed from the dataset, as were singletons and doubletons. After filtering, samples with less than 3000 sequence reads were excluded from the dataset. The final ASV table contained 4496 ASVs and 61 samples with read counts greater than 3000. All statistical analyzes were performed in the R environment (v. 4.2.0) using the Bioconductor v3.15 packages TreeSummarizedExperiment (Huang et al., 2021), phyloseq (McMurdie et al., 2013), mia (Ernst et al., 2022), and microViz (Barnett et al., 2021) and visualized using the package ggplot2 (Wickham, 2009). Prokaryotic community similarity between biofilm samples as a function of environmental parameters was evaluated using non-metric multidimensional scaling (NMDS) based on the Bray-Curtis dissimilarity distance. Permutational multivariate

analysis of variance (PERMANOVA) was used to assess the extent to which microbial communities were affected by sampling seasons, locations, selected environmental parameters, and biofilm color.

3.3. Activity of Bizovac and Tuhelj biofilms in different substrates

For the screening of microbial activity patterns, fresh biofilm samples were collected in spring 2021 from two geothermal sources with contrasting characteristics, the Bizovac well and the Tuhelj spring. These sources were chosen based on their distinct features, including one being a natural spring and the other a well with limited light availability, their geographic distance (Figure 6 a), as well as differences in geochemistry (e.g., double temperature difference and sulfide concentration) and microbial community composition observed during seasonal sampling. Biofilms from the Bizovac well displayed an atypical community composition, not dominated by phylum Cyanobacteria, and experienced moderately sulfidic, high-temperature conditions, while all biofilms from the low-temperature, non-sulfidic Tuhelj spring were dominated by phylum Cyanobacteria.

The combination of CARD-FISH and BONCAT was applied to investigate the identity and activity of microorganisms inhabiting these two contrasting hot spring biofilms, supplied with substrates stimulating either phototrophic, chemoorganotrophic, or chemolithotrophic activity. To evaluate microbial activity of hot spring biofilms sustained by various reducing equivalent sources, a series of incubation experiments were designed with sodium acetate, pyruvate, glucose, thiosulfate, and in the presence of light. Standard LED light from the incubator was used to stimulate phototrophic activity. Since the redox gradients in the studied hot springs, including Bizovac well and Tuhelj spring, were partially characterized by the presence of sulfide-oxygen transition zones, thiosulfate was provided as a reducing equivalent source to stimulate chemolithotrophic activity. Unlike sulfide, thiosulfate is stable under oxic conditions, non-toxic at elevated concentrations, and most sulfide oxidizers can utilize thiosulfate (Kappler and Dahl, 2001). Since previous studies demonstrated that members of Cyanobacteria phylum release glucose, acetate, and pyruvate through glycogen degradation under dark and anaerobic conditions, and considering that a variety of bacteria from diverse taxonomic groups possess the essential metabolic pathways for their utilization, these substrates have been used as reducing equivalents to stimulate chemoorganotrophic activity (Nguyen et al., 2017; Thiel et al., 2017; Hagemann and Hess, 2018; Melis et al., 2020; Chuang et al., 2021). The combination of BONCAT and CARD-FISH was performed as presented in Figure 6.
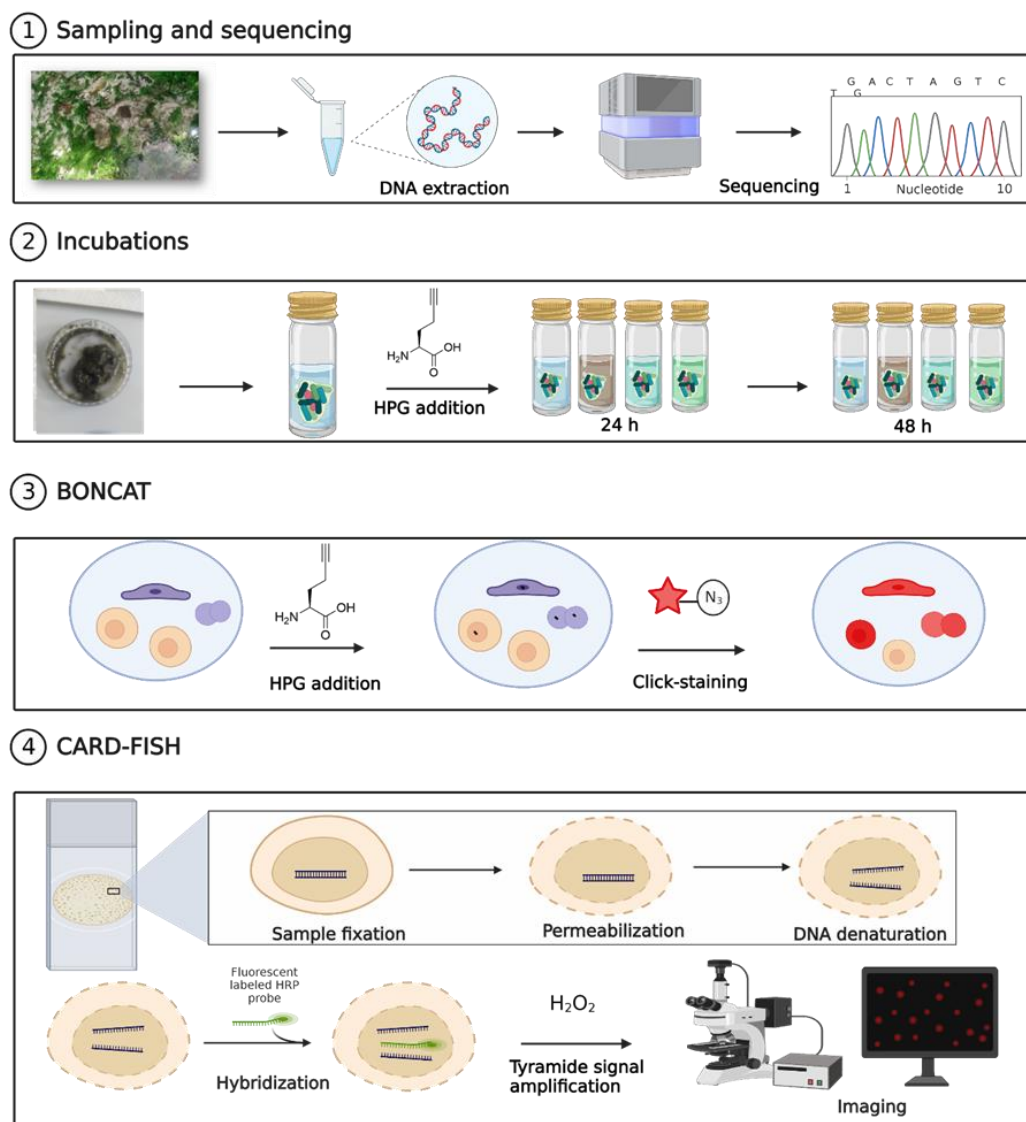
Figure 6. Schematic overview of the experimental workflow applied for characterization of hot spring biofilms collected in spring 2021: (1) characterization of the biofilm microbial community composition; (2) incubation with the l-methionine analogue HPG under different substrate amendment for 24 h and 48 h; (4) BONCAT visualization of active cells; (3) CARD-FISH hybridization of target populations, sample imaging and image analysis.

3.3.1. Incubations of biofilms

For each incubation setup (Figure 6), 0.5 g wet weight of biofilm material was suspended in 10 mL of sterile filtered (0.2 μm pore size) corresponding geothermal water in glass vials and incubated for 48 h at source temperature. To monitor activity, l-homopropargylglycine (HPG) was added to the sample at a final concentration of 50 μmol L^{-1} along with substrates (sodium

acetate, glucose, pyruvate or sodium thiosulfate) at a final concentration of 1 mmol L^{-1}. The acetate, pyruvate, and glucose solutions were prepared by dissolving the appropriate weight of substrate in autoclaved MQ water, while the thiosulfate media stock was prepared according to (Hidayat et al., 2017). To assess native activity, a set of incubations without substrate amendment was performed, only with the addition of HPG. To stimulate phototrophic activity, another set of incubations with HPG addition only was exposed to standard LED light of the incubator, while all other incubations were conducted in the dark to minimize the effects of additional photosynthetically produced substrates on the experiment. After 24 and 48 h, samples were removed from the incubator and 2 mL of 0.5 % Tween 20 (Promega) was added (Reichart et al., 2020). Samples were then macerated, vortexed at maximum speed for 5 min, sonicated (Microson XL 2000, Misonix Inc., New York) at standard instrument settings for 1 min (Pin et al., 2021), and centrifuged at 500 × g for 5 min to separate the particles from the cell fraction (Reichart et al., 2020). The supernatant was sequentially filtered through polycarbonate filters with pore sizes of 10 μm and 3 μm to remove filamentous Cyanobacteria and ease microscopy. The final filtrate was fixed with paraformaldehyde at a final concentration of 3 % for 1 h at room temperature in the dark (Pin et al., 2021). Samples were then filtered onto a filter with a pore size of 0.2 μm and stained with 4′,6-diamidino-2-phenylindole (DAPI, 10 μg μL^{-1}). The filters were examined with inverted fluorescence microscope (ZEISS, Germany) and stored at −20 °C until the CLICK reaction was performed.

3.3.2. BONCAT procedure

BONCAT was performed according to (Hatzenpichler and Orphan, 2015). Briefly, filter pieces were placed sequentially in 50, 80, and 96 % EtOH for 3 min to dehydrate and permeabilize the cells. For the Cu(I)-catalyzed CLICK reaction, a dye premix was prepared, consisting of 1.25 μL of a 20 mmol L^{-1} CuSO$_4$ solution, 1 μL of a 2.5 mmol L^{-1} Cy5-azide dye, and 2.5 μL of a 50 mmol L^{-1} THPTA chelating agent. While allowing the dye premix to react, 12.5 μL each of freshly prepared 100 mmol L^{-1} sodium ascorbate and 100 mmol L^{-1} aminoguanidine hydrochloride were added to 221 μL of sterilized phosphate-buffered saline (PBS). After mixing the dye premix with the remainder of the buffer, the filters were added directly to the CLICK mixture and incubated in the dark at room temperature for 1 h to label active microbial cells. Subsequently, the filters were washed three times with PBS for 3 min each to remove unreacted reagents, dehydrated in 50 % EtOH for 3 min, and stored at −20 °C until the CARD-FISH procedure.

3.3.3. CARD-FISH procedure

CARD-FISH was performed following the protocol (Schmidt et al., 2012). Briefly, after the filters thawed, they were dehydrated in a series of EtOH and embedded in 0.1 % low melting point agarose. To facilitate HRP probe penetration into the microbial cells, the cells were permeabilized with a 10 mg mL^{-1} lysozyme solution for 1 h and a 60 U mL^{-1} achromopeptidase solution for 30 min, both at 37 °C, followed by incubation in 0.1 mol L^{-1} HCl for 1 min at room temperature. Inactivation of endogenous peroxidases was achieved by 3 % H$_2$O$_2$ treatment. Subsequently, 1.5 μL of a 50 ng μL^{-1} HRP probe solution was added to 400 μL of hybridization buffer of the appropriate stringency (Table 3). Filters were added directly to the solution and hybridized overnight at 46 °C. To improve the detection of microorganisms, the fluorescence signal was amplified by CARD. Before amplifying the fluorescence signal, the removal of unbound probes was performed in a washing buffer for 10 min at 48 °C, heated in a water bath, followed by 5 min incubation in Triton-X–PBS. The filters were then added to a mixture of 1 mL amplification buffer and 2 μL tyramide solution (either Cy3 or Atto-488 dye), incubated at 46 °C for 20 min, and washed in Triton-X–PBS, MQ water, and absolute EtOH. After drying, filters were embedded in Citifluor-Vectashield solution containing DAPI (10 μg μL^{-1}) on slides. Oligonucleotide probes for CARD-FISH were selected based on 16S rRNA gene amplicon analysis of biofilms from previous seasons, and the NONEUB probe served as a negative control for all hybridizations.

Table 3. 16S rRNA-targeted oligonucleotide probes and hybridization conditions used for CARD-FISH experiments.

Probe	Specificity	Sequence (5'-3')	FA (% vol/vol)[a]	References
EUBI*	Most Bacteria	5'- GCT GCC TCC CGT AGG AGT -3'	35	Amann et al., 1995
EUBII*	Planctomycetota	5'- GCA GCC ACC CGT AGG TGT -3'	35	Daims et al., 1999
EUBIII*	Verrucomicrobiota	5'- GCT GCC ACC CGT AGG TGT -3'	35	Daims et al., 1999
Gam42a#	Gammaproteobacteria	5'- GCC TTC CCA CAT CGT TT -3'	35	Manz et al., 1992
CFX1223	Chloroflexota	5'- CCA TTG TAG CGT GTG TGT MG -3'	35	Björnsson et al., 2002

[a] FA, formamide concentration in the hybridization buffer
*Used in equimolar mixture EUBI-III mix
#Used without Bet42a competitor

3.3.4. Images Processing and Analysis

Samples were imaged using an epifluorescence microscope (model DMi8; Leica, Germany) equipped with the Thunder Imaging System at a resolution of 2048×2048 pixels. Z-stacks of 4–10 image fields were acquired for each sample, both in each channel individually as well as their overlay. The final images represent the maximum projection of all stacks. After inspection of the samples on the microscope, biovolume analysis was performed using *daime* software (v. 2. 2. 3, Daims et al., 2006). The images were processed with 2D filter histogram stretching to improve signal-to-noise ratio and eliminate background noise before automatic segmentation in ISODATA or Custom mode. After examining the results of the different segmentation methods for each sample, the biovolume fractions of BONCAT positive cells/cell aggregates against CARD-FISH positive ones and vice versa were determined considering % congruency of the signals.

3.4. Activity at single-cell resolution of biofilms from Bizovac and Tuhelj, their functionality and metabolic potential

In autumn 2021, fresh biofilm samples were collected from two contrasting geothermal sources: the Bizovac well and the Tuhelj spring (Figure 6 a). To investigate the changes in activity and diversity at single-cell resolution, the combination of BONCAT and FACS was applied to hot spring biofilms, supplied with substrates stimulating either chemoorganotrophic or chemolithotrophic microbial activity. To evaluate the response of microorganisms to different sources of reducing equivalents, a series of incubation experiments were performed with sodium acetate, pyruvate, thiosulfate, potassium tetrathionate or thiocyanate. Incubation experiments with biofilms collected from the same sources in spring 2021 showed that the activity of certain microbial groups decreased when incubated with acetate, while the addition of pyruvate and glucose resulted in similar activity patterns for all investigated taxonomic groups. Similarly, the addition of thiosulfate resulted in a significant increase in activity for all taxonomic groups studied. Therefore, based on the results of the previous activity screening, acetate and pyruvate were selected as reducing equivalents to assess chemoorganotrophic activity, while other sulfur compounds were selected along with thiosulfate to determine chemolithotrophic substrate preferences of biofilms collected in autumn 2021. The combination of BONCAT and FACS was performed as presented in Figure 7.

3.4.1. Incubations of biofilms

For each incubation setup (Figure 7), 0.25 g wet weight of biofilm material was suspended in 10 mL of sterile filtered (0.2 μm pore size) corresponding geothermal water in glass vials and incubated for 48 h at source temperature.
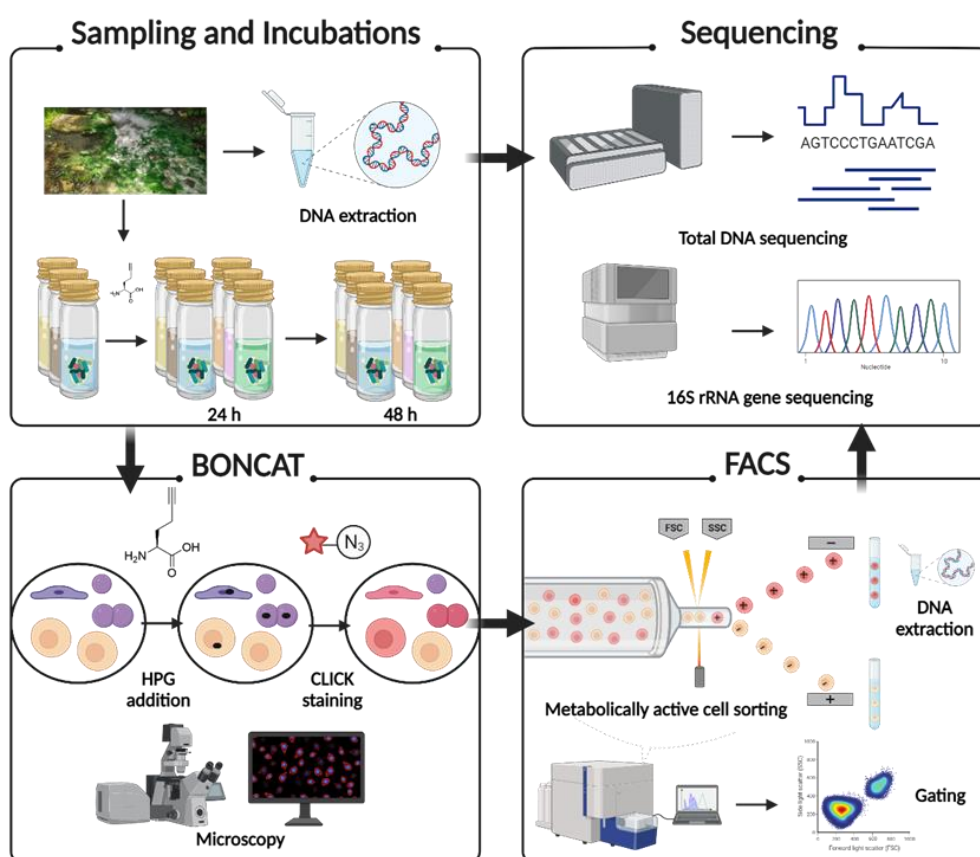
Figure 7. A schematic overview of the experimental workflow to characterize hot spring biofilms collected in autumn 2021: microbial community composition, metabolic capacity, and functionality of initial biofilms were characterized by 16S rRNA gene amplicon sequencing and metagenomic sequencing; biofilms were incubated with the l-methionine analogue HPG under various substrate amendments in the dark for 24 h and 48 h, respectively; the BONCAT method was used to label and visualize active cells; the FACS method was used to sort the active biomass in different substrates, and the sorted samples were characterized by 16S rRNA gene amplicon sequencing.

As described in 3.3.2., HPG was added to the sample at a final concentration of 50 μmol L^{-1} along with various substrates to monitor microbial activity. Substrate solutions were prepared

at a final concentration of 1 mmol L^{-1} by dissolving the appropriate weight of substrate in autoclaved MQ water. In addition to the substrate amended incubations, a set of control incubations was conducted without the addition of any substrates, with only HPG added to assess native microbial activity. All incubations were performed in the dark and at source temperature. After 24 and 48 h, biofilms were removed from the incubator, 2 mL of 0.5 % Tween 20 (Promega) was added (Reichart et al., 2020) and samples were macerated, vortexed at maximum speed for 5 min and sonicated for 1 min (Pin et al., 2021). To separate the particles from the cell fractions, samples were centrifuged at 500 × g for 5 min (Reichart et al., 2020). The supernatant was then filtered using a 5 µm syringe filter to remove filamentous Cyanobacteria and ease microscopy. For sample fixation, cells were pelleted by centrifugation (8000 × g for 10 min), washed twice in sterile PBS, and fixed using a 50 % (v/v) ethanol/PBS solution for 10 min at room temperature (Sakoula et al., 2021). The fixed biomass was washed once with PBS and stored at -20 °C until CLICK labelling was performed.

3.4.2. BONCAT procedure

To select adequate dyes for CLICK reaction and FACS, biofilm samples were first checked for autofluorescence by lambda scanning on the Leica TCS Sp8x confocal laser microscope (CLSM; Leica Microsystems, Netherlands) equipped with a 405 nm UV diode. After staining with DAPI, series of fluorescence images were acquired at different wavelengths (channels) to create a spectral scan of the biofilm samples. For scanning, the microscope laser was used over the entire spectrum (415-780 nm) with a bandwidth of 40 nm, encompassing a total of 20 steps, and the intensity of the emitted light was measured sequentially. For each sample and channel, 3 spectra were recorded, and the data were used to generate a plot of fluorescence intensity versus wavelength for each pixel or region of interest in the samples.

Prior to CLICK labelling, samples were subjected to a series of ethanol dehydrations, washed with PBS, and pelleted by centrifugation for 3 min at 3000 x g (Sakoula et al., 2022). CLICK reaction was performed in plastic microcentrifuge tubes (1.5 ml) at a final volume of 250 µl following the protocols (Sakoula et al., 2022; Hatzenpichler and Orphan, 2015). The biomass was resuspended in 221 µl sterile PBS and mixed with 12.5 µl each of freshly prepared 100 mM sodium ascorbate solution and 100 mM aminoguanidine hydrochloride solution. After 3 min of incubation in the dark, dye premix containing 1.25 µl of a 20 mM CuSO$_4$ solution, 1.25 µl of a 100 mM THPTA, and 0.3 µl of a 5 mM Cy3- or Cy5- azide dye was added to the reaction tubes and then incubated for 60 min, at room temperature in the dark. CLICK reaction was terminated

by centrifuging the samples at 3000 x g for 6 min, the cell pellets were washed thoroughly three times with sterile PBS to eliminate unbound dye and either stored at –80 °C in Gly-TE buffer (10 mM Tris-HCl, 1 mM EDTA pH 8.0, 5 % v/v glycerol) or processed directly. After staining with DAPI, BONCAT positive cells were visualised using a fluorescence microscope with Thunder Imaging System (model DMi8; Leica, Germany) and manually counted to determine cell density and volume required for FACS (1) on a flow cytometer (BD FACSMelody, New Jersey, United States).

$$TCC/BCC = \frac{\pi\, r^2 \times K \times N\,(dapi/boncat)}{A \times N\,(grid) \times V\,(sample)} \qquad V\,(FACS) = \frac{WCC}{TCC} \qquad (1)$$

TCC/BCC – total/boncat cell count, cell mL^{-1}

r – filtration column radius, 9500 µm

K – dilution factor, 1.00

N (dapi/boncat) – number of DAPI/Boncat positive cells

A – grid area, 15133.65 $µm^2$

N (grids) – number of counted grids for each sample, 10

V (sample) - Volume of filtered sample, 0.01 mL

V (FACS) – volume of sample for optimal cell sorting, mL

WCC – wanted cell counts, 5×10^5 cell mL^{-1}

3.4.3. FACS procedure

Sorting of active biomass was performed according to the manufacturer's protocol (URL 4). Based on the initial cell density determined for FACS (1), samples were diluted with sterile PBS to ensure a final event rate of <10.000 events s^{-1}. The signal from PBS was recorded to remove potentially generated background noise. Control incubations with HPG-only addition, particularly labelled with Cy3-azide dye, as well as DAPI and Cy5-azide dye were used to determine a gating strategy to remove artefacts and exclude populations with off-target labelling or passive dye accumulation. Gating was set for double positive DAPI-BONCAT cells, considering thresholds for forward signal scatter (FSC, approximate to cell size) and side signal scatter (SSC, approximate to granularity). Sorting was performed in purity mode, processing 80 % of the events for an optimal flow rate, with sample agitation at 100 rpm. For efficient DNA extraction and 16S rRNA sequencing, 50 000 events per sample were sorted. Examples of sorting reports and gating setup can be found in **Appendix 1**.

3.4.4. 16S rRNA amplicon sequencing and analysis of sorted samples

Amplicon sequencing of the 16S rRNA gene from the sorted samples was performed as described in 3.2. The hypervariable V4 region was amplified, samples were barcoded, purified, normalized, and prepared for sequencing as previously described (Pjevac et al., 2021). Sequencing was conducted in pair-end mode using the Illumina MiSeq platform (Illumina, Inc., San Diego, California). Raw sequencing data underwent amplicon pool extraction with standard FASTQ workflow parameters (BaseSpace, Illumina). PhiX contamination was removed using BBDuk from the BBtools package. Demultiplexing was performed using the Python package "demultiplex". ASVs were inferred in pooled mode using the DADA2 R package version 1.20.0 (R 4.1.1) and further classified using the SILVA reference database (SILVA release 138) with the SINA classifier, version 1.6.1. Statistical analyses were performed in the R environment (v. 4. 2. 0) using Bioconductor v 3.15 packages, including TreeSummarizedExperiment (Huang et al., 2021), phyloseq (McMurdie et al., 2013), mia (Ernst et al., 2022), and microViz (Barnett et al., 2021). Results were visualized using the ggplot2 package (Wickham, 2009). This analysis allowed comparison between sorted and initial samples, enabling the determination of changes in biofilm prokaryotic community abundance, diversity, and activity in response to addition of mentioned substrates.

3.4.5. Metagenome sequencing and analysis

Total DNA sequencing was performed on the initial samples before the incubation experiment. DNA preparation for sequencing followed the protocol described in the Ligation Sequencing Kit (SQK-LSK112, Oxford Nanopore Technologies). To obtain long-read data for metagenomic analysis, samples were sequenced using the PromethION P24 platform with MinKNOW operating software (v. 21.10.8) on two different flow cell types, R10.3 and R10.4 (all versions specified by Oxford Nanopore Technologies, United Kingdom). Long-reads, although more error-prone, enable the assembly of long repeat regions and more complete genomes (Buttler and Drown, 2023).

For the R10.4 pore, long-reads were basecalled with Guppy (v. 5.0.17) using Super Accuracy Mode and assembled using flye (v. 2.9-b1768) with "–nano-hq" option (Kolmogorov et al. 2019). To ensure the extensive amounts and lengths of precise data and more complete genomes, the assembly underwent three rounds of polishing with minimap2 (v. 2.17, Li, 2018) and racon (v. 1.4.3, Vaser et al., 2017), followed by two rounds of polishing with Medaka

models (v. 1.4.4, URL 5). For the R10.3 specific part, long-reads were basecalled with bonito (v. 0.3.5) and assembled using flye (v. 2.9-b1768) with "–nano-hq" option (Kolmogorov et al. 2019). The assembly was polished three times with minimap2 (v. 2.17, Li, 2018) and racon (v. 1.4.3, Vaser et al., 2017) models, and finally, once with Illumina short reads (NovaSeq 6000, Eurofins Genomics Europe Sequencing GmbH, Germany). The R10.3+LSK112 data were polished with Illumina short reads because this data version has been discontinued, and Medaka models were never released for it.

After the reads were mapped to the assemblies, the read mappings were converted using samtools (v. 1.12, Li et al., 2009) for the binning process with metabat2 (v. 2.15, Kang et al. 2019). Contigs labelled as circular by the assembler were extracted as independent bins before the automatic binning process. Classification of reads was performed using kraken (v. 2.1.2). All generated metagenomes were co-assembled and binned into combined metagenome-assembled genomes (MAGs). The quality of the reconstructed MAGs was assessed using QUAST (v. 5.0.2, Gurevich et al., 2013) and CheckM (v. 1.1.1, Parks et al., 2015), followed by taxonomic classification using GTDBtk (v. 1.5.1, Chaumeil et al. 2020).

Analysis of MAGs was performed using a modified script (URL 6) with the software METABOLIC, a toolkit for profiling metabolic and biogeochemical traits and functional networks in microbial communities based on microbial genomes as described in (Zhou et al., 2022). Prediction of genes on good quality MAGs (completeness > 50 %, contamination <10 %) and contigs longer than 1 kbp from the entire metagenomic assembly was performed using Prodigal (Hyatt et al., 2010). To generate a broad range of HMM (Hidden Markov model) profiles of metabolic genes, three sets of HMM-based databases were integrated (Zhou et al., 2022): KOfam containing HMM profiles for KEGG/KO with predefined score thresholds (release July 2019, Aramaki et al., 2019), TIGRfam (release 15.0, Selengut et al., 2007) and Pfam (release 32.0, Finn et al.,2014). Methods for manual curation of these HMM databases are described in (Zhou et al., 2022). HMM databases were used as a reference for hmmsearch (Finn et al., 2011) to find protein hits of input genomes. The KEGG database was used to assign pathways, brite, and modules of KOs (Kanehisa et al., 2023). For carbohydrate-active enzymes (CAZymes), dbCAN2 was used to annotate proteins with default settings (Zhang et al., 2018). All statistical analyses and visualization were done in the R environment (version 4. 2. 0.) using the packages phyloseq (McMurdie and Holmes, 2013), vegan (Oksanen et al., 2020), dplyr (Wickham et al., 2023) and ggplot2 (Wickham, 2016).

4. RESULTS

Parts of chapter 4 (4.1. - 4.3.) are published in (Kostešić et al., 2023).

4.1. Environmental characteristics and description of the sampling sites

The sampled geothermal springs and wells (n = 12) differed significantly in their geochemistry (Tables 4 - 7). Among them, the Topusko well (TEB) and the Bizovac well (B) had the highest temperatures, reaching 64.8 °C each, while the Đakovačka Breznica well (DB) had the lowest recorded temperature, 12.9 °C.

Table 4. Physicochemical properties of spring water measured *in situ* or collected directly above biofilm samples in autumn 2019.

Autumn 2019						
Samples	**K**	**DB**	**TOP**	**TEB**	**T**	**VK**
pH	7	7.2	6.82	6.76	6.99	7.16
T °C	41.8	12.9	46.2	64.8	32.1	40.7
DIC mg/L	60.8	114	52	52.9	74.1	101
DOC mg/L	0.12	4.4	0.05	0.13	0.13	0.13
TN mg/L	<1	3	<1	<1	<1	3
EC mS/cm	509	839	602	627	533	1160
Ca^{2+} mg/L	52.4	114.7	78.9	83.7	66.5	123.6
Cl^- mg/L	1.7	3.2	9.1	10.6	1.5	52
K^+ mg/L	2.6	1	10.6	11.8	2	11.9
Mg^{2+} mg/L	31.9	33.4	18.4	19.3	38.2	26.6
Na^+ mg/L	8.7	27	16.9	18.7	7.5	97.7
HCO_3^- mg/L	305	580	265	270	378	510
NH_4^+ mg/L	0.1	2.2	0.3	0.3	0.2	0.8
NO_3^- mg/L	<0.1	4	<0.1	<0.1	<0.1	4.6
SO_4^{2-} mg/L	35	11.1	90.7	104.9	31.5	153.8
O_2 mg/L	0.14	0.4	1.7	0	0.08	0
SiO_2 mg/L	25.2	30.7	35.2	43.5	20.9	51.4
H_2S mg/L	0.08	15.8	0.8	1.2	0.48	1.2

Considering Table 1 (Novak, 1968), DB well can be classified as cold water, Jana (J), Šemnica (S) and Tuhelj (T) springs as hypothermic waters, and all other sampled sites (B, VK, V, TEB, TOP, Z, K, D) as hyperthermic waters. The pH values of the sampled water spanned from 6.3 to 8.3, denoting a range from weakly acidic to mildly alkaline. An inversely proportional relationship was observed between the pH and the concentration of dissolved gasses (CO_2, NH_3, H_2S), with higher gas concentration associated with lower pH and vice versa. The Bizovac well (B) sampled in spring 2021 had the highest concentrations of ammonia (18.4 mg L^{-1}) and total nitrogen (TN, 16 mg L^{-1}), while the DB well collected in spring 2020 had the highest H_2S concentration (18.8 mg L^{-1}). Concentrations of SO_4^{2-} ranged from 9.3 to 196.9 mg L^{-1}.

Table 5. Physicochemical properties of spring water measured in situ or collected directly above biofilm samples in spring 2019.

Spring 2020											
Samples	**K**	**DB**	**TOP**	**T**	**VK**	**V**	**D**	**Z**	**S**	**J**	**B**
pH	6.99	7.21	6.72	6.99	7.14	6.4	6.77	8.02	7.18	7.17	7.45
T °C	42.2	13.9	46.5	32.3	40	59	45.8	45	28.7	24.3	64
DIC mg/L	54.9	105.9	52	70.6	66.7	68.6	64.7	98	64.7	70.6	186.3
DOC mg/L	0.11	0.11	0.11	0.11	0.7	0.07	0.23	1.88	0.13	0.14	3.77
TN mg/L	<1	<1	<1	<1	0	0	<1	6.4	<1	<1	6.5
EC mS/cm	508	840	600	603	1197	1161	591	840	570	550	4860
Ca^{2+} mg/L	50.9	114.7	78.3	64.9	123.7	121.3	75.6	4.1	65.3	64.5	32.7
Cl^- mg/L	2.6	8.6	16.9	2.1	109	105.9	2.1	3.9	2.5	2.7	1360.7
K^+ mg/L	2.7	0.3	10.6	2	12.2	12	3.4	3.3	1.6	1.7	86.5
Mg^{2+} mg/L	30.9	30.3	18.1	37.1	26.2	25.7	24.5	0.5	34.9	33.1	13.3
Na^+ mg/L	8.7	25.2	16.7	7	94.4	92.4	13.2	193.2	3.8	3.2	1125.7
HCO_3^- mg/L	280	540	265	360	340	350	330	500	330	360	950
NH_4^+ mg/L	0.13	0.72	0.35	0.22	0.38	0.92	0.38	9.03	<0.01	0.02	8.82
NO_3^- mg/L	1	<0.1	<0.1	1.4	1.5	0.1	<0.1	<0.1	0.3	1	<0.1
SO_4^{2-} mg/L	36.9	18.3	104.1	32.5	196.9	179.2	52.5	24.3	44	9.5	10.3
O_2 mg/L	0.01	0.8	0.5	0.07	1.2	0	0.08	0.2	2.8	6.3	0
SiO_2 mg/L	23.5	31.9	37	19.8	50.8	53	40	30.5	15.6	13.6	65.3
H_2S mg/L	0.08	18.8	0.8	0.48	1.2	12	0.01	2.4	<0.01	<0.01	1.8

Ammonia and sulfate content can be attributed to natural processes such as decomposition of organic matter within quaternary deposits infiltrated by geothermal water, dissolution of hydrogen sulfide and ammonia gas in the subsurface, and weathering of sulfides (Marković et al., 2012). Considering Table 1 (Novak, 1968), both DB and B wells, along with Topusko well (TEB), Varaždin spring (VK), Varaždin well (V), and Zelina well (Z), can be classified as sulfur sources. The highest O_2 concentration, 6.8 mg L^{-1}, was observed in Jana spring (J) collected in autumn 2020.

Table 6. Physicochemical properties of spring water measured in situ or collected directly above biofilm samples in autumn 2020.

Autumn 2020								
Samples	**DB**	**TEB**	**T**	**VK**	**V**	**Z**	**J**	**K**
pH	7.36	6.74	6.97	7.1	6.27	8.28	7.35	7.01
T °C	13.23	46.5	32.4	41	56.7	39.5	23.65	42
DIC mg/L	105.5	55.2	78.2	100	100.5	115.5	80.1	65.2
DOC mg/L	0.66	0.6	0.11	0.7	0.72	1.3	0.3	0.33
TN mg/L	1.9	<1	<1	0	<1	5.8	<1	<1
EC mS/cm	604	603	604	1190	1172	523	500	512
Ca^{2+} mg/L	114.1	84.2	66.5	127	125.3	4.3	65.6	52.6
Cl^- mg/L	10.7	18.3	1.3	105	109.7	2.9	1.7	1.6
K^+ mg/L	0.9	10.7	1.9	12	12.2	3.2	1.6	2.6
Mg^{2+} mg/L	33.1	18.5	38.2	27.1	26.8	0.6	33.3	31.9
Na^+ mg/L	27	17.9	7	97.9	95.9	202.5	2.9	8.5
HCO_3^- mg/L	512	276	378	370	380	556	380	322
NH_4^+ mg/L	2.1	0.29	0.2	0.3	0.77	7.66	0.01	0.11
NO_3^- mg/L	1.9	0.7	1.3	1.5	1.9	1.3	1.6	0.7
SO_4^{2-} mg/L	17.3	97.7	31.2	180.3	167.4	21.9	9.3	35
O_2 mg/L	0.72	1	0.02	1.2	0	5.19	6.8	0.02
SiO_2 mg/L	30.9	36.3	20.3	103	105.3	31.2	13.4	23.4

Notably, in addition to the highest temperature, TN and ammonia concentration, the Bizovac well had the highest anion concentration (2580 mg L^{-1} HCO_3^-, 1360.7 mg L^{-1} Cl^-, 7.8 mg L^{-1}

NO_3^-), as well as the highest DIC and DOC concentrations among all sampled sources (Tables 4 – 7). In general, DIC ranged from 52 to 390 mg L^{-1}, DOC from 0.05 to 86 mg L^{-1}, and essential cation contents were in the following ranges: Ca^{2+} from 4.1 to 127, Mg^{2+} from 0.5 to 38.2, K^+ from 0.3 to 86.5 and Na^+ from 2.9 to 1826.9 mg L^{-1} (Tables 4 – 7).

Table 7. Physicochemical properties of spring water measured in situ or collected directly above biofilm samples from the Bizovac well and the Tuhelj spring, on which incubation experiments were conducted.

Samples	Spring 2021		Autumn 2021	
	T	B	T	B
pH	6.99	7.6	6.98	7.75
T °C	33	64	32.3	64.8
DIC mg/L	75.1	390	76.2	323.3
DOC mg/L	0.14	35.5	0.12	86
TN mg/L	<1	16	<1	12.4
EC mS/cm	602	4830	569	8913
Ca^{2+} mg/L	65.5	7.5	66.5	7.7
Cl^- mg/L	1.7	688.1	1.4	1270.9
K^+ mg/L	1.9	13.5	2	11.8
Mg^{2+} mg/L	32.9	1.4	38.2	2.2
Na^+ mg/L	6.7	1147.4	7.3	1826.9
HCO_3^- mg/L	380	1950	378	2580
NH_4^+ mg/L	0.11	18.4	0.2	15.8
NO_3^- mg/L	<0.1	7.8	0.7	4.9
SO_4^{2-} mg/L	30.8	20.4	31.4	11.2
O_2 mg/L	0	0	0.05	2.16
SiO_2 mg/L	21.8	69.3	20.6	68
H_2S mg/L	0.16	1.8	0.48	2.1

In the context of seasonality, the sources showed slight variations in their geochemistry, which can be related to the influence of hydrological conditions and the amount of water pumped from deeper parts of the aquifer (Tables 4 - 7).

4.2. Taxonomic composition and diversity of biofilm prokaryotic communities through seasons

Based on 16S rRNA gene amplicon sequencing, microorganisms inhabiting 61 biofilm samples collected over three seasonal and two additional samplings were clustered into 4496 ASVs.
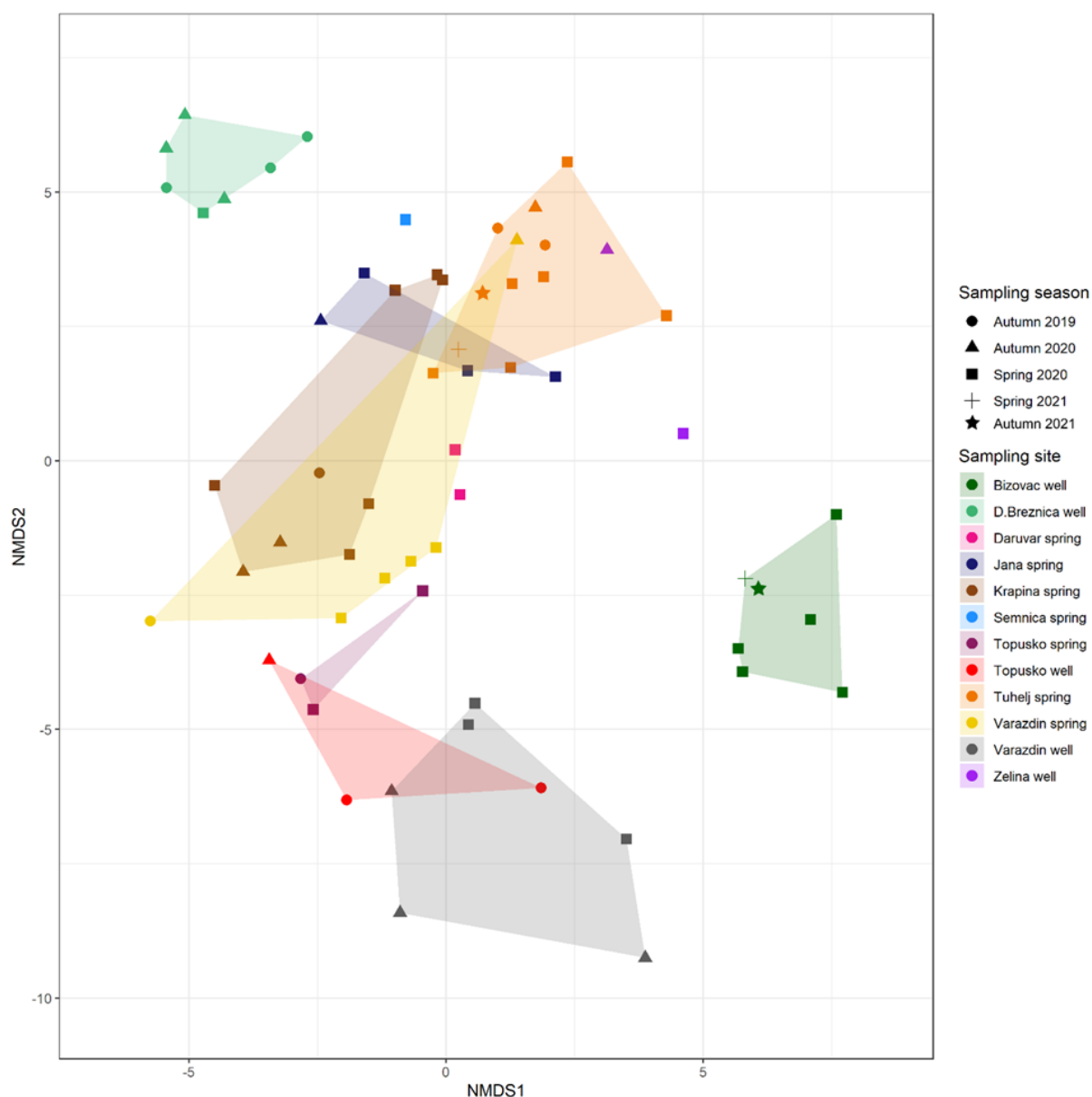

Figure 8. NMDS (Bray-Curtis dissimilarity) clustering of hot spring biofilm microbial communities. Samples are colored by sampling location, while shapes represent the sampling seasons.

The NMDS analysis (Bray-Curtis dissimilarity) showed that the microbial community of biofilms was predominantly clustered according to their spring or well of origin (Figure 8). This result was further verified by PERMANOVA, which confirmed the spring source as a significant factor influencing biofilm community composition ($R^2 = 0.42$, $p < 0.001$). Among the measured environmental parameters, temperature ($R^2 = 0.8$, $p < 0.001$) and electric conductivity (correlated with concentrations of sodium, potassium, and chlorine ions) ($R^2 = 0.5$, $p < 0.001$) best explained community structure (Table 8). Season of sampling ($R^2 = 0.06$, $p = 0.08$) and biofilm sample color ($R^2 = 0.08$, $p = 0.89$) did not significantly correlate with observed community structure at the ASV level.

Table 8. Tested environmental parameters using NMDS based on Bray-Curtis dissimilarity distances.

Parameters	Distance	r2	p-value
pH	Bray-Curtis	0.396426	0.001
T °C	**Bray-Curtis**	**0.846393**	**0.001**
DIC (mg/L)	Bray-Curtis	0.268837	0.001
DOC (mg/L)	Bray-Curtis	0.107403	0.055
EC (mS/cm)	Bray-Curtis	0.477058	0.001
Ca^{2+} (mg/L)	Bray-Curtis	0.359249	0.001
Cl^- (mg/L)	Bray-Curtis	0.474361	0.001
K^+ (mg/L)	Bray-Curtis	0.511882	0.001
Mg^{2+} (mg/L)	Bray-Curtis	0.380571	0.001
Na^+ (mg/L)	Bray-Curtis	0.498542	0.001
NH_4^+ (mg/L)	Bray-Curtis	0.404466	0.001
NO_3^- (mg/L)	Bray-Curtis	0.276962	0.001
O_2 (mg/L)	Bray-Curtis	0.059064	0.189
SiO_2 (mg/L)	Bray-Curtis	0.568962	0.001
SO_4^{2-} (mg/L)	Bray-Curtis	0.503213	0.001
H_2S (mg/L)	Bray-Curtis	0.074191	0.123

Overall, biofilm communities were highly diverse, with ASVs affiliating with 52 bacterial and 10 archaeal phyla. Almost all analyzed biofilms were dominated by Cyanobacteria phylum (Figure 9). In addition to Cyanobacteria, phyla Pseudomonadota, Chloroflexota and

Bacteroidota also had high relative abundances in all biofilm samples (Figure 9). The relative abundance of Archaea was comparatively low in all samples (7 ± 3 % on average). Unlike most samples, biofilms from the Bizovac well were not dominated by the Cyanobacteria phylum. Instead, phyla Pseudomonadota, Chloroflexota, Deinococcota, and Bacteroidota accounted for large fractions of the community composition in the biofilms from this site (Figure 9). At the family and genus level, prokaryotic community composition was highly site-specific (Figure 10 and Figure 11).
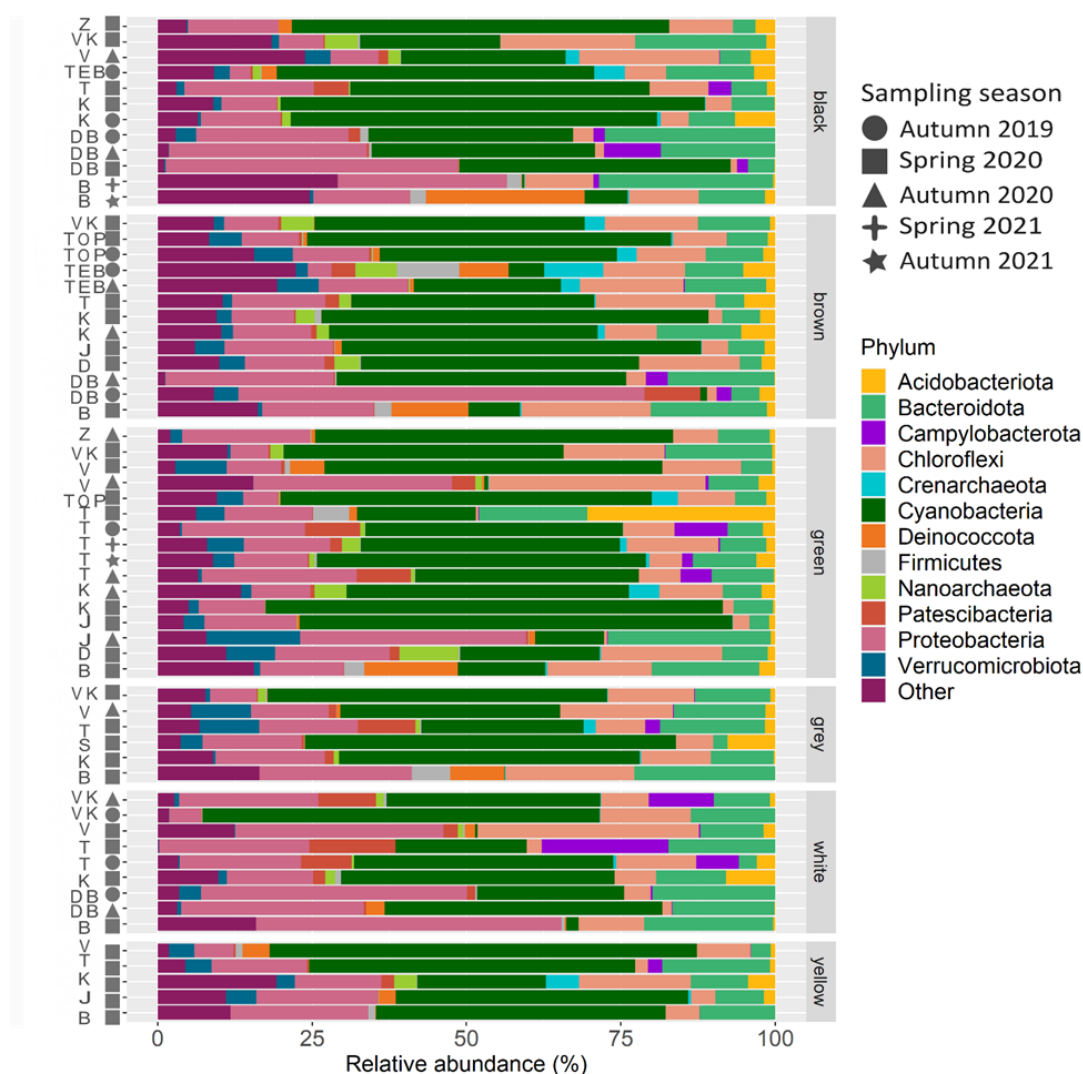
Figure 9. Microbial community composition clustered at phylum level. Phyla where cumulative relative abundance of ASVs exceeded 5 % in at least one biofilm sample are displayed, while the residual community is clustered as "Other." Samples are grouped based on the color of biofilm samples. Sampling locations are indicated by the sampling site abbreviations, while shapes represent the sampling seasons.

Figure 10. Bubble plot of the average relative abundance (circle size) of 30 most abundant families, colored according to their phylum affiliation. Samples are grouped based on the color of biofilm samples. Sampling locations are indicated by the sampling site abbreviation, while shapes represent the sampling seasons.

Figure 11. Microbial community composition at the genus level. Bubble plot of the average relative abundance (circle size) of 30 most abundant genera, colored according to their phylum affiliation. Samples are grouped based on the color of biofilm samples. Sampling locations are indicated by the sampling site abbreviation, while shapes represent the sampling seasons.

Leptolyngbyaceae and *Nostocaceae* were the relatively most abundant cyanobacterial families in all biofilms, apart from samples from the sulfidic cold spring DB, where *Trychonema*-related ASV (family *Phormidiaceae,* Figure 10 and Figure 11) dominated the cyanobacterial community. In the samples from Bizovac well, Cyanobacteria were not only less abundant overall, but also distinctly different from the cyanobacterial communities of the other biofilms, with ASVs predominantly associated with unicellular colony-forming members of the genus

Gloeocapsa (family *Chroococcidiopsaceae*; Figure 10 and Figure 11). In general, Bizovac biofilms exhibited high diversity, with only a few highly abundant individual genera and a distinct community composition compared to samples from other geothermal sites (Figures 9 - 11). Among the thiotrophic members of the community, unicellular gammaproteobacterial *Halothiobacillaceae* family (genus *Thiofaba*) dominated biofilms from the Bizovac well in all three sampling seasons. Additionally, filamentous gammaproteobacterial populations (family *Thiotrichaceae*, genus *Thiothrix*, Figure 10 and Figure 11) and ASVs related to the genus *Sulfurovum* (phylum Campylobacterota, Figure 10 and Figure 11) were detected in the samples from all other sites.

The initial community of freshly collected (spring 2021) biofilms from the Bizovac well used for the activity screening experiments was again dominated by the phyla Bacteroidota (28.1 %), Pseudomonadota (27.3 %), and Chloroflexota (11.1 %), while the biofilms from the Tuhelj spring were again dominated by the phylum Cyanobacteria (41.5 %), but the phyla Pseudomonadota (13.8 %) and Chloroflexota (14.7 %) were also relatively abundant (Figure 9).

The initial community of freshly collected (autumn 2021) biofilms from the Bizovac well used for the activity experiment at single-cell resolution was dominated by phyla Deinococcota (25.7 %) and Pseudomonadota (15.7 %), Chloroflexota (11.3 %) and Bacteroidota (10.7 %). Biofilms from the Tuhelj spring were again dominated by phylum Cyanobacteria (53.3 %), but phyla Pseudomonadota (11.9 %), Bacteroidota (10.3 %) and Chloroflexota (5.4 %) were also relatively abundant (Figure 9).

4.3. Activity patterns of Bizovac and Tuhelj biofilms detected with BONCAT-CARD-FISH method

By combining sequencing methods with quantitative analyses of BONCAT and CARD-FISH, a detailed description of community structure is provided and the taxonomic identity of active cells under different incubation conditions are determined.

The microbial communities of the freshly collected biofilms in spring 2021 were characterized by 16S rRNA gene amplicon sequencing and confirmed compositional similarity to previously analyzed biofilm samples collected in 2019 and 2020 from the respective source environments (Figure 9 - 12).
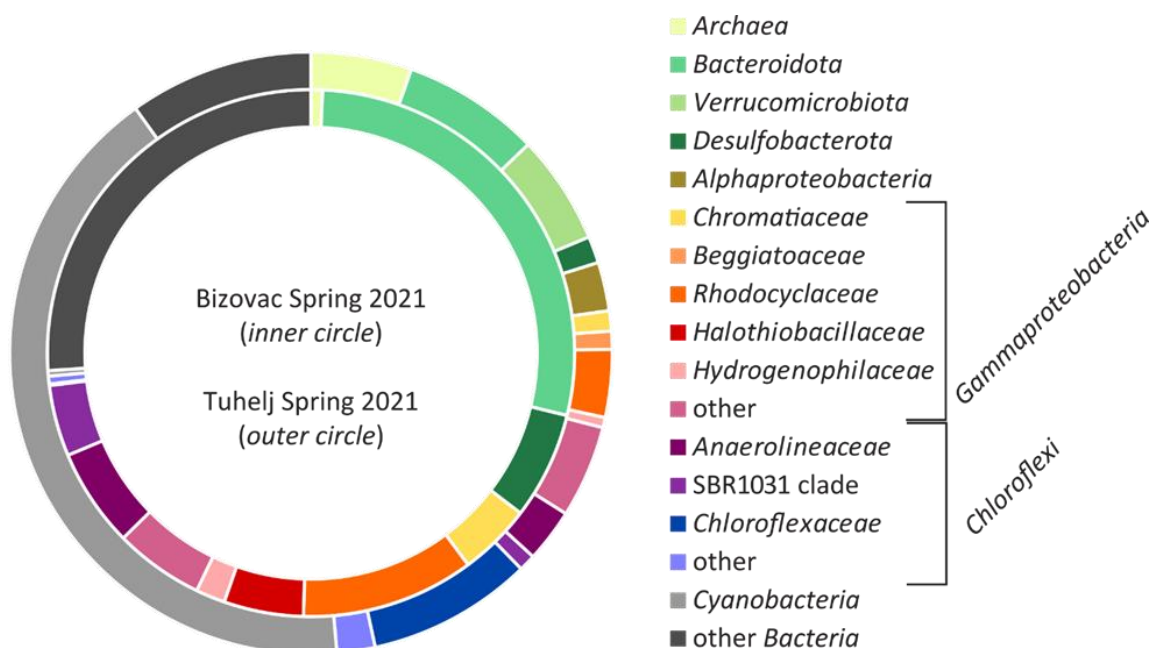
Figure 12. Family-level microbial community composition of Bizovac and Tuhelj biofilms, collected in spring 2021, on which incubation experiments were performed.

As expected, the active fraction of the bacterial biofilm community (defined as a CARD-FISH signal with the probe mixture EUBI-III, targeting most bacteria, and a positive BONCAT signal) was lowest when the biofilm samples were incubated in the dark without the substrate addition (i.e., HPG-only control). The active fraction of cells in the incubations without substrate addition was very similar in both biofilm samples: after 24 h of incubation, 33 % and 35 % of EUBI-III positive cells displayed a BONCAT signal in Bizovac and Tuhelj biofilm incubations, respectively (Figure 13, Table 9). Moreover, the fraction of active cells in the HPG-only controls did not change significantly after 48 h of incubation in either biofilm (Figure 13, Table 9). The result indicated that the native energy and substrate sources were nearly depleted or that all microorganisms capable of utilizing these under the applied experimental conditions became active within 48 h. The 48 h incubation time point was therefore chosen to further investigate the effects of different substrate additions on the fraction and identity of active biofilm populations. All results of BONCAT-CARD-FISH method can be found in **Appendix 2**.
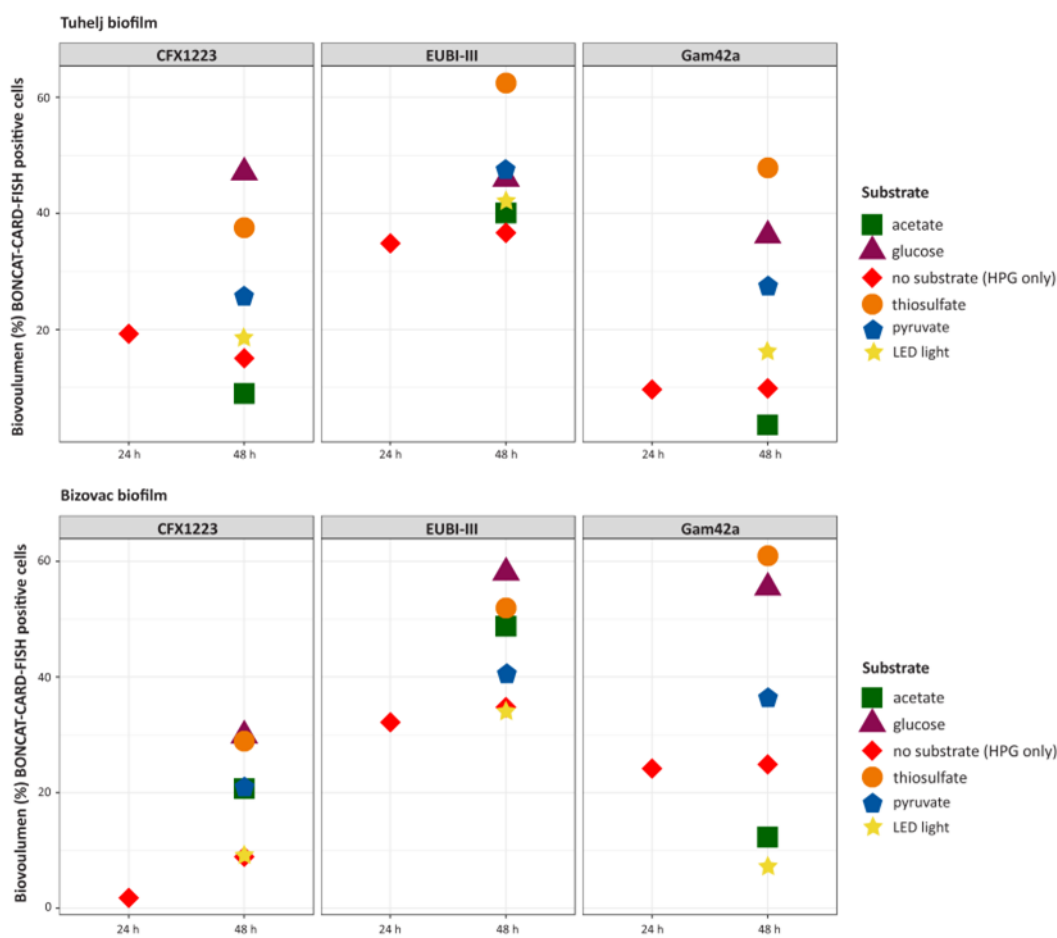
Figure 13. Biovolume of the active fraction (i.e., displaying BONCAT signal) of cells displaying a positive CARD-FISH signal with probes specifically targeting the Chloroflexota phylum (CFX1223), the Gammaproteobacteria class (Gam42a), or all bacteria (EUBI-III mix) after 24 h without substrate amendment (HPG-only), and 48 h without substrate amendment (HPG-only) and in incubations amended with glucose, pyruvate, acetate or thiosulfate and in the presence of light.

The addition of glucose, pyruvate, acetate, and thiosulfate resulted in a significant increase in the active bacterial fraction (defined by a positive signal with the EUBI-III mix probe and a positive BONCAT signal) after 48 h of incubation (Figure 13). The glucose amendment resulted in the highest total biovolume of active cells in the Bizovac biofilms (58 %). The thiosulfate amendment had the greatest effect on the total active cell fraction in the Tuhelj biofilms (62.5 %), while the activity stimulated by acetate, pyruvate and glucose additions was significantly lower (Figure 13, Table 9). Moreover, the activity stimulated by acetate and glucose supplements in the Tuhelj biofilms was lower than the activity stimulated by the same substrates in the Bizovac biofilms (Figure 13, Table 9).

Table 9. Biovolume (based on *daime* image analysis) of CARD-FISH-BONCAT positive cells in biofilm incubation experiments.

Biofilm	Substrate	Time point	Probe	Histogram stretching	Segmentation method	% biovolume	% congruency
Tuhelj	acetate	48	Gamm42a	50-200	Custom:5-255	3.6	50
Tuhelj	glucose	48	Gamm42a	40-200	Custom:30-255	36.2	31
Tuhelj	pyruvate	48	Gamm42a	30-150	Custom:60-255	28.5	41
Tuhelj	thiosulfate	48	Gamm42a	30-200	Custom:90-255	47.9	56
Tuhelj	HPG+Dark	24	Gamm42a	20-150	Custom:5-255	9.7	37
Tuhelj	HPG+Dark	48	Gamm42a	20-150	Isodata	9.9	46
Tuhelj	HPG+Light	48	Gamm42a	50-200	Custom:5-255	16.4	24
Bizovac	acetate	48	Gamm42a	50-200	Custom:5-255	12.3	42
Bizovac	glucose	48	Gamm42a	20-150	Isodata	55.5	65
Bizovac	pyruvate	48	Gamm42a	20-150	Custom:5-255	36.9	69
Bizovac	thiosulfate	48	Gamm42a	20-150	Custom:5-255	61	71.5
Bizovac	HPG+Dark	24	Gamm42a	20-150	Custom:5-255	24.2	88
Bizovac	HPG+Dark	48	Gamm42a	30-150	Custom:20-150	24.9	48
Bizovac	HPG+Light	48	Gamm42a	20-150	Isodata	7.1	74
Tuhelj	acetate	48	CFX1223	30-150	Custom:60-255	9	57
Tuhelj	glucose	48	CFX1223	70-255	Custom:90-255	47.1	46
Tuhelj	pyruvate	48	CFX1223	60-200	Custom:5-255	25.5	41
Tuhelj	thiosulfate	48	CFX1223	30-150	Custom:5-255	37.6	29
Tuhelj	HPG+Dark	24	CFX1223	50-200	Custom:30-255	19.3	32
Tuhelj	HPG+Dark	48	CFX1223	0-10	Custom:30-255	15.1	84
Tuhelj	HPG+Light	48	CFX1223	50-200	Custom:5-255	18.2	52
Bizovac	acetate	48	CFX1223	20-150	Isodata	20.7	96
Bizovac	glucose	48	CFX1223	1-150	Isodata	29.9	95
Bizovac	pyruvate	48	CFX1223	20-150	Custom:5-255	20.1	44
Bizovac	thiosulfate	48	CFX1223	20-150	Custom:5-255	28.9	40
Bizovac	HPG+Dark	24	CFX1223	20-255	Isodata	1.8	73
Bizovac	HPG+Dark	48	CFX1223	20-150	Custom:5-255	8.9	11
Bizovac	HPG+Light	48	CFX1223	20-150	Custom:5-255	9.5	38
Tuhelj	acetate	48	EUBI-III	70-200	Custom:5-255	40.1	33
Tuhelj	glucose	48	EUBI-III	20-150	Isodata	46	95
Tuhelj	pyruvate	48	EUBI-III	30-200	Custom:5-255	48.3	29
Tuhelj	thiosulfate	48	EUBI-III	40-200	Custom:5-255	62.5	43
Tuhelj	HPG+Dark	24	EUBI-III	30-200	Custom:5-255	34.9	48
Tuhelj	HPG+Dark	48	EUBI-III	20-150	Custom:30-255	36.7	23
Tuhelj	HPG+Light	48	EUBI-III	100-200	Custom:5-255	42	19
Bizovac	acetate	48	EUBI-III	20-150	Isodata	48.8	60
Bizovac	glucose	48	EUBI-III	50-200	Isodata	58.1	53
Bizovac	pyruvate	48	EUBI-III	20-150	Isodata	40.5	80
Bizovac	thiosulfate	48	EUBI-III	20-190	Isodata	52	99
Bizovac	HPG+Dark	24	EUBI-III	30-150	Custom:30-255	33.2	40
Bizovac	HPG+Dark	48	EUBI-III	20-150	Isodata	35.3	94
Bizovac	HPG+Light	48	EUBI-III	20-190	Isodata	34.8	97

In contrast, the activity in Tuhelj biofilms stimulated by pyruvate amendment (Figure 13, Figure 14 A - B) and the presence of light was higher than the activity in Bizovac biofilms stimulated by the same substrates (Figure 13, Table 9). Interestingly, bacterial activity stimulated by the presence of light in Bizovac biofilms did not differ from the substrate free HPG-only control, after 48 h (35.3 %; 34.8 %; Table 9, Figure 13). Because Gammaproteobacteria- and Chloroflexota-related ASVs were the most abundant noncyanobacterial ASVs in both biofilms (Figure 12), the contributions of these taxa were selected for a more detailed analysis of the observed responses to substrate changes using BONCAT–CARD- FISH.

The class Gammaproteobacteria accounted for 22.8 % of the initial population in the Bizovac biofilms, with high relative abundances of the families *Rhodocyclaceae* (10.6 %), *Hallothiobacillaceae* (4.9 %), and *Hydrogenophilaceae* (1.8 %), which are known to harbor thiosulfate oxidizers (Figure 12). In the Tuhelj biofilms, Gammaproteobacteria- related ASVs accounted for 11.2 % of the total microbial population, with most ASVs belonging to the families *Rhodocyclaceae* (3.6 %), *Chromatimaceae* (1.1 %), and *Beggiatoaceae* (1.0 %) (Figure 12). The fraction of active Gammaproteobacteria cells (defined as a CARD-FISH signal with the Gam42a probe and a positive BONCAT signal) remained constant when comparing 24 h and 48 h incubations without substrate amendment (HPG-only, Figure 13). Under these conditions, approximately 25 % of the gammaproteobacterial cells were active in the Bizovac biofilms, while only 10 % of the gammaproteobacterial population was active in the Tuhelj biofilms (Table 9, Figure 13). Glucose and thiosulfate additions resulted in very similar responses of the gammaproteobacterial class in the Bizovac biofilms, with 56 % and 61 % of translationally active cells after 48 h of incubation, respectively (Figure 13, Figures 14 C-D, Table 9). The addition of pyruvate resulted in a slightly less pronounced increase in gammaproteobacterial activity in the Bizovac biofilms over the same period (16.9 %, Table 9, Figure 13). In contrast, the addition of acetate and the presence of light negatively affected the activity of gammaproteobacterial cells in the Bizovac biofilms, with a BONCAT signal detected in only 12.5 % and 7.1 % of Gam42-positive cells after 48 h of incubation, respectively (Figure 13, Table 9). In the Tuhelj biofilms, the addition of thiosulfate resulted in a significant increase in the active fraction of gammaproteobacterial cells with 48 % translationally active Gam42a-positive cells after 48 h of incubation (Figure 13, Table 9). Glucose and pyruvate amendments also increased the activity of the gammaproteobacterial class in the Tuhelj biofilms, with 36 % and 28.5 % of cells displaying activity after 48 h, respectively (Figure 13, Table 9). Compared to the HPG-only control incubated in the dark, the presence of light slightly increased the

gammaproteobacterial activity (16.4 %) in Tuhelj biofilms after 48 h of incubation (Table 9, Figure 13). As previously observed in the Bizovac biofilms, acetate addition also suppressed the activity of the gammaproteobacterial class in the Tuhelj biofilms. After 48 h of incubation with acetate, only 3.6 % of the gammaproteobacterial cells were translationally active (Figure 13, Table 9).

In the Bizovac biofilms, phylum Chloroflexota had a lower relative abundance than t class Gammaproteobacteria. Almost all ASVs associated with Chloroflexota (11.1 %) belonged to the SBR1031 clade (4.4 %) or the family *Anaerolineaceae* (6.1 %, Figure 12). In the Tuhelj biofilms, Chloroflexota-related ASVs had a higher relative abundance than Gammaprotobacteria class and accounted for the majority of the noncyanobacterial microbial community (14.7 %). Most ASVs in the Tuhelj samples belonged to the families *Chloroflexaceae* (8.9 %) and *Anaerolineaceae* (2.9 %, Figure 12). In the Bizovac biofilms, less than 2 % of Chloroflexota cells (defined as a CARD-FISH signal with the CFX1223 probe and a positive BONCAT signal) were active after 24 h, while 9 % of cells were active after 48 h of incubation without substrate amendment (HPG-only, Table 9, Figure 13). In the Tuhelj biofilms, the activity of Chloroflexota cells was much higher in the treatments without substrate addition (HPG-only) than in the Bizovac biofilms, with 19 % and 15 % of active CFX1223 positive cells after 24 h and 48 h of incubation, respectively (Figure 13, Table 9). In both biofilms, the presence of light did not have a major effect on the activity of Chloroflexota cells compared to the activity in the HPG-only control treatments. After 48 h incubation in the light, 9.5 % of Chloroflexota cells in the Bizovac biofilm were active, while 18.2 % of CFX1223 cells in the Tuhelj samples showed a positive BONCAT signal (Figure 13, Figures 14 E-F, Table 9). Like the activity in the control treatment, the response of Chloroflexota populations in the Bizovac biofilms to glucose and thiosulfate additions was lower than the response of the gammaproteobacterial population. After 48 h of incubation in these substrates, 30 % and 29 % of the populations were active, respectively (Figure 13, Table 9). However, unlike Gammaproteobacteria class, the Chloroflexota population in the Bizovac biofilms responded with increased activity to acetate amendment, mirroring the pattern observed during pyruvate incubation: 20.7 % and 20.1 % of active Chloroflexota cells after 48 h of incubation, respectively (Figure 13, Table 9). In contrast, incubation with acetate in the Tuhelj biofilms resulted in lower Chloroflexota activity compared with the control treatments. After 48 h of incubation with acetate addition, only 9 % of Chloroflexota cells were active (Figure 13, Table 9). The addition of glucose resulted in the highest increase, while the addition of pyruvate

resulted in the lowest increase in activity and percentage of active Chloroflexota cells in the Tuhelj biofilms (47 % and 25.5 % after 48 h of incubation, respectively). Lastly, 37 % of the Chloroflexota populations in the Tuhelj biofilms were active after 48 h of incubation in thiosulfate amended setups (Figure 13, Table 9).
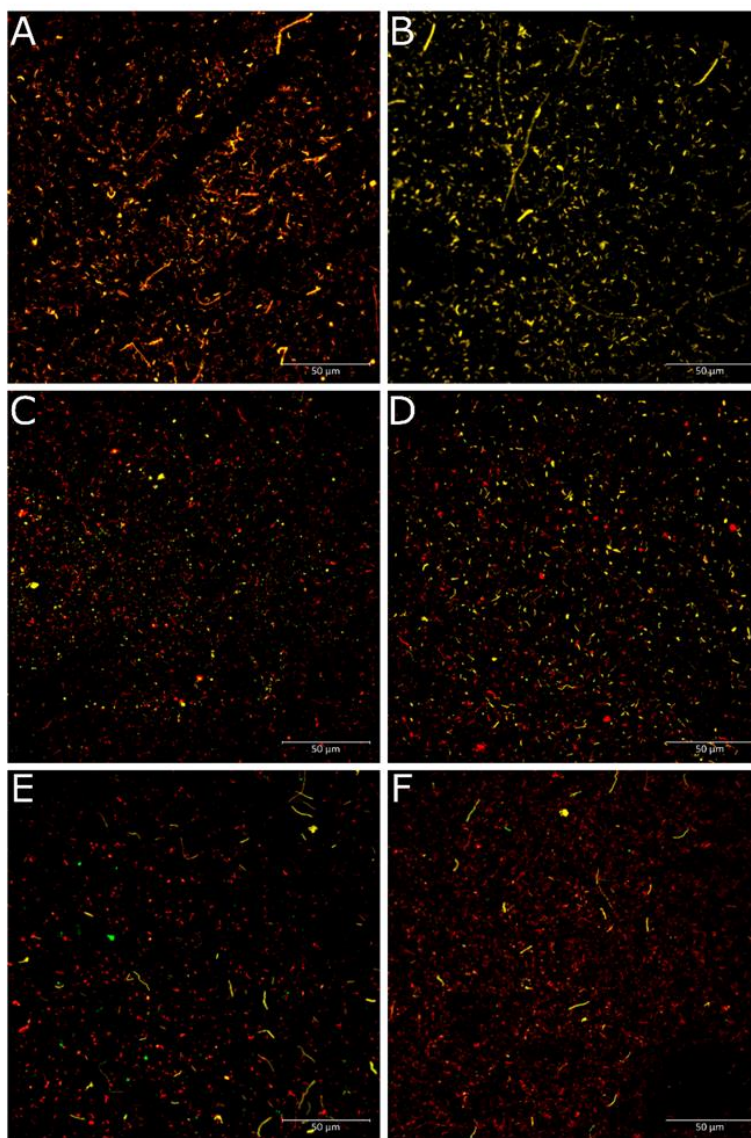

Figure 14. Images of incubated biofilms labelled with Cy5 (RED) for BONCAT signal and Cy3 (YELLOW) or Atto-488 (GREEN) for CARD-FISH signal: EUBI-III in Tuhelj biofilms incubated for 24 (A) and 48 (B) h in pyruvate; Gam42a in Bizovac biofilms incubated for 24 (C) and 48 (D) h in glucose; CFX1223 in Tuhelj biofilms incubated for 24 (E) and 48 (F) h with light.

4.4. Metabolic capacity of Bizovac and Tuhelj biofilms

4.4.1. Activity patterns of biofilms at the single-cell resolution

By combining sequencing methods with BONCAT and FACS, a detailed description of community structure on a single- cell resolution is provided, as well as insights into changes in the taxonomic composition of the biofilms following incubation with various additives. The microbial communities of the freshly collected biofilms in autumn 2021 were characterized by 16S rRNA gene amplicon sequencing. This analysis confirmed compositional similarities to previously analyzed biofilm samples collected in 2019 and 2020 from their respective source environments. The only notable difference was a higher relative abundance of phylum Deinococcota in the biofilms from the Bizovac well (Figure 9 - 11).

When incubated in the dark without the addition of substrate (i.e., the HPG-only control), the active fraction of the biofilm community was very similar in both biofilm samples (Table 10). After 24 h of incubation, 18 % of the cells in the Tuhelj biofilms and 18.6 % of the cells in the Bizovac biofilms exhibited a positive BONCAT signal (Table 10). The percentage of active cells did not change significantly after 48 h of incubation in either biofilm (Table 10), indicating that either the native energy and substrate sources were nearly depleted or that all microorganisms capable of utilizing these under the applied experimental conditions became active within the specified time frame.

In the Tuhelj biofilms, the addition of pyruvate, thiosulfate, and tetrathionate resulted in an increase in the active fraction after 48 h of incubation (Table 10). The addition of thiosulfate again led to the highest percentage of active cells in the Tuhelj biofilms (48.5 % after 24 h and 58.7 % after 48 h, Table 10). The pyruvate and tetrathionate amendments led to similar percentage of active cells after 24 h incubation (26.1 % and 21.4 %, respectively), but differed at 48 h time point, with the addition of pyruvate resulting in a higher activity increase (36.9 %, Table 10). In contrast, the addition of acetate resulted in a lower active fraction in the Tuhelj biofilms compared to the HPG-only controls, with only 10.1 % active cells after 48 h of incubation (Table 10). The thiocyanate amendment resulted in nearly the same percentage of active cells as in the HPG-only controls after 24 h but decreased slightly to 15.5 % during the 48 h incubation (Table 10).

For the Bizovac sample, incubation with all additives resulted in increased activity compared to the HPG-only controls (Table 10). Like in the Tuhelj biofilms, the highest percentage of active cells in the Bizovac biofilms was displayed upon incubation with thiosulfate with 31.5 % after 24 h and 56.3 % of active cells after 48 h of incubation (Table 10). In contrast to the

Tuhelj biofilm, the addition of acetate in the Bizovac biofilms resulted in an activity increase with 47.2 % of active cells after 48 h incubation (Table 10). Although acetate, thiosulfate, and tetrathionate amendments resulted in almost the same percentage of active cells after 24 h, the addition of tetrathionate in the Bizovac biofilm eventually resulted in the lowest increase in activity after 48 h among the substrates tested (22.5 %, Table 10). The addition of pyruvate and thiocyanate led to similar percentage of active cells in the Bizovac biofilms after 24 h (24.2 % and 25 %, respectively), but the active fraction in the incubation with pyruvate did not change during the 48 h, whereas the addition of thiocyanate resulted in 33.9 % of active cells after 48 h incubation (Table 10).

Table 10. Percentage of DAPI-BONCAT positive cells in biofilm incubation experiments and calculated cell density.

| Substrate	DAPI	Boncat	TCC	BCC	% Boncat	WCC	V for FACS (mL)
Tuhelj_24 h							
HPG	399	72	7.48E+07	1.35E+07	18.0 %	5.00E+05	6.69E-03
HPG + Acetate	275	35	5.15E+07	6.56E+06	12.7 %	5.00E+05	9.70E-03
HPG + Pyruvate	449	117	8.41E+07	2.19E+07	26.1 %	5.00E+05	5.94E-03
HPG + $Na_2S_2O_3$	656	318	1.23E+08	5.96E+07	48.5 %	5.00E+05	4.07E-03
HPG + $K_2S_4O_6$	388	83	7.27E+07	1.56E+07	21.4 %	5.00E+05	6.88E-03
HPG + KSCN	774	140	1.45E+08	2.62E+07	18.1 %	5.00E+05	3.45E-03
Tuhelj_48 h							
HPG	585	101	1.10E+08	1.89E+07	17.3 %	5.00E+05	4.56E-03
HPG + Acetate	425	43	7.96E+07	8.06E+06	10.1 %	5.00E+05	6.28E-03
HPG + Pyruvate	609	225	1.14E+08	4.22E+07	36.9 %	5.00E+05	4.38E-03
HPG + $Na_2S_2O_3$	774	454	1.45E+08	8.51E+07	58.7 %	5.00E+05	3.45E-03
HPG + $K_2S_4O_6$	549	140	1.03E+08	2.62E+07	25.5 %	5.00E+05	4.86E-03
HPG + KSCN	646	100	1.21E+08	1.87E+07	15.5 %	5.00E+05	4.13E-03
Bizovac_24 h							
HPG	587	109	1.10E+08	2.04E+07	18.6 %	5.00E+05	4.55E-03
HPG + Acetate	171	54	3.20E+07	1.01E+07	31.6 %	5.00E+05	1.56E-02
HPG + Pyruvate	339	82	6.35E+07	1.54E+07	24.2 %	5.00E+05	7.87E-03
HPG + $Na_2S_2O_3$	308	97	5.77E+07	1.82E+07	31.5 %	5.00E+05	8.66E-03
HPG + $K_2S_4O_6$	876	275	1.64E+08	5.15E+07	31.4 %	5.00E+05	3.05E-03
HPG + KSCN	724	181	1.36E+08	3.39E+07	25.0 %	5.00E+05	3.69E-03
Bizovac_48 h							
HPG	400	83	7.49E+07	1.56E+07	20.8 %	5.00E+05	6.67E-03
HPG + Acetate	544	257	1.02E+08	4.81E+07	47.2 %	5.00E+05	4.91E-03
HPG + Pyruvate	196	47	3.67E+07	8.81E+06	24.0 %	5.00E+05	1.36E-02
HPG + $Na_2S_2O_3$	613	345	1.15E+08	6.46E+07	56.3 %	5.00E+05	4.35E-03
HPG + $K_2S_4O_6$	369	83	6.91E+07	1.56E+07	22.5 %	5.00E+05	7.23E-03
HPG + KSCN	540	183	1.01E+08	3.43E+07	33.9 %	5.00E+05	4.94E-03
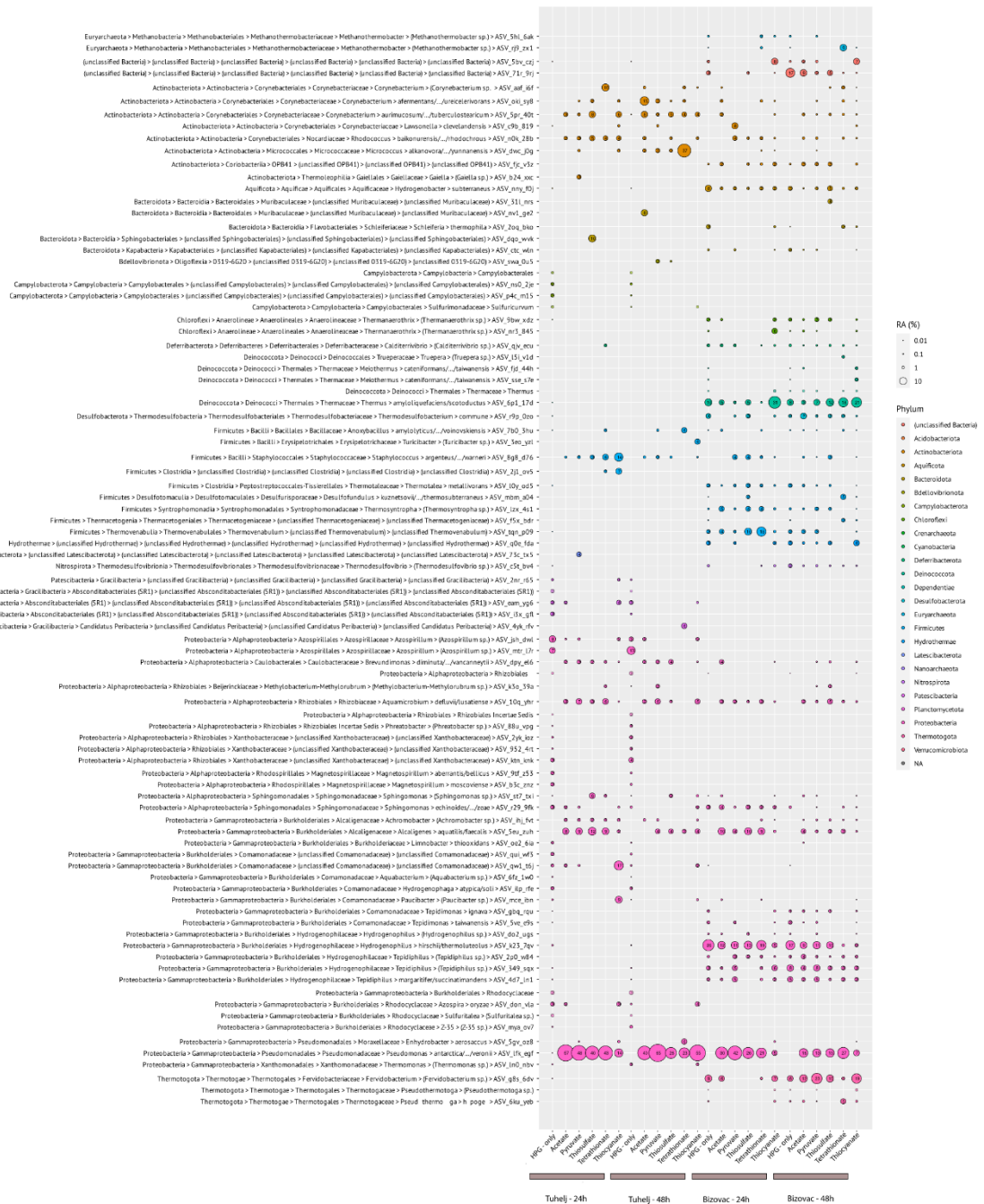
Figure 15. Relative abundance of sorted biofilms from Bizovac and Tuhelj source incubated in different substrates. Relative abundance (RA) shown for higher taxonomic ranks are exclusive of the relative abundance for separately shown lower taxonomic ranks. Taxa are NOT collapsed if RA ≥ 1 % in at least 1 sample(s). The highest rank(s) are never collapsed.

After counting the cell density (Table 10), the active fraction of the biofilm samples detected by the BONCAT method was sorted by FACS. Subsequently, DNA of the sorted samples was extracted and 16S rRNA gene amplicon analysis was performed (Figure 15). After incubation of the Bizovac biofilms in different substrates, changes in the relative abundance of some microbial groups were detected (Figure 15), so these populations were selected for more detailed analysis of the results obtained by the BONCAT- FACS-seq method.

As shown in Figure 15, after 24 h of incubation, the genus *Fervidobacterium* of the phylum Thermotogota was found in higher abundance only in the HPG-only control (9.5 %) and in the incubation with acetate addition (6 %). In contrast, after 48 h of incubation, this genus had a relative abundance of 6 % in the HPG-only control but exhibited a much higher relative abundance in the incubations with substrate additions (Figure 15). The highest relative abundance of this genus (23 %) was detected in the incubation with pyruvate, while higher relative abundances were also observed in the incubations with thiocyanate (19 %), thiosulfate (10 %), and acetate (12 %, Figure 15)

The orders Thermovenabulales and Syntrophomonadales from the phylum Bacillota also had significantly higher relative abundances in the incubations with substrate additions compared to the HPG-only control, as did *Thermus* from the phylum Deinococcota (Figure 15). In the HPG-only control, the relative abundance of Syntrophomonadales was 1 % after 24 h (Figure 15). At the same time point, the highest relative abundance of this order was observed when incubated with acetate (5 %), and similar abundance was observed after incubation with thiosulfate and tetrathionate (4 % each, Figure 15). The relative abundance of Thermovenabulales in the HPG-only control was 2 % at both time points (Figure 15). The highest relative abundance of this order was observed after 24 h of incubation with tetrathionate (18 %, Figure 15). Increased abundance of this order was also observed after 24 h of incubation with thiosulfate (at 10 %). The genus *Thermus* had a relative abundance of 10 % in the HPG-only control after 24 h of incubation, which decreased with all substrate incubations except thiocyanate, where it increased to 31 % relative abundance after 24 h (Figure 15). After 48 h of incubation, this genus was detected at a relative abundance of 8 % in the HPG-only control, which increased significantly in the incubations with thiosulfate (12 %), tetrathionate (18 %), and thiocyanate (21 %, Figure 15).

In contrast, the *Hydrogenophilus* and *Tepidiphilus* genera of the *Hydrogenophilaceae* family in the Bizovac sample had lower relative abundances in most incubations with substrate additions

compared to the HPG-only control at both time points (as shown in Figure 15). For the genus *Hydrogenophilus*, the relative abundance after 24 and 48 h of incubation in the HPG-only control was 26 % and 17 %, respectively. Addition of acetate resulted in a decrease in relative abundance (12 % and 9 % after 24 and 48 h of incubation, respectively), while incubation with pyruvate resulted in the same relative abundance of this genus at both time points (11 %, Figure 15). Thiosulfate resulted in a relative abundance of 13 % of *Hydrogenophilus* after 24 h and 10 % after 48 h of incubation, and tetrathionate resulted in 19 % and 10 % after 24 and 48 h of incubation, respectively (Figure 15). The addition of thiocyanate resulted in the most significant decrease in relative abundance of the genus *Hydrogenophilus* in both time points (Figure 15). Two ASVs related to the genus *Tepidiphilus* showed higher abundance when incubated with acetate (5 % each) than in the HPG-only control after 24 h (Figure 15). However, in all other incubations, lower abundance of this genus was observed after 24 h (Figure 15). After 48 h of incubation, genus *Tepidiphilus* was detected at a relative abundance of 13 % in the HPG-only control, which decreased significantly (no more than 5 % in all incubations), except for the incubation with pyruvate, where relative abundance of *Tepidiphilus* remained the same as in the HPG-only control (Figure 15).

4.4.2. Metagenome analysis

The analysis of both thermal biofilms revealed the presence of diverse metabolic processes, including those associated with carbohydrate metabolism, lipopolysaccharide (glycan) metabolism, cofactor and vitamin metabolism, xenobiotic (aromatic) degradation, biosynthesis of terpenoids and polyketides (specifically, terpenoid backbone biosynthesis, macrolide biosynthesis, and polyketide sugar unit biosynthesis), as well as various energy metabolism pathways. Regarding photosynthesis-related processes, the Tuhelj biofilm exhibited the presence of genes associated with Photosystem II, Photosystem I, and Anoxygenic Photosystem II. In contrast, the Bizovac biofilm only contained genes linked to Anoxygenic Photosystem II, indicating differences in the photosynthetic capabilities between these two biofilms.

The Tuhelj biofilm contained a total of 83 MAGs with completeness levels exceeding 50 % and contamination levels below 5 %. Among these MAGs, three exhibited circular genomes, all of which were taxonomically classified under the phylum Cyanobacteria, specifically within the *Microcoleaceae* and *Microcystaceae* families. In terms of primary producers within the biofilm,

19 MAGs were attributed to the phylum Cyanobacteria, while 8 were associated with the phylum Chloroflexota, primarily within the *Chloroflexaceae* family. Additionally, 16 MAGs were linked to the phylum Pseudomonadota, with an equal distribution between Alpha- and Gammaproteobacteria. All gammaproteobacterial MAGs belonged to the *Burkholderiaceae* family, except for one MAG affiliated with the *Xanthobacteraceae* family. Furthermore, the biofilm exhibited a diverse microbial composition, with 3 MAGs each associated with the phyla Verrucomicrobiota, Planctomycetota, Armatimonadota, and Acidobacteriota, respectively. Additionally, 7 MAGs were identified within the Bacteroidota phylum, 4 within the Desulfobacterota phylum, 2 within the Myxococcota phylum, and single representatives within the Actinobacteriota and Campylobacterota (specifically, *Sulfurovaceae* family) phyla.

The analysis of the carbon cycle in the Tuhelj biofilm (Figure 16) revealed the presence of all essential metabolic steps, encompassing the Calvin cycle, Crassulacean acid metabolism (CAM) in both dark and light conditions, the reductive citrate cycle (Arnon-Buchanan cycle), the phosphate acetyltransferase-acetate kinase pathway, glucogenesis, glycolysis (Embden-Meyerhof pathway), the Entner-Doudoroff pathway, pyruvate oxidation, and all functional modules of the citrate cycle, along with the pentose phosphate pathway. Notably, the sole process absent within this cycle was methanogenesis (Figure 16).
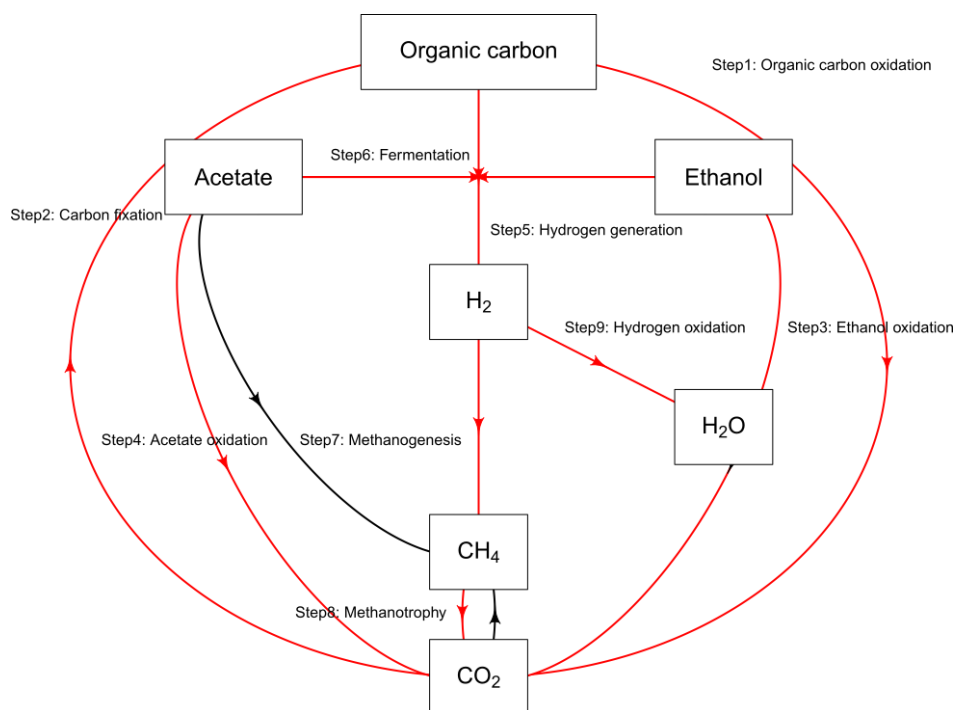

Figure 16. Microbially mediated carbon cycling in Tuhelj biofilm. Red arrows indicate complete pathways of respective step.
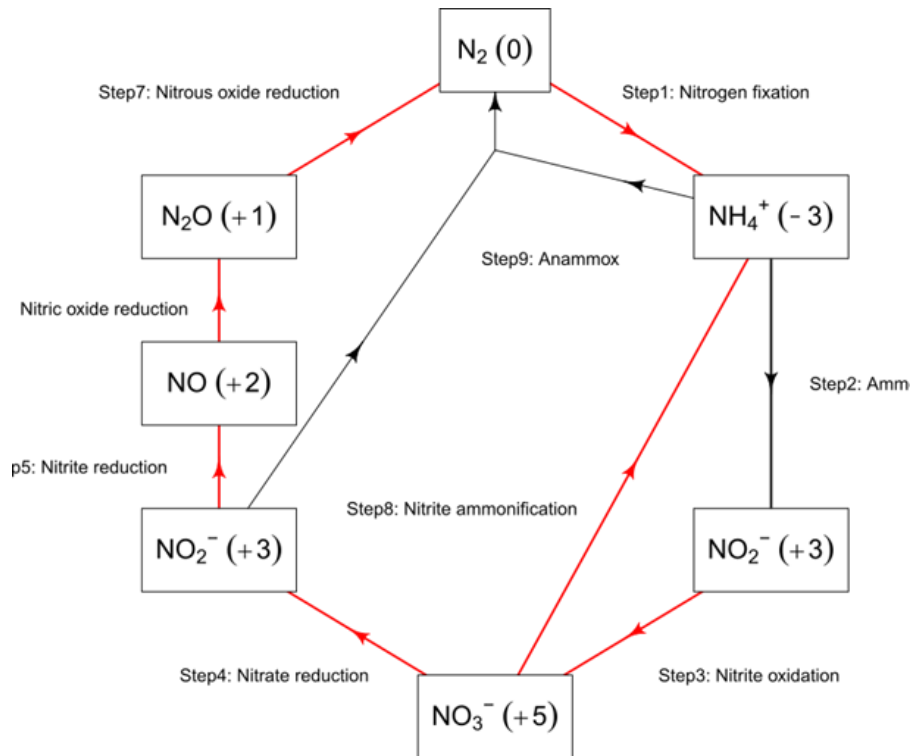
Figure 17. Microbially mediated nitrogen cycling in Tuhelj biofilm. Red arrows indicate complete pathways of respective step.

In the context of the nitrogen cycle within the Tuhelj biofilm (Figure 17), all fundamental stages were identified, apart from the oxidation of ammonium ions to nitrite and the anammox process, which involves the conversion of ammonium and nitrite into dinitrogen gas in anaerobic conditions by autotrophic microorganisms. Furthermore, a sulfur cycle was observed in the Tuhelj biofilm (Figure 18) encompassing all key components, including assimilatory sulfate reduction, dissimilatory sulfate reduction, and thiosulfate oxidation mediated by the SoX complex.
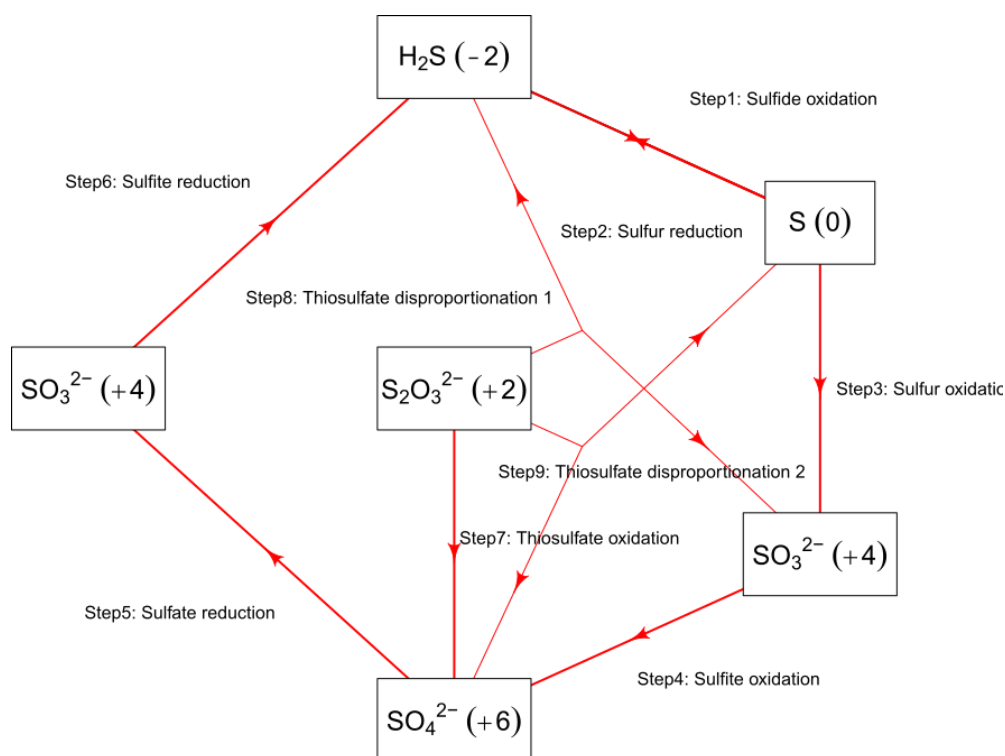
Figure 18. Microbially mediated sulfur cycling in Tuhelj biofilm. Red arrows indicate complete pathways of respective step.

Additionally, the genomic content of the Tuhelj biofilm included genes associated with diverse redox processes, such as metal reduction, arsenate oxidoreduction, and selenate reduction (Figure 19).

Figure 19. Microbially mediated metal reduction, arsenate oxidoreduction and selenate reduction in Tuhelj biofilm. Red arrows indicate complete pathways of respective step.

The Bizovac biofilm contained 36 MAGs with a completeness level exceeding 50 % and contamination levels lower than 5 %. among which 15 were circular. Three MAGs were identified within the Archaea kingdom, with one circular MAG associated with the *Methanothermobacteraceae* family. Regarding the Bacteria domain, a balanced distribution of MAGs was observed across various phyla. Specifically, six MAGs were attributed to the phylum Bacteroidota, with two of these exhibiting circular structures and affiliations with the *Schleiferiaceae* and *Ignavibacteriaceae* families. Similarly, six MAGs were linked to the phylum Chloroflexota, three of which were circular, and associated with the A4b, EnvOPS12, and *Caldilineaceae* family. The phylum Pseudomonadota was also represented with 6 MAGs among which one circular MAG was associated with the *Immundisolibacteraceae* family. Moreover, two MAGs each were associated with the phyla Acidobacteriota, Plantomycetota, and Nitrospirota (among which one circular MAG belonged to the *Thermodesulfovibrionaceae* family). Additionally, single MAGs were attributed to the Desulfobacterota and Cyanobacteria phyla. The remaining MAGs, all of which were circular, were affiliated with the Actinobacteriota, Armatimonadota, Bipolaricaulota, Deinococcota, Dictyoglomota, WOR-3, and Aquificota phylum.

Within Bizovac microbial community, a diverse array of carbon fixation pathways was identified (Figure 20). These encompassed both dark and light Crassulacean Acid Metabolism (CAM), the Reductive Acetyl-CoA Pathway (Wood-Ljungdahl pathway), as well as the Embden-Meyerhof and Entner-Doudoroff pathways, which facilitate the conversion of glucose into pyruvate. Furthermore, citrate cycle (TCA cycle, Krebs cycle) and various processes within the pentose phosphate pathway were also detected, as well as methanogenesis and formaldehyde assimilation pathways (Figure 20).

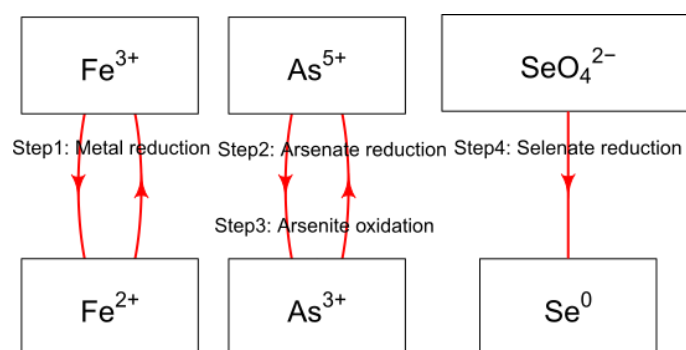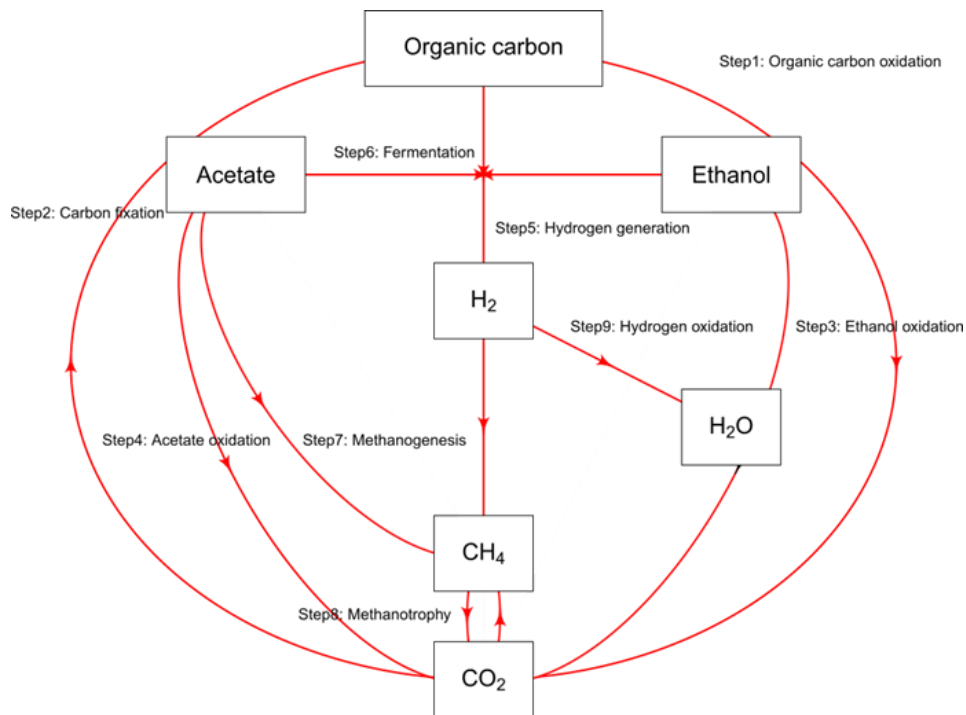Figure 20. Microbially mediated carbon cycling in Bizovac biofilm. Red arrows indicate complete pathways of respective step.
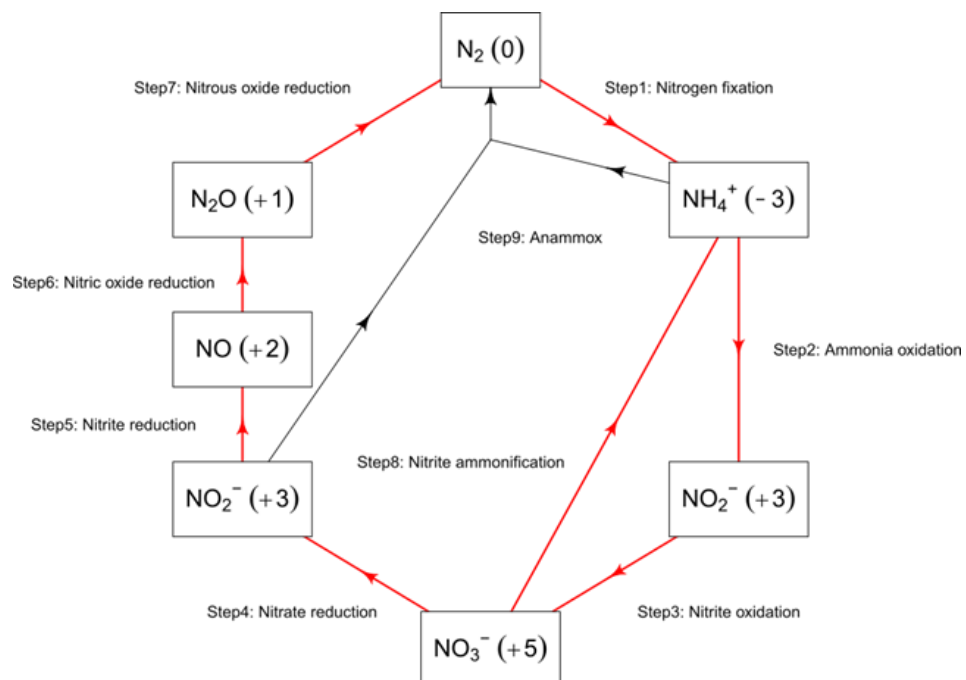

Figure 21. Microbially mediated nitrogen cycling in Bizovac biofilm. Red arrows indicate the complete pathways of respective step.

In terms of nitrogen cycling, a comprehensive suite of pathways was identified in the Bizovac biofilm, as illustrated in Figure 21. These encompassed the complete pathways for Dissimilatory Nitrate Reduction to Ammonium (DNR), Assimilatory Nitrate Reduction (ANR), denitrification, and nitrogen fixation. Notably, the genes responsible for nitrogen fixation were affiliated with three distinct groups: Nitrospirota (specifically, the *Thermodesulfovibrio* genus), Aquificota, and Cyanobacteria, as illustrated in Figure 22. Similarly, ANR genes were detected in MAGs associated with Gammaproteobacteria, Cyanobacteria, Actinobacteriota and Desulfobacterota (Figure 22).

Figure 22. Distribution of sulfur and nitrogen cycling genes detected in Bizovac biofilm.
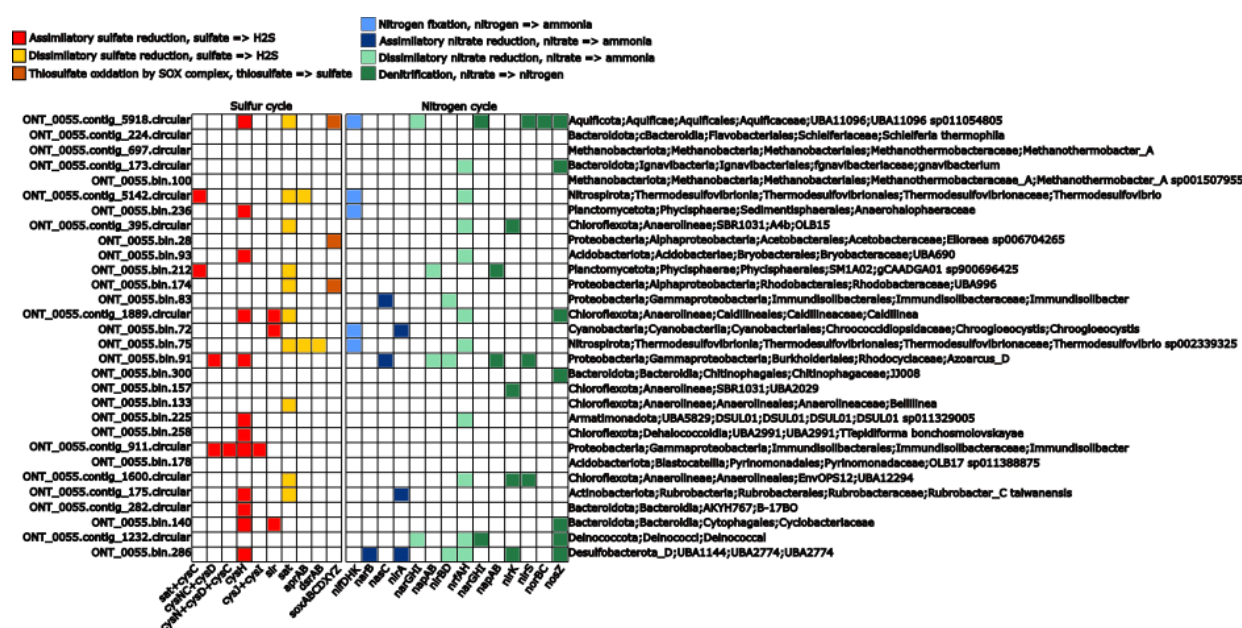
In the context of the sulfur cycle, the Bizovac biofilm displayed complete assimilatory sulfate reduction process, as depicted in Figure 22 and Figure 23. Notably, this process was primarily associated with the phylum Pseudomonadota (Figure 22). Dissimilatory sulfate reduction process was mainly associated with ASVs belonging to phyla Chloroflexota and Nitrospirota (Figure 22). Additionally, within this biofilm, two MAGs from the alphaproteobacterial class contain genes linked to thiosulfate oxidation, as presented in Figure 22. These findings underscore the multifaceted nature of sulfur cycling within the microbial community originating from the Bizovac source. Notably, MAG associated with *Aquificaceae* family revealed genes associated with all steps involved in both sulfur and nitrogen cycling (Figure 22).
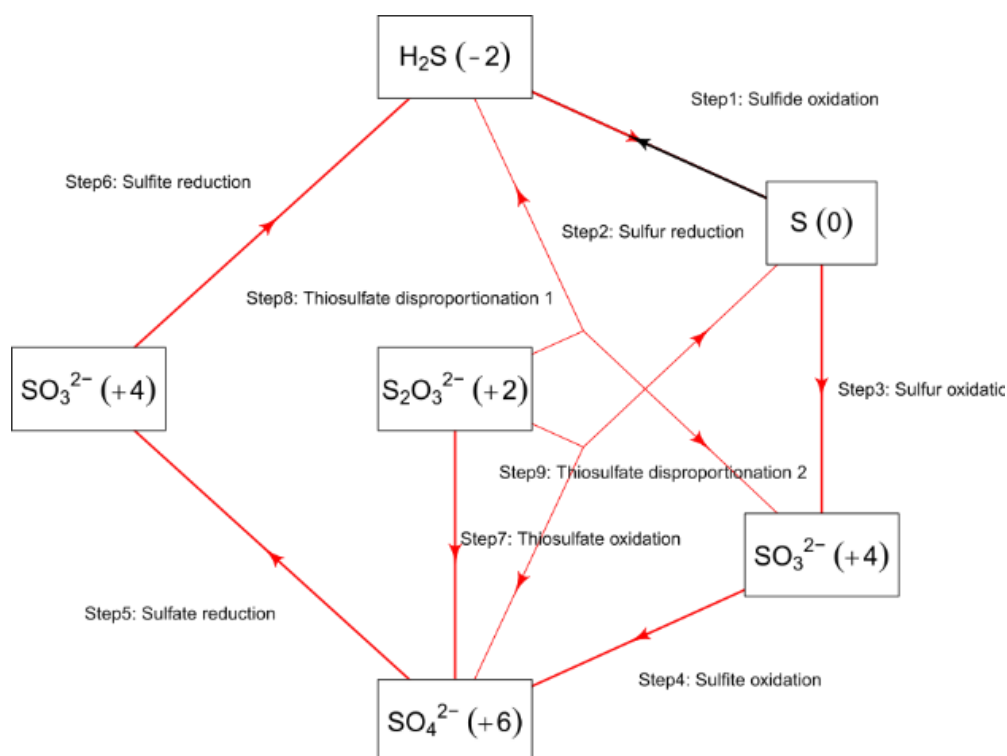
Figure 23. Microbially mediated sulfur cycling in Bizovac biofilm. Red arrows indicate the complete pathways of respective step.
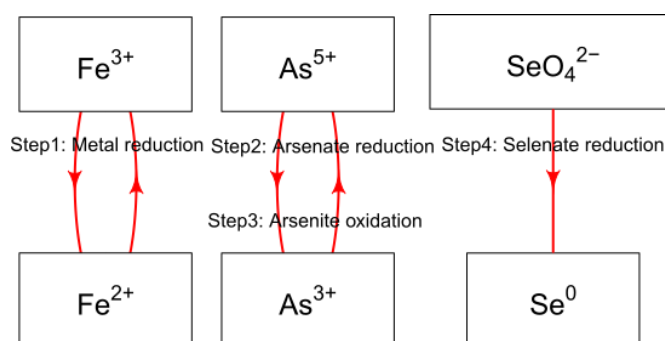
Figure 24. Microbially mediated metal reduction, Arsenate oxidoreduction and Selenate reduction. Red arrows indicate the complete pathways of respective step.

Like observations in the Tuhelj biofilm, the Bizovac biofilm featured the presence of genes involved in processes such as metal reduction, arsenate oxidoreduction, and selenate reduction, as illustrated in Figure 22.

5. DISCUSSION

5.1. Influence of seasonality and physiochemical parameters on geothermal biofilms

The microbial composition of hot spring biofilms has often been described as influenced by the elevated temperature in these environments (e.g., Sompong et al., 2005; Purcell et al., 2007; Msarah et al., 2018; Prieto-Barajas et al., 2018). However, a recent study of 925 hot springs in New Zealand showed that temperature has a significant effect on microbial beta diversity only at values above 80 °C (Power et al., 2018). Although geothermal spring temperatures in this study were lower (max. 65 °C), temperature and sample origin were the main determinants of biofilm microbial structure. Contrary to expectations, no significant effect of sampling season or biofilm color on the microbial community composition was observed. The most abundant microbial groups in the sampled biofilms were consistent with previous studies (Portillo et al., 2009; Huang et al., 2011; Coman et al., 2013; Coman et al., 2015; Alcamán-Arias et al., 2018; Mackenzie et al., 2013; Guo et al., 2020; Toshchakov et al., 2021), with Cyanobacteria dominating in the biofilms of all sampling sites except the Bizovac well, and Chloroflexota, Pseudomonadota, and Bacteroidota having high relative abundance in all biofilms.

Cyanobacterial genera related to *Leptolyngbya*, which dominated most of the analyzed biofilms, were also found abundantly in the upper layer of alkaline microbial mats from the Garga hot spring (Rozanov et al., 2017). The genus *Tychonema*, detected in biofilms from the cold well DB, was also recently found abundantly in biofilms from hydrothermal systems in Italy with temperatures moderately above ambient (Della Porta et al., 2022). As expected, the microbial communities in the biofilms were significantly different from the communities of geothermal water in the same springs. Geothermal waters from the same sampling sites were dominated by ASVs affiliating to Crenarchaeota, Nanoarchaeota, Campylobacterota, and various Pseudomonadota lineages (Mitrović et al., 2022), while almost all biofilm samples were dominated by Cyanobacteria (Kostešić et al., 2023). As for thiotrophs, the genera detected in water samples from the same sites (e.g., *Sulfuricurvum* and *Sulfurimonas* among the Camplyobacterota, and *Thiobacillus* among the Gammaproteobacteria (Mitrović et al., 2022) differed from the dominant genera in the biofilm samples (*Sulfovorum*, *Thiofaba*, *Thiotrix*, *Hydrogenophillus*), all previously detected in hot spring biofilms at other sites with similar temperatures (e.g., Valeriani et al., 2018). As for Archaea, while diverse crenarchaeal, micrarchaeal, and nanoarchaeal lineages dominated in many water samples from the same springs (Mitrović et al., 2022) they were not abundant in the biofilm samples (Figure 9, Kostešić et al., 2023). The highest abundance of Creanarchaeota was found in the biofilm of Topusko

well (TEB), the sampling site with the highest temperature (64.8 °C) in this dataset. Consistent with this observation, comparison of mats from a geothermal spring in Romania at different temperature ranges revealed that the relative abundance of Archaea was low at 32 °C (< 0.5 %) but increased significantly at 65 °C (36 %) (Coman et al., 2015). Similarly, Alcaman et al. reported a temperature value of 58 °C as the turnover point for phototrophs, with Cyanobacteria dominating the lower temperature range and Chloroflexota being more abundant in the 58-66 °C range (Alcamán-Arias et al., 2018). Three of high-temperature sampling sites (Topusko (TEB), Varazdin (V), and Bizovac (B) well) had temperatures around this tipping point (Table 4 – 7), but only the biofilms from Bizovac well were dominated by Chloroflexota (genera *Candidatus Chlorotrix* and *Chloroflexus*; Figure 11) rather than Cyanobacteria. All other sampling sites with high and moderate temperatures were indeed dominated by Cyanobacteria (Figure 9), confirming that temperature is not the only driver for the previously observed community switch among primary producers.

5.2. Activity patterns of Bizovac and Tuhelj biofilms

Based on the differences in microbial community composition and spring geochemistry observed during seasonal sampling, fresh biofilms were collected from Bizovac well and Tuhelj spring and subjected to a series of incubation experiments to investigate the phototrophic and chemoorganotrophic and chemolithotrophic activity of the community members. The majority of the analyzed hot spring biofilms, including those from Tuhelj spring, were dominated by Cyanobacteria, the dominant photosynthetic primary producers in these systems. In contrast, primary producers in the Bizovac biofilms were mainly associated with Chloroflexota phylum. Therefore, the presence of light in the incubation experiments was a logical choice for assessing microbial activity in these samples. Subsequently, Cyanobacteria are likely a major source of organic carbon substrates, sustaining growth and activity of chemoorganotrophic microorganisms in hot spring biofilms. However, because hot spring biofilms grow at a redox interface, a fraction of the microbial community might also be adapted to derive energy from reduced inorganic substrates through chemolithotrophic metabolism, as evidenced, for example, by the presence of various and diverse thiotrophs in most biofilm samples (Figure 12). Therefore, thiosulfate was selected as a substrate to evaluate chemolithotrophic activity related to the geochemical gradients on which the biofilms reside on. Glucose, pyruvate, and acetate were selected as carbon substrates to simulate the activity of chemoorganotrophs, *in situ* supplied with organic compounds via photosynthetic primary production. In the biofilms

recovered from both sources, the thiotrophs putatively able to oxidize the thiosulfate provided as substrate belonged predominantly to various gammaproteobacterial lineages.

The Bizovac biofilm contained more ASVs affiliated with putative thiotrophs and Gammaproteobacteria in general compared to Cyanobacteria-dominated biofilms from the Tuhelj spring (Figures 9 - 12). ASVs related to *Chromatiaceae* and *Hallothiobacillaceae* were identified as putative thiotrophs in the Bizovac sample, whereas *Chromatiaceae* and Beggiatoaceae ASVs were found in the Tuhelj biofilms (Figure 12, Wasmund et al., 2017). Other abundant gammaproteobacterial families in both samples were *Rhodocyclaceae* and *Hydrogenophilaceae* (Figure 12). The *Rhodocyclaceae* family is metabolically diverse and consists of photoautotrophic, heterotrophic, and organotrophic members. This family has also been found abundantly in sulfidic hot springs in Northern Baikal (Chernitsyna et al., 2023) and in microbial mats of hot springs in Eritrea (Ghilamicael et al., 2017). The most abundant ASVs of the family *Rhodocyclaceae* detected in the Bizovac biofilm belonged to the genus *Azoarcus* (8 %). Although primarily classified as denitrifying chemolithoheterotrophs, numerous studies reported *Azoarcus* to be denitrifying, desulfurizing core bacteria in bioreactor experiments under mixotrophic conditions (Xu et al., 2014; Li et al., 2016; Zhang et al., 2019; Liu et al., 2020; Gao et al., 2022). The only currently known sulfur-oxidizing denitrifying species, *Azoarcus taiwanensis*, was isolated from a hot spring biofilm in Taiwan (Lee et al., 2014). Members of the family *Hydrogenophilaceae* are thermophilic heterotrophs and autotrophs that can use hydrogen as an electron donor (Boden et al., 2017). A new species of this family was recently isolated from microbial mats of hot springs in Japan that can grow with thiosulfate and elemental sulfur under aerobic conditions and is unable to utilize hydrogen (Kawai et al., 2022). Almost all *Hallothiobacilaceae* ASVs in the Bizovac sample belonged to the genus Thiofaba (4.8 %; Figure 12). The type of strain of this genus, *Thiofaba teidiphila*, was isolated from the biofilm of a hot spring in Japan and characterized as an obligate chemolithoautotrophic bacterium that uses thiosulfate, elemental sulfur, sulfide, and tetrathionate as electron donors (Mori and Suzuki, 2008). In addition, a larger fraction of the microbial community in the Bizovac biofilms belonged to the Desulfobacterota - a phylum harboring various microorganisms involved mainly in the reductive but also in the oxidative sulfur cycle (Wasmund et al., 2017). Moreover, considerable amounts of sulfide were detectable *in situ* in the water samples from the Bizovac well, but not in the water from the Tuhelj spring (Table 4 – 7), indicating sulfide oxidation, but also S disproportionation (Singh et al., 2019). Therefore, it is hypothesized that either a larger fraction of the microbial community in the Bizovac biofilms is capable of chemolithotrophic activity by utilizing thiosulfate as a source of reducing

equivalents, or that the observed changes in the activity of the non-thiotrophic fraction, despite the relatively short incubation time, were the result of cross-feeding interactions in which the activity of the putative thiotrophs led to the accumulation of hydrogen and small organic molecules. Contrary to expectations, the overall increase in the total active cell fraction and, in particular the active gammaproteobacterial fraction, was more pronounced in the thiosulfate-amendment incubations in the Tuhelj biofilms (Figure 13), in which ASVs related to the known thiotrophs were less abundant (Figure 12). Because the community in the Bizovac biofilms was dominated by chemolithoheterotrophic *Rhodocyclaceae*, it is possible that the availability of suitable organic carbon sources limited the metabolic activity of thiotrophs in the experiments. In both biofilm samples, the response to glucose addition in the gammaproteobacterial cell fraction was in the same range of activity increase as in the incubations amended with thiosulfate (Figure 13). These results are consistent with the chemoorganoheterotrophy and mixotrophy expected for many of the community members detected here. The class Gammaproteobacteria contains the largest diversity of obligate and generalist hydrocarbonoclastic bacteria (Gutierrez, 2019), many of which are known for their implication in acetate assimilation (Winkel et al., 2014; Dyksma et al., 2018). However, contrary to expectation, incubation with acetate resulted in decreased fractions of active gammaproteobacterial populations in both biofilms. Compared to glucose, acetate is a low-energy carbon source and has been shown to have an inhibitory effect on some microorganisms, reducing their growth rate (Kutscha and Pflügl, 2020). Nevertheless, since the overall response of the microbial community to acetate amendment was increased activity, the used acetate concentration does not appear to be inhibitory.

In both biofilms, the increase in the active cell fraction of Chloroflexota in incubations with thiosulfate was almost equivalent to the activity increase in glucose treatments (Figure 13). This result was surprising, as the majority of Chloroflexota ASVs in both samples were not related to known thiotrophs. Almost all Chloroflexota ASVs in the Bizovac sample belonged to clade SBR1031 and family *Anaerolineaceae*. These were previously found to occur in microbial mats at temperatures of 25 – 60 °C in hot springs of the Tibetan Plateau (Wang et al., 2017), Costa Rica (Uribe-Lorío et al., 2019), and Saudi Arabia (Yasir et al., 2020). Most members of the *Anaerolineaceae* are known to be mesophilic or thermophilic chemoheterotrophs that grow mainly under anaerobic conditions and metabolize sugars fermentatively (Yamada and Sekiguchi, 2018). In addition to fermentative sugar metabolism, SBR1031 members also encode key genes for acetogenic dehydrogenation (Xia et al., 2016). Therefore, the stimulation of Chloroflexota by thiosulfate amendments observed in this experiment was unexpected. It is

possible that either members of Chloroflexota with yet undescribed metabolism are present in the biofilm samples or that, despite the relatively short incubation time, observed findings are the results of microbial interactions in which compounds produced and released by thiosulfate oxidizers, such as the thiotrophic gammaproteobacterial community, actually stimulated Chloroflexota. On the other hand, Chloroflexota ASVs from the initial Tuhelj biofilms, apart from the *Anaerolineaceae* family, were mostly associated with members of the *Chloroflexaceae* family, which are known to grow photoautotrophically, suggesting an ecological role as primary producers in the hot spring environment (Gupta et al., 2013), but have also been previously shown to utilize acetate (Nübel et al., 2002). Nevertheless, the acetate amendment in this biofilm resulted in slightly reduced activity of Chloroflexota, contrary to expectations.

5.4. Bizovac and Tuhelj functionality and genes of biotechnological importance

5.4.1. Activity patterns in biofilm samples

Biofilms sampled in autumn 2021 confirmed microbial composition with seasonal sampling and additional sampling performed in spring 2021 (Fig 9 -11). In the Bizovac sample, the dominant phyla were Deinococcota (25.7 %) and Pseudomonadota (15.7 %), accompanied by Chloroflexota (11.3 %) and Bacteroidota (10.7 %). In contrast, the biofilms from the Tuhelj spring were primarily composed of Cyanobacteria (53.3 %), with notable proportions of Pseudomonadota (11.9 %), Bacteroidota (10.3 %), and Chloroflexota (5.4 %, Figure 9). The incubation experiment conducted on biofilms from Bizovac and Tuhelj sampled in autumn 2021 aligned with results obtained in previous incubation experiment conducted on biofilms from the same sources sampled in spring 2021 (Figure 13, Table 9).

In Tuhelj biofilm, acetate addition again led to decreased activity of microbial population in both time points (24 and 48 h) and resulted in lowest percentage of BONCAT positive cells among all incubation setups (Table 10). Thiocyanate addition in incubation of Tuhelj biofilms led to almost similar activity as the one observed in HPG-only controls (Table 10). Pyruvate and thiosulfate triggered the highest proportion of active cells in the Tuhelj biofilms. This, coupled with findings from previous experiments, strongly suggests that thiosulfate is the preferred substrate in biofilms from Tuhelj spring. The heightened activity observed with pyruvate addition aligns with expectations, as pyruvate is an intermediate product in microbial glucose utilization. This pattern supports the idea of chemoorganoheterotrophy and mixotrophy expected among many community members (Figure 9 - 11, Gutierrez, 2019).

In Bizovac biofilms, microbial activity was lowest upon incubation with HPG-only control for both time points (24 and 48 h, Table 10). Compared to HPG-control, addition of pyruvate and thiocyanate led to slight increase in microbial activity which stayed almost constant through 48 h incubation (Table 10). This result was expected, as thiocyanate (SCN^-) utilization is a specialized metabolic trait rarely observed in bacterial species, while those able to utilize thiocyanate grow much slower than in incubations with thiosulfate (Sorokin et al., 2001). Conversely, thiosulfate once again led to the highest microbial activity in Bizovac biofilms throughout the 48 h incubation (Table 10), associated with the presence of many thiosulfate utilizers detected in biofilms from this source. Detailed discussions on sulfur metabolism in Bizovac biofilm will follow in subsequent sections.

5.4.2. 16S rRNAamplicon sequence analysis of sorted samples

Using a BONCAT-FACS -seq approach on biofilms collected in autumn 2021 and subjected to incubations with various substrates, significant alterations in the relative abundance of certain microbial populations within Bizovac biofilms were observed. These populations were further selected for more detailed investigation. Notably, thermophilic genera, including *Fervidobacterium* from the phylum Thermotogota, *Thermosyntropha* and unclassified *Thermovenabulum* from the phylum Bacillota, as well as *Thermus* from the phylum Deinococcota, all commonly associated with hot springs, displayed pronounced increases in relative abundance during incubations with substrate additions compared to the HPG-only control (Figure 15).

The genus *Fervidobacterium* exhibited the highest relative abundance during incubation with pyruvate, with substantial increases also observed during incubation with thiocyanate, thiosulfate, and acetate additions (Figure 15). Members of the genus *Fervidobacterium* are typically anaerobes known for their fermentative metabolism of carbohydrates (Ravot et al., 1995; Gumerov et al., 2011. These microorganisms have previously been identified as essential members of the cellulose-degrading community in Yellowstone hot springs (Vishnivetskaya et al., 2015). While their primary mode of carbon acquisition involves heterotrophic metabolism by utilizing organic compounds like glucose and pyruvate, certain *Fervidobacterium* species exhibit metabolic versatility, enabling the utilization of inorganic compounds such as thiosulfate under specific conditions. For instance, *Fervidobacterium islandicum* and strain SEBR 2665, isolated from an oil well, have demonstrated the ability to reduce thiosulfate to sulfide (Ravot et al., 1995). This highlights the adaptability of *Fervidobacterium* species, which

adapt to their local environment and develop specialized metabolic strategies to exploit available resources.

The genus *Thermosyntropha* from the Firmicutes phylum exhibited higher relative abundance during incubation with acetate, thiosulfate, and tetrathionate (Figure 15). An anaerobic thermophilic strain, L-60T, of this genus was isolated from a Chinese hot spring (Zhang et al., 2012). This strain was able to utilize sulfate, sulfite, thiosulfate, nitrate, fumarate, or Fe (III) as electron acceptors (Zhang et al., 2012).

The highest relative abundance of the *Thermovenabulum* was observed during the 24 h incubation period in the presence of tetrathionate (Figure 15). A similar increase in abundance within this genus was also observed after a 24 h incubation with thiosulfate (Figure 15). Notably, a strain type of *Thermovenabulum* was isolated from microbial mats in thermal waters in the Great Artesian Basin, with temperatures similar to those in the Bizovac source (Ogg et al., 2010). In cultivation experiments, this strain showed growth in the presence of electron acceptors such as Fe (III), Mn (IV), thiosulfate, and elemental sulfur (Ogg et al., 2010).

The *Thermus* genus exhibited significantly higher relative abundance after a 48 h incubation period in the presence of thiosulfate, tetrathionate, and thiocyanate (Figure 15). This observed increase in relative abundance is consistent with the known phenotype of thiosulfate oxidation in this genus. The combination of the higher relative abundance across all incubations with sulfur substrates and considering the physiological and genomic characteristics of strains such as *Thermus tenuipuniceus* (Zhou et al., 2018), a recently described representative isolated from a terrestrial geothermal spring, and *Thermus thermophilus* strain JL-18 (Murugapiran et al., 2013), provides strong basis for the hypothesis that *Thermus* genera from Bizovac biofilm possesses the metabolic capability to utilize thiosulfate as an electron donor. It is also worth noting that several strains of the *Thermus* genus are known for their ability to reduce metals, making them valuable candidates for bioremediation applications (Ranawat et al., 2018).

In contrast, the genera *Hydrogenophilus* and *Tepidiphilus* of the *Hydrogenophilaceae* family in the Bizovac sample exhibited lower relative abundances in most substrate incubations compared to the HPG-only control at both time points (Figure 15). For the genus *Hydrogenophilus*, the addition of acetate resulted in a decreased relative abundance after both 24 and 48 h of incubation (Figure 15), whereas incubation with pyruvate resulted in a consistent relative abundance of this genus at both time points (11 %, Figure 15). The addition of thiosulfate and tetrathionate also led to lower relative abundances of this genus after 24 and 48 h of incubation, respectively, while the addition of thiocyanate resulted in the most significant decrease in relative abundance of the *Hydrogenophilus* genus at both time points (Figure 15).

Two ASVs related to the genus *Tepidiphilus* exhibited higher abundance after 24 h of incubation with acetate than in the HPG-only control (Figure 15). However, lower abundances of this genus were observed after 24 h with all other substrate additions (Figure 15). Compared to the HPG-only control, the relative abundance of the genus *Tepidiphilus* was lower after 48 h in all incubations with substrate additions, except for the incubation with pyruvate, where the relative abundance of *Tepidiphilus* remained consistent with the HPG-only control (Figure 15). These results were rather surprising, as most species of the genera *Hydrogenophilus*, such as *Hydrogenophilus thermoluteolus* (Hayashi et al., 1999) and *Hydrogenophilus islandicus* (Vésteinsdóttir et al., 2011), originally isolated from a hot spring, are characterize as facultative chemolithoautotrophs that can use hydrogen as an electron donor, carbon dioxide as a carbon source and acetate and pyruvate as electron donors and carbon sources. Similarly, several species of the *Tepidiphilus* genus, isolated from terrestrial hot springs, have been primarily characterized as chemolithotrophic or mixotrophic microorganisms capable of utilizing inorganic electron donors like reduced sulfuric compounds or hydrogen (Podar et al., 2018). Nevertheless, the addition of acetate, pyruvate, and sulfur substrates did not result in an overall positive effect on the relative abundance of either of these genera (Figure 15). This outcome suggests that other microorganisms in the Bizovac biofilm community, stimulated by the added substrates, produced compounds or metabolites that negatively affected relative abundance of *Hydrogenophilus* and *Tepidiphilus*. Alternatively, other microorganisms in the biofilm community, such as members of phyla Thermotogota or Bacillota, may possess higher affinities or more efficient metabolic pathways for rapidly utilizing the added substrates, thus leaving fewer resources available for genera like *Hydrogenophilus* and *Tepidiphilus*.

5.4.3. Functional annotation of genes in biofilm samples

Both experiments with biofilm incubations showed a significant increase in metabolic activity when the biofilms were incubated with thiosulfate. Therefore, sulfur metabolism was selected for more detailed analysis. All metabolic pathways involved in the sulfur cycle (Wu et al., 2021) were detected in the Bizovac biofilms (Figure 22): assimilative sulfur reduction (ASR), dissimilative sulfur reduction (DSR) and sulfur oxidation (SoX). ASR relates to the assimilation of sulfur as a substrate for the synthesis of biological molecules and includes cys family genes (Wu et al., 2021). DSR pathway, in which sulfur compounds are used as electron acceptors, includes the dsr and apr genes, while SoX is mainly associated with energy processes that utilize sulfur compounds in processes related to electron transfer and includes the SoX family of

proteins involved in thiosulfate metabolism (Wu et al., 2021). The soxB gene, encoding the thiosulfohydrolase soxB, is the most conserved component of the sulfur-oxidizing SoX system and catalyzes the dissimilative oxidation of thiosulfate and other sulfur compounds (Sakurai et al., 2010). It has been found in several SOB including Chlorobiota, Pseudomonadota (Alpha- and Gamma- proteobacteria) and Acidithiobacillia members (Yamamoto et al., 2011). In the Bizovac biofilm, the complete set of SOX genes was detected in MAG from the family *Aquificaceae* and 2 MAGs from the class Alphaproteobacteria (families *Acetobacteraceae* and *Rhodobacteraceae,* Figure 22*)*. These results, together with the results of the BONCAT-CARD-FISH experiment and the BONCAT-FACS-seq experiment, suggest that the thiosulfate metabolic activity in the Bizovac biofilms is carried out by several members of the Pseudomonadota community. In addition to thiosulfate oxidation, MAG which belongs to the *Aquificaceae* family, also showed the ability for assimilatory and dissimilatory sulfate reduction, dissimilatory nitrate reduction, and denitrification (Figure 22). Members of the phylum Aquificota are commonly found in thermal biofilms (e.g., Malygina et al., 2023).

Genes involved in ASR were found to be the most diverse in the Bizovac biofilm, belonging to many different phyla including MAGs associated with *Thermodesulfovibrio* (Nitrospirota phylum), Plantomycetota phylum, Acidobacteriota phylum, *Azoarcus* and *Immunidisolibacter* genera of the class Gammaproteobacteria, *Anaerolineaceae* family, and Cyanobacteria. Except for ASR, *Thermodesulfovibrio* MAG revealed the presence of all DSR genes (dsrAB, sat, aprAB, Figure 22). Moreover, all Chloroflexota MAGs from Bizovac biofilm displayed ability of dissimilatory sulfate reduction (Figure 22). This pathway was also mainly associated with the dominant primary producers in the Porcelana hot springs (Konrad et al., 2023). In this spring with temperature similar to the Bizovac source, Chloroflexota were the most abundant and active taxa for both sulfate-to-sulfite and sulfite-to-sulfide reactions (Konrad et al., 2023). The changes in diversity and activity of various sulfur-metabolizing bacteria in microbial biofilms from Bizovac demonstrated their significant role in hot spring environments.

6. CONCLUSIONS

The overall research and results presented in this doctoral thesis provide insight into the biodiversity of the microbial community of geothermal biofilms and their ecological role, expanding the current knowledge of thermal ecosystems.

The main final remarks of this thesis can be summarized in the following conclusions:

1. Thermal biofilms are stable systems through seasons in terms of their geochemistry and microbial community composition.

2. Temperature and sample origin are the main determinants of biofilm community composition in geothermal environments.

3. BONCAT-CARD-FISH method can be successfully applied on geothermal biofilms and presents fast and straightforward way for linking taxonomic identity and metabolic activity of this microenvironments.

4. BONCAT-FACS method is a non-destructive approach that allows downstream sequencing of active biofilm populations and can provide information on a single-cell resolution in relatively short period of time

5. Addition of acetate led to lower metabolic activity for Gammaproteobacteria and Chloroflexota populations in incubations of biofilms from Bizovac and Tuhelj

6. Presence of light did not affect activity od microbial populations in incubations of biofilms from Bizovac and Tuhelj.

7. Glucose and thiosulfate led to the highest increased in metabolic activity in incubations of biofilms from Bizovac and Tuhelj sources.

8. Both biofilms from Bizovac and Tuhelj sources possess complete biogeochemical cycles, as well as genes involved in metal reduction, arsenate oxidoreduction and selenate reduction.

9. Genes involved in sulfur metabolism in Bizovac biofilms are associated with members of phyla Pseudomonadota and Nitrospirota as well as primary producers Chloroflexota.

7. REFERENCES

Acar Kirit, H., Bollback, J. P., Lagator, M (2022) The Role of the Environment in Horizontal Gene Transfer. *Mol. Biol. Evol.* **39** (11), msac220.

Achtman, M., Wagner, M. (2008) Microbial diversity and the genetic nature of microbial species. *Nat. Rev. Microbiol.* **6** (6), 431-440.

Adams, A., Thompson, K. D. (2011) Development of diagnostics for aquaculture: challenges and opportunities. *Aquac. Res.* **42**, 93–102.

Albertsen, M., Karst, S. M., Ziegler, A. S., Kirkegaard, R. H., Nielsen, P. H. (2015) Back to basics—the influence of DNA extraction and primer choice on phylogenetic analysis of activated sludge communities. *PloS One* **10** (7), e0132783.

Alcamán-Arias, M. E., Pedrós-Alió, C., Tamames, J., Fernández, C., Pérez-Pantoja, D., Vásquez, M., Díez, B. (2018) Diurnal changes in active carbon and nitrogen pathways along the temperature gradient in porcelana hot spring microbial mat. *Front. Microbiol.* **9**, 2353.

Alcolombri, U., Pioli, R., Stocker, R., Berry, D. (2022) Single-cell stable isotope probing in microbial ecology. *ISME Commun.* **2** (1), 1-9.

Ali, S., Khan, S. A., Hamayun, M., Lee, I. J. (2023) The Recent Advances in the Utility of Microbial Lipases: A Review. *Microorganisms* **11** (2), 510.

Amann, R. I., Fuchs, B. M. (2008) Single-cell identification in microbial communities by improved fluorescence in situ hybridization techniques. *Nat. Rev. Microbiol.* **6** (5), 339–348.

Amann, R. I., Krumholz, L., Stahl, D. A. (1990) Fluorescent - oligonucleotide probing of whole cells for determinative, phylogenetic, and environmental studies in microbiology. *J Bacteriol.* **172** (2), 762–770.

Amann, R. I., Ludwig, W., Schleifer, K. H. (1995) Phylogenetic identification and in situ detection of individual microbial cells without cultivation. *Microbiol. Rev.* **59** (1), 143–169.

Amidzadeh, Z., Behbahani, A. B., Erfani, N., Sharifzadeh, S., Ranjbaran, R., Moezi, L., Aboualizadeh, F., Okhovat, M. A., Alavi, P., Azarpira, N. (2014) Assessment of different permeabilization methods of minimizing damage to the adherent cells for detection of intracellular RNA by flow cytometry. *Avicenna J. Med. Biotechnol.* **6** (1), 38–46.

Anantharaman, K., Brown, C. T., Hug, L. A., Sharon, I., Castelle, C. J., Probst, A. J., Thomas, B.C., Singh, A., Wilkins, M. J., Karaoz, U., Brodie, E. L. (2016) Thousands of microbial genomes shed light on interconnected biogeochemical processes in an aquifer system. *Nat. Commun.* **7**, 13219.

Apprill, A., McNally, S., Parsons, R., Weber, L. (2015) Minor revision to V4 region SSU rRNA 806R gene primer greatly increases detection of SAR11 bacterioplankton. *Aquat. Microb. Ecol.* **75**, 129–137.

Aramaki, T., Blanc-Mathieu, R., Endo, H., Ohkubo, K., Kanehisa, M., Goto, S., Ogata, H. (2020) KofamKOALA: KEGG ortholog assignment based on profile HMM and adaptive score threshold. *Bioinformatics* **36** (7), 2251–2252.

Arnórsson, S., Bjarnason, J.Ö., Giroud, N., Gunnarsson, I., Stefánsson, A. (2006) Sampling and analysis of geothermal fluids. *Geofluids* **6** (3), 203–216.

Azeredo, J., Azevedo, N. F., Briandet, R., Cerca, N., Coenye, T., Costa, A. R., Desvaux, M., Di Bonaventura, G., Hébraud, M., Jaglic, Z., Kačániová, M., Knøchel, S., Lourenço, A., Mergulhão, F., Meyer, R. L., Nychas, G., Simões, M., Tresse, O., Sternberg, C. (2017) Critical review on biofilm methods. *Crit. Rev. Microbiol.* **43** (3), 313–351.

Babin, B. M., Atangcho, L., van Eldijk, M. B., Sweredoski, M. J., Moradian, A., Hess, S., Tolker-Nielsen, T., Newman, D. K., Tirrell, D. A. (2017) Selective proteomic analysis of antibiotic-tolerant cellular subpopulations in Pseudomonas aeruginosa biofilms. *mBio* **8** (5), e01593-17.

Barathi, S., Aruljothi, K. N., Karthik, C., Padikasan, I. A., Ashokkumar, V. (2022) Biofilm mediated decolorization and degradation of reactive red 170 dye by the bacterial consortium isolated from the dyeing industry wastewater sediments. *Chemosphere* **286** (Pt 3), 131914.

Barnett, D. J., Arts, I. C., Penders, J. (2021) microViz: an R package for microbiome data visualization and statistics. *J. Open Source Softw.* **6** (63), 3201.

Bauld, J., Brock, T. D. (1973) Ecological studies of *Chloroflexis*, a gliding photosynthetic bacterium. *Archiv. Mikrobiol.* **92**, 267–284.

Baumgartner, L. K., Reid, R. P., Dupraz, C., Decho, A. W., Buckley, D. H., Spear, J. R., Przekop, K. M., Visscher, P. T. (2006) Sulfate reducing bacteria in microbial mats: Changing paradigms, new discoveries. *Sediment. Geol.* **185**, 131–145.

Berg, G., Rybakova, D., Fischer, D., Cernava, T., Vergès, M. C., Charles, T., Chen, X., Cocolin, L., Eversole, K., Corral, G. H., Kazou, M., Kinkel, L., Lange, L., Lima, N., Loy, A., Macklin, J. A., Maguin, E., Mauchline, T., McClure, R., Mitter, B., Ryan, M., Sarand, I., Smidt, H., Schelkle, B., Roume, H., Kiran, G. S., Selvin, J., Souza, R. S. C., van Overbeek, L., Singh, B. K., Wagner, M., Walsh, A., Sessitsch, A., Schloter, M. (2020) Microbiome definition re-visited: old concepts and new challenges. *Microbiome* **8** (1), 103.

Bidnenko, E., Mercier, C., Tremblay, J., Tailliez, P., Kulakauskas, S. (1998) Estimation of the state of the bacterial cell wall by fluorescent In situ hybridization. *Appl. Environ. Microbiol.* **64** (8), 3059–3062.

Biller, S. J., Berube, P. M., Dooley, K., Williams, M., Satinsky, B. M., Hackl, T., Hogle, S. L., Coe, A., Bergauer, K., Bouman, H. A., Browning, T. J., Corte, D., Hassler, C., Hulston, D., Jacquot, J. E., Maas, E. W., Reinthaler, T., Sintes, E., Yokokawa, T., Chisholm, S. W. (2019) Marine microbial metagenomes sampled across space and time. *Sci. data* **6**, 180176.

Bird, R. E., Lemmel, S. A., Yu, X., Zhou, Q. A. (2021) Bioorthogonal Chemistry and Its Applications. *Bioconjug. Chem.* **32** (12), 2457–2479.

Björnsson, L., Hugenholtz, P., Tyson, G. W. Blackall, L. L. (2002) Filamentous Chloroflexi (green non-sulfur bacteria) are abundant in wastewater treatment processes with biological nutrient removal. *Microbiology* **148** (Pt 8), 2309–2318.

Boden, R., Hutt, L.P., Rae, A.W. (2017) Reclassification of *Thiobacillus aquaesulis* (Wood & Kelly, 1995) as *Annwoodia aquaesulis* gen. nov., comb. nov., transfer of *Thiobacillus* (Beijerinck, 1904) from the Hydrogenophilales to the Nitrosomonadales, proposal of Hydrogenophilalia class. nov. within the "Proteobacteria," and four new families within the orders Nitrosomonadales and Rhodocyclales. *Int. J. Syst. Evol. Microbiol.* **67** (5), 1191–1205.

Boomer, S.M., Noll, K.L., Geesey, G.G., Dutton, B.E. (2009) Formation of multilayered photosynthetic biofilms in an alkaline thermal spring in Yellowstone national Park, Wyoming. *Appl. Environ. Microbiol.* **75** (8), 2464–2475.

Boughner, L.A., and Singh, P. (2016) Microbial Ecology: Where are we now? *Postdoc J.* **4** (11), 3-17.

Bowers, R. M., Kyrpides, N. C., Stepanauskas, R., Harmon-Smith, M., Doud, D., Reddy, T. B. K., Schulz, F., Jarett, J., Rivers, A. R., Eloe-Fadrosh, E. A., Tringe, S. G., Ivanova, N. N., Copeland, A., Clum, A., Becraft, E. D., Malmstrom, R. R., Birren, B., Podar, M., Bork, P.,

Weinstock, G. M., Garrity, G. M., Dodsworth, J. A., Yooseph, S., Sutton, G., Glöckner, F. O., Gilbert, J. A., Nelson, W. C., Hallam, S. J., Jungbluth, S. P., Ettema, T. J. G., Tighe, S., Konstantinidis, K. T., Liu, W. T., Baker, B. J., Rattei, T., Eisen, J. A., Hedlund, B., McMahon, K. D., Fierer, N., Knight, R., Finn, R., Cochrane, G., Karsch-Mizrachi, I., Tyson, G. W., Rinke, C.; Lapidus, A., Meyer, F., Yilmaz, P., Parks, D. H., Eren, A. M., Schriml, L., Banfield, J. F., Hugenholtz, P., Woyke, T. (2017) Minimum information about a single amplified genome (MISAG) and a metagenome-assembled genome (MIMAG) of bacteria and archaea. *Nat. Biotechnol.* **35** (8), 725–731.

Braissant, O., Astasov-Frauenhoffer, M., Waltimo, T., Bonkat, G. (2020) Review of methods to determine viability, vitality, and metabolic rates in microbiology. *Front. Microbiol.* **11**, 547458.

Brock, T. D. (1969) Vertical zonation in hot spring algal mats. *Phycologia* **8**, 201–205.

Brock, T. D. (1987) The study of microorganisms in situ: progress and problems. *Symp. Soc. Gen. Microbiol.* **41**, 1–17.

Brock, T. D., Brock, M. L. (1969) Effect of light intensity on photosynthesis by thermal algae adapted to natural and reduced sunlight. *Limnol. Oceanogr.* **14**, 334–341.

Brock, T. D., Freeze, H. (1969) *Thermus aquaticus* gen. n. and sp. n., a non-sporulating extreme thermophile. *J. Bacteriol.* **98** (1), 289–297.

Brown, C. T., Hug, L. A., Thomas, B. C., Sharon, I., Castelle, C. J., Singh, A., Wilkins, M. J., Wrighton, K. C., Williams, K. H., Banfield, J. F. (2015) Unusual biology across a group comprising more than 15 % of domain Bacteria. *Nature* **523** (7559), 208–211.

Burmølle, M., Ren, D., Bjarnsholt, T., Sørensen, S. J. (2014) Interactions in multispecies biofilms: do they actually matter? *Trends Microbiol.* **22** (2), 84–91.

Buttler, J. Drown, D.M. (2023) Accuracy and Completeness of Long Read Metagenomic Assemblies. *Microorganisms* **11** (1), 96.

Callahan, B. J., McMurdie, P. J., Rosen, M. J., Han, A. W., Johnson, A. J., Holmes, S. P. (2016a) DADA2: High-resolution sample inference from Illumina amplicon data. *Nat. Methods* **13** (7), 581–583.

Callahan, B. J., Sankaran, K., Fukuyama, J. A., McMurdie, P. J., & Holmes, S. P. (2016) Bioconductor Workflow for Microbiome Data Analysis: from raw reads to community analyses. *F1000Res.* **5**, 1492.

Cardenas, E., Tiedje, J. M. (2008) New tools for discovering and characterizing microbial diversity. *Curr. Opin. Biotechnol.* **19** (6), 544–549.

Castro, L., Blázquez, M. L., González, F., Muñoz, J. Á. (2021) Biohydrometallurgy for Rare Earth Elements Recovery from Industrial Wastes. *Molecules* **26** (20), 6200.

Chaudhary, P., Singh, S., Chaudhary, A., Sharma, A., Kumar, G. (2022) Overview of biofertilizers in crop production and stress management for sustainable agriculture. *Front. Plant. Sci.* **13**, 930340.

Chaumeil, P. A., Mussig, A. J., Hugenholtz, P., Parks, D. H. (2019) GTDB-Tk: a toolkit to classify genomes with the Genome Taxonomy Database. *Bioinformatics* **36** (6), 1925–1927.

Cheng, K. C., Catchmark, J. M., Demirci, A. (2009) Enhanced production of bacterial cellulose by using a biofilm reactor and its material property analysis. *J. Biol. Eng.* **3**, 12.

Cheng, J. H., Zhang, X. Y., Wang, Z., Zhang, X., Liu, S. C., Song, X. Y., Zhang, Y. Z., Ding, J. M., Chen, X. L., Xu, F. (2021) Potential of Thermolysin-like Protease A69 in Preparation of Bovine Collagen Peptides with Moisture-Retention Ability and Antioxidative Activity. *Mar. Drugs.* **19** (12), 676.

Chernitsyna, S., Elovskaya, I., Pogodaeva, T., Bukin, S., Zakharenko, A., Zemskaya, T. (2023) Bacterial Communities in a Gradient of Abiotic Factors Near a Sulfide Thermal Spring in Northern Baikal. *Diversity* **15** (2), 298.

Chien, A., Edgar, D. B., Trela, J. M. (1976) Deoxyribonucleic acid polymerase from the extreme thermophile *Thermus aquaticus*. *J. Bacteriol.* **127** (3), 1550–1557.

Chuang, D. S. W., Liao, J. C. (2021) Role of cyanobacterial phosphoketolase in energy regulation and glucose secretion under dark anaerobic and osmotic stress conditions. *Metab. Eng.* **65**, 255–262.

Clarridge J. E. (2004) Impact of 16S rRNA gene sequence analysis for identification of bacteria on clinical microbiology and infectious diseases. *Clin. Microbiol. Rev.* **17** (4), 840–862.

Coman, C., Chiriac, C. M., Robeson, M. S., Ionescu, C., Dragos, N., Barbu-Tudoran, L., Andrei, A. Ş., Banciu, H. L., Sicora, C., Podar, M. (2015) Structure, mineralogy, and microbial diversity of geothermal spring microbialites associated with a deep oil drilling in Romania. *Front. Microbiol.* **6**, 253.

Coman, C., Drugă, B., Hegedus, A., Sicora, C., Dragoş, N. (2013) Archaeal and bacterial diversity in two hot spring microbial mats from a geothermal region in Romania. *Extremophiles* **17** (3), 523–534.

Costa, A. M., Mergulhão, F. J., Briandet, R., Azevedo, N. F. (2017) It is all about location: how to pinpoint microorganisms and their functions in multispecies biofilms. *Future Microbiol.* **12**, 987–999.

Costerton J. W. (1995) Overview of microbial biofilms. *J. Ind. Microbiol.* **15** (3), 137–140.

Costerton, J. W., Lewandowski, Z., Caldwell, D. E., Korber, D. R., Lappin-Scott, H. M. (1995) Microbial biofilms. *Annu. Rev. Microbiol.* **49**, 711–745.

Cox, M. J., Cookson, W. O., Moffatt, M. F. (2013). Sequencing the human microbiome in health and disease. *Hum. Mol. Genet.* **22** (R1), R88–R94.

Cui, J. L., Chen, C., Qin, Z. H., Yu, C. N., Shen, H., Shen, C. F., Chen, Y. X. (2012). *Ying yong sheng tai xue bao (The journal of applied ecology)* **23** (11), 3218–3226.

Ćuković Ignjatović, N., Vranješ, A., Ignjatović, D., Milenić, D., Krunić, O. (2021) Sustainable Modularity Approach to Facilities Development Based on Geothermal Energy Potential. *Appl. Sci.* **11**, 2691.

Daims, H., Brühl, A., Amann, R., Schleifer, K. H., Wagner, M. (1999) The domain-specific probe EUB338 is insufficient for the detection of all bacteria: development and evaluation of a more comprehensive probe set. *Syst. Appl. Microbiol.* **22**, 434-444.

Daims, H., Lücker, S., Wagner, M. (2006) daime, a novel image analysis program for microbial ecology and biofilm research. *Environ. Microbiol.* **8** (2), 200–213.

Damer, B., Deamer D. (2015) Coupled phases and combinatorial selection in fluctuating hydrothermal pools: a scenario to guide experimental approaches to the origin of cellular life. *Life* **5** (1), 872–887

Damer, B., Deamer, D. (2020) The hot spring hypothesis for an origin of life. *Astrobiology* **20** (4), 429–52.

DeCastro, M. E., Rodríguez-Belmonte, E., González-Siso, M. I. (2016) Metagenomics of thermophiles with a focus on discovery of novel thermozymes. *Front. Microbiol.* **7**, 1521.

Della Porta, G., Hoppert, M., Hallmann, C., Schneider, D., Reitner, J. (2022) The influence of microbial mats on travertine precipitation in active hydrothermal systems (Central Italy). *Depositional Rec.* **8** (1), 165–209.

de los Ríos, A., Grube, M., Sancho, L. G., Ascaso, C. (2007) Ultrastructural and genetic characteristics of endolithic cyanobacterial biofilms colonizing Antarctic granite rocks. *FEMS Microbiol. Ecol.* **59** (2), 386–395.

Des Marais, D. J., Walter, M. R. (2019) Terrestrial Hot Spring Systems: Introduction. *Astrobiology* **19** (12), 1419–1432.

D'Imperio, S., Lehr, C. R., Breary, M., McDermott, T. R. (2007) Autecology of an arsenite chemolithotroph: sulfide constraints on function and distribution in a geothermal spring. *Appl. Environ. Microbiol.* **73** (21), 7067–7074.

Di Salvo, E., Lo Vecchio, G., De Pasquale, R., De Maria, L., Tardugno, R., Vadalà, R., Cicero, N. (2023) Natural Pigments Production and Their Application in Food, Health and Other Industries. *Nutrients* **15** (8), 1923.

Dobretsov, S., Abed, R. M. M., Al Maskari, S. M. S., Al Sabahi, J. N., Victor, R. (2011) Cyanobacterial mats from hot springs produce antimicrobial compounds and quorum-sensing inhibitors under natural conditions. *J. Appl. Phycol.* **23** (6), 983–993.

Doemel, W. N., Brock, T. D. (1977) Structure, growth, and decomposition of laminated algal-bacterial mats in alkaline hot springs. *Appl. Env. Microbiol.* **34** (4), 433–452.

Donlan, R. M., Costerton, J. W. (2002) Biofilms: survival mechanisms of clinically relevant microorganisms. *Clin. Microbiol. Rev.* **15** (2), 167–193.

Du, Z., Behrens, S. F. (2021) Tracking de novo protein synthesis in the activated sludge microbiome using BONCAT-FACS. *Water Res.* **205**, 117696.

Duman, M., Altun, S., Saticioglu, I. B. (2022) General Assessment of Approaches to the Identification of Aquatic Bacterial Pathogens: A Methodological Review. *N. Am. J. Aquac.* **84** (1), 405-426.

Dumorné, K., Córdova, D. C., Astorga-Eló, M., Renganathan, P. (2017) Extremozymes: A Potential Source for Industrial Applications. *J. Microbiol. Biotechnol.* **27** (4), 649–659.

Dyksma, S., Lenk, S., Sawicka, J. E., Mußmann, M. (2018) Uncultured *Gammaproteobacteria* and *Desulfobacteraceae* Account for Major Acetate Assimilation in a Coastal Marine Sediment. *Front Microbiol.* **9**, 3124.

Eloe-Fadrosh, E. A., Paez-Espino, D., Jarett, J., Dunfield, P. F., Hedlund, B. P., Dekas, A. E., Grasby, S. E., Brady, A. L., Dong, H., Briggs, B. R., Li, W. J., Goudeau, D., Malmstrom, R., Pati, A., Pett-Ridge, J., Rubin, E. M., Woyke, T., Kyrpides, N. C., Ivanova, N. N. (2016) Global metagenomic survey reveals a new bacterial candidate phylum in geothermal springs. *Nat. Commun.* **7**, 10476.

Emerson, D., Agulto, L., Liu, H., Liu, L. (2008) Identifying and Characterizing Bacteria in an Era of Genomics and Proteomics. *BioScience* **58** (10), 925-936.

Ferrari, B. C., Tujula, N., Stoner, K., Kjelleberg, S. (2006) Catalyzed reporter deposition-fluorescence in situ hybridization allows for enrichment-independent detection of microcolony-forming soil bacteria. *Appl. Environ. Microbiol.* **72** (1), 918–922.

Finn, R. D., Bateman, A., Clements, J., Coggill, P., Eberhardt, R. Y., Eddy, S. R., Heger, A., Hetherington, K., Holm, L., Mistry, J., Sonnhammer, E. L., Tate, J., Punta, M. (2014) Pfam: the protein families database. *Nucleic Acids Res.* **42**, D222–D230.

Finn, R. D., Clements, J., Eddy, S. R. (2011) HMMER web server: interactive sequence similarity searching. *Nucleic Acids Res.* **39**, W29–37.

Franco-Duarte, R., Černáková, L., Kadam, S., Kaushik, K. S., Salehi, B., Bevilacqua, A., Corbo, M. R., Antolak, H., Dybka-Stępień, K., Leszczewicz, M., Relison Tintino, S., Alexandrino de Souza, V. C., Sharifi-Rad, J., Coutinho, H. D. M., Martins, N., Rodrigues, C. F. (2019) Advances in Chemical and Biological Methods to Identify Microorganisms-From Past to Present. *Microorganisms* **7** (5), 130.

Gallo, G., Aulitto, M., Contursi, P., Limauro, D., Bartolucci, S., Fiorentino, G. (2021) Bioprospecting of Extremophilic Microorganisms to Address Environmental Pollution. *J. Vis. Exp.* **178**, 10.3791/63453.

Gao, S., Li, Z., Hou, Y., Wang, A., Liu, Q., Huang, C. (2022) Effects of different carbon sources on the efficiency of sulfur-oxidizing denitrifying microorganisms. *Environ Res.* **204** (Pt A), 111946.

Gevers, D., Cohan, F. M., Lawrence, J. G., Spratt, B. G., Coenye, T., Feil, E. J., Stackebrandt, E., Van de Peer, Y., Vandamme, P., Thompson, F. L., Swings, J. (2005) Opinion: Re-evaluating prokaryotic species. *Nat. Rev. Microbiol.* **3** (9), 733–739.

Ghilamicael, A. M., Budambula, N. L. M., Anami, S. E., Mehari, T., Boga, H. I. (2017) Evaluation of prokaryotic diversity of five hot springs in Eritrea. *BMC Microbiol.* **17** (1), 203.

Gianfaldoni, S., Tchernev, G., Wollina, U., Roccia, M. G., Fioranelli, M., Gianfaldoni, R., Lotti, T. (2017) History of the Baths and Thermal Medicine. *Open Access Maced. J. Med. Sci.* **5** (4), 566–568.

Gillis, M., Vandamme, P., De Vos, P., Swings, J., Kersters, K. (2001) Polyphasic taxonomy. In: *Bergey's Manual of Systematic Bacteriology 1* (Boone, D. R. and Castenholtz, R. W. eds.), Springer, New York, 43-48.

Ginolhac, A., Jarrin, C., Gillet, B., Robe, P., Pujic, P., Tuphile, K., Bertrand, H., Vogel, T. M., Perrière, G., Simonet, P., Nalin, R. (2004) Phylogenetic analysis of polyketide synthase I domains from soil metagenomic libraries allows selection of promising clones. *Appl. Environ. Microbiol.* **70** (9), 5522–5527.

Guerrieri, N., Fantozzi, L., Lami, A., Musazzi, S., Austoni, M., Orrù, A., Marziali, L., Borgonovo, G., Scaglioni, L. (2022) Biofilm and Rivers: The Natural Association to Reduce Metals in Waters. *Toxics* **10** (12), 791.

Gumerov, V. M., Mardanov, A. V., Beletsky, A. V., Bonch-Osmolovskaya, E. A., Ravin, N. V. (2011) Molecular analysis of microbial diversity in the Zavarzin Spring, Uzon Caldera, Kamchatka. *Microbiology* **80**, 244–251.

Guo, L., Wang, G., Sheng, Y., Sun, X., Shi, Z., Xu, Q., Mu, W. (2020) Temperature governs the distribution of hot spring microbial community in three hydrothermal fields, Eastern Tibetan Plateau Geothermal Belt, Western China. *Sci. Total Environ.* **720**, 137574.

Gupta, R., Beg, Q. K., Lorenz, P. (2002) Bacterial alkaline proteases: molecular approaches and industrial applications. *Appl. Microbiol. Biotechnol.* **59** (1), 15–32.

Gupta, R., Gigras, P., Mohapatra, H., Goswami, V. K., Chauhan, R. (2003) Microbial α-amylases: a biotechnological perspective. *Process Biochem.* **38** (11), 1599-1616.

Gupta, R. S., Chander, P., George, S. (2013) Phylogenetic framework and molecular signatures for the class Chloroflexi and its different clades; proposal for division of the class Chloroflexia class. nov. [corrected] into the suborder Chloroflexineae subord. nov., consisting of the emended family Oscillochloridaceae and the family Chloroflexaceae fam. nov., and the suborder Roseiflexineae subord. nov., containing the family Roseiflexaceae fam. nov. *Antonie van Leeuwenhoek* **103** (1), 99–119.

Gurevich, A., Saveliev, V., Vyahhi, N., Tesler, G. (2013) QUAST: Quality Assessment Tool for Genome Assemblies. *Bioinformatics* **29** (8), 1072–75.

Gutierrez, T. (2019) Aerobic hydrocarbondegrading Gammaproteobacteria: Porticoccus. In: *Hydrocarbon and lipid microbiology protocols* (McGenity, T. J., Timmis, K. N., Nogales, B. eds). Springer, Berlin.

Guzmán-Soto, I., McTiernan, C., Gonzalez-Gomez, M., Ross, A., Gupta, K., Suuronen, E. J., Mah, T. F., Griffith, M., Alarcon, E. I. (2021) Mimicking biofilm formation and development: Recent progress in *in vitro* and *in vivo* biofilm models. *iScience* **24** (5), 102443.

Gürtler, V., Stanisich, V. A. (1996) New approaches to typing and identification of bacteria using the 16S-23S rDNA spacer region. *Microbiology* **142** (Pt 1), 3–16.

Hagemann, M., Hess, W. R. (2018) Systems and synthetic biology for the biotechnological application of cyanobacteria. *Curr. Opin. Biotechnol.* **49**, 94–99.

Hall-Stoodley, L., Costerton, J. W., Stoodley, P. (2004) Bacterial biofilms: from the natural environment to infectious diseases. *Nat. Rev. Microbiol.* **2** (2), 95–108.

Hamilton, T. L., Bennett, A. C., Murugapiran, S. K., Havig, J. R. (2019) Anoxygenic Phototrophs Span Geochemical Gradients and Diverse Morphologies in Terrestrial Geothermal Springs. *mSystems* **4** (6), e00498-19.

Haque, M. M., Mosharaf, M. K., Khatun, M., Haque, M. A., Biswas, M. S., Islam, M. S., Islam, M. M., Shozib, H. B., Miah, M. M. U., Molla, A. H., Siddiquee, M. A. (2020) Biofilm

Producing Rhizobacteria With Multiple Plant Growth-Promoting Traits Promote Growth of Tomato Under Water-Deficit Stress. *Front. Microbiol.* **11**, 542053.

Hatzenpichler, R., Connon, S. A., Goudeau, D., Malmstrom, R. R., Woyke, T., Orphan, V. J. (2016) Visualizing in situ translational activity for identifying and sorting slow-growing archaeal-bacterial consortia. *Proc. Natl. Acad. Sci. U S A* **113** (28), E4069–E4078.

Hatzenpichler, R., Krukenberg, V., Spietz, R. L., Jay, Z. J. (2020) Next-generation physiology approaches to study microbiome function at single cell level. *Nat. Rev. Microbiol.* **18** (4), 241–256.

Hatzenpichler, R., Orphan, V.J. (2015) Detection of protein-synthesizing microorganisms in the environment via bioorthogonal noncanonical amino acid tagging (BONCAT). In: *Hydrocarbon and lipid microbiology protocols* (McGenity, T. J., Timmis, K. N., Nogales, B. eds). Springer, Berlin, 145–157.

Hatzenpichler, R., Scheller, S., Tavormina, P. L., Babin, B. M., Tirrell, D. A., Orphan, V. J. (2014) In situ visualization of newly synthesized proteins in environmental microbes using amino acid tagging and click chemistry. *Environ. Microbiol.* **16** (8), 2568–2590.

Hayashi, N. R., Ishida, T., Yokota, A., Kodama, T., Igarashi, Y. (1999) Hydrogenophilus thermoluteolus gen. nov., sp. nov., a thermophilic, facultatively chemolithoautotrophic, hydrogen-oxidizing bacterium. *Int. J. Syst. Bacteriol.* **49** (Pt 2), 783–786.

Hazen, T. C., Rocha, A. M., Techtmann, S. M. (2013) Advances in monitoring environmental microbes. *Curr. Opin. Biotechnol.* **24** (3), 526–533.

Hein, J. E., Fokin, V. V. (2010) Copper-catalyzed azide-alkyne cycloaddition (CuAAC) and beyond: new reactivity of copper(I) acetylides. *Chem. Soc. Rev.* **39** (4), 1302–1315.

Hidayat, M. Y., Saud, H. M., Samsudin, A. A. (2017) Isolation and characterization of sulphur oxidizing bacteria isolated from hot spring in Malaysia for biological deodorisation of hydrogen sulphide in chicken manure. *Media Peternakan* **40** (3), 178–187.

Houghton, K. M., Carere, C. R., Stott, M. B., McDonald, I. R. (2019) Thermophilic methanotrophs: in hot pursuit. *FEMS Microbiol. Ecol.* **95** (9), fiz125.

Huang, Q., Dong, C. Z., Dong, R. M., Jiang, H., Wang, S., Wang, G., Fang, B., Ding, X., Niu, L., Li, X., Zhang, C., Dong, H. (2011) Archaeal and bacterial diversity in hot springs on the Tibetan Plateau, China. *Extremophiles* **15** (5), 549–563.

Huang, R., Soneson, C., Ernst, F. G. M., Rue-Albrecht, K. C., Yu, G., Hicks, S. C., Robinson, M. D. (2020) TreeSummarizedExperiment: a S4 class for data with hierarchical structure. *F1000Res.* **9**, 1246.

Huson, D. H., Beier, S., Flade, I., Górska, A., El-Hadidi, M., Mitra, S., Ruscheweyh, H. J., Tappu, R. (2016) MEGAN Community Edition - Interactive Exploration and Analysis of Large-Scale Microbiome Sequencing Data. *PLoS Comput. Biol.* **12** (6), e1004957.

Hyatt, D., Chen, G. L., Locascio, P. F., Land, M. L., Larimer, F. W., Hauser, L. J. (2010) Prodigal: prokaryotic gene recognition and translation initiation site identification. *BMC Bioinformatics* **11**, 119.

Ibáñez, A., Garrido-Chamorro, S., Coque, J. J. R., Barreiro, C. (2023) From Genes to Bioleaching: Unraveling Sulfur Metabolism in Acidithiobacillus Genus. *Genes* **14** (9), 1772.

Ivanišević, G. (2008) Natural Health Resorts in Croatia. Croatian Academy of Medical Sciences, Committe for Health Tourism and Natural Remedies.1-70.'

Izquierdo, E., Delgado, A. (2018) Click chemistry in sphingolipid research. *Chem Phys Lipids.* **215**, 71–83.

Janda, J. M., Abbott, S. L. (2007) 16S rRNA gene sequencing for bacterial identification in the diagnostic laboratory: pluses, perils, and pitfalls. *J. Clin. Microbiol.* **45** (9), 2761–2764.

Jardine, J. L. (2022) Potential bioremediation of heavy metal ions, polycyclic aromatic hydrocarbons and biofilms with South African hot spring bacteria. *Bioremediat. J.* **26** (3), 261-269.

Jiang, D., Armour, C. R., Hu, C., Mei, M., Tian, C., Sharpton, T. J., Jiang, Y. (2019) Microbiome Multi-Omics Network Analysis: Statistical Considerations, Limitations, and Opportunities. *Front. Genet.* **10**, 995.

Kanehisa, M., Goto, S. (2000) KEGG: kyoto encyclopedia of genes and genomes. *Nucleic Acids Res.* **28** (1), 27–30.

Kang, D. D., Li, F., Kirton, E., Thomas, A., Egan, R., An, H., Wang, Z. (2019) MetaBAT 2: an adaptive binning algorithm for robust and efficient genome reconstruction from metagenome assemblies. *PeerJ.* **7**, e7359.

Kappler, U., Dahl, C. (2001) Enzymology and molecular biology of prokaryotic sulfite oxidation. *FEMS Microbiol Lett.* **203** (1), 1–9.

Kawai, S., Ishikawa, M., Hanada, S., Haruta, S. (2022) *Hydrogenophilus thiooxidans* sp. nov., a moderately thermophilic chemotrophic bacterium unable to grow on hydrogen gas, isolated from hot spring microbial mats. *Int. J. Syst. Evol. Microbiol.* **72** (5), 10.1099/ijsem.0.005355.

Khadka, S., Khadka, D., Poudel, R. C., Bhandari, M., Baidya, P., Sijapati, J., Maharjan, J. (2022) Production Optimization and Biochemical Characterization of Cellulase from *Geobacillus* sp. KP43 Isolated from Hot Spring Water of Nepal. *Biomed. Res. Int. 2022*, 6840409.

Kim, O. S., Cho, Y. J., Lee, K., Yoon, S. H., Kim, M., Na, H., Park, S. C., Jeon, Y. S., Lee, J. H., Yi, H., Won, S., Chun, J. (2012) Introducing EzTaxon-e: a prokaryotic 16S rRNA gene sequence database with phylotypes that represent uncultured species. *Int. J. Syst. Evol. Microbiol.* **62** (Pt 3), 716–721.

Kindaichi, T., Ito, T., Okabe, S. (2004) Ecophysiological interaction between nitrifying bacteria and heterotrophic bacteria in autotrophic nitrifying biofilms as determined by microautoradiography-fluorescence in situ hybridization. *Appl. Environ. Microbiol.* **70** (3), 1641–1650.

Klatt, J. M., Meyer, S., Häusler, S., Macalady, J. L., de Beer, D., Polerecky, L. (2016) Structure and function of natural sulphide-oxidizing microbial mats under dynamic input of light and chemical energy. *ISME J.* **10** (4), 921–933.

Kochhar, N., I K, K., Shrivastava, S., Ghosh, A., Rawat, V. S., Sodhi, K. K., Kumar, M. (2022) Perspectives on the microorganism of extreme environments and their applications. *Curr. Res. Microb. Sci.* **3**, 100134.

Kolmogorov, M., Yuan, J., Lin, Y., Pevzner, P. A. (2019) Assembly of long, error-prone reads using repeat graphs. *Nat. Biotechnol.* **37** (5), 540–546.

Konrad, R., Vergara-Barros, P., Alcorta, J., Alcamán-Arias, M.E., Levicán, G., Ridley, C., Díez, B. (2023) Distribution and Activity of Sulfur-Metabolizing Bacteria along the Temperature Gradient in Phototrophic Mats of the Chilean Hot Spring Porcelana. *Microorganisms* **11** (7), 1803.

Kostešić, E., Mitrović, M., Kajan, K., Marković, T., Hausmann, B., Orlić, S., Pjevac, P. (2023) Microbial Diversity and Activity of Biofilms from Geothermal Springs in Croatia. *Microb. Ecol.* 10.1007/s00248-023-02239-1. Online publication <https://doi.org/10.1007/s00248-023-02239-1>. Accessed October 02, 2023.

Kourmentza, C., Plácido, J., Venetsaneas, N., Burniol-Figols, A., Varrone, C., Gavala, H. N., Reis, M. A. M. (2017) Recent Advances and Challenges towards Sustainable Polyhydroxyalkanoate (PHA) Production. *Bioengineering* **4** (4), 55.

Krsmanovic, M., Biswas, D., Ali, H., Kumar, A., Ghosh, R., Dickerson, A. K. (2021) Hydrodynamics and surface properties influence biofilm proliferation. *Adv. Colloid Interface Sci.* **288**, 102336.

Keller-Costa, T., Kozma, L., Silva, S. G., Toscan, R., Gonçalves, J., Lago-Lestón, A., Kyrpides, N. C., Nunes da Rocha, U., Costa, R. (2022) Metagenomics-resolved genomics provides novel insights into chitin turnover, metabolic specialization, and niche partitioning in the octocoral microbiome. *Microbiome* **10** (1), 151.

Kubota, K. (2013) CARD-FISH for environmental microorganisms: Technical advancement and future applications. *Microbes Environ.* **28** (1), 3–12.

Kutscha, R., Pflügl, S. (2020) Microbial Upgrading of Acetate into Value-Added Products-Examining Microbial Diversity, Bioenergetic Constraints and Metabolic Engineering Approaches. *Int. J. Mol. Sci.* **21** (22), 8777.

Lederberg, J., Sagan, C. (1962) Microenvironments for life on Mars. *Proc. Natl. Acad. Sci. USA* **48** (9), 1473–1475.

Lee, D. J., Wong, B. T., Adav, S. S. (2014) Azoarcus taiwanensis sp. nov., a denitrifying species isolated from a hot spring. *Appl. Microbiol. Biotechnol.* **98** (3), 1301–1307.

Leizeaga, A., Estrany, M., Forn, I., Sebastián, M. (2017) Using Click-Chemistry for Visualizing *in Situ* Changes of Translational Activity in Planktonic Marine Bacteria. *Front. Microbiol.* **8**, 2360.

Li, H. (2018) Minimap2: Pairwise Alignment for Nucleotide Sequences. *Bioinformatics* **34** (18), 3094–3100.

Li, X., Chopp, D. L., Russin, W. A., Brannon, P. T., Parsek, M. R., Packman, A. I. (2015) Spatial patterns of carbonate biomineralization in biofilms. *Appl. Environ. Microbiol.* **81** (21), 7403–7410.

Li, H., Handsaker, B., Wysoker, A., Fennell, T., Ruan, J., Homer, N., Marth, G., Abecasis, G., Durbin, R., 1000 Genome Project Data Processing Subgroup (2009) The Sequence Alignment/Map format and SAMtools. *Bioinformatics* **25** (16), 2078–2079.

Li, W., Lin, J., Zhang, L., Zhu, K., Liu, X., Wang, Z., Cao, B., Guo, P. (2016) Mixotrophic denitrification desulfurization wastewater treatment process: bioreactor performance and analysis of the microbial community. *Pol. J. Environ. Stud.* **25** (6), 2491–2497.

Li, L., Ma, Z. S. (2019) Global microbiome diversity scaling in hot springs with DAR (Diversity-area relationship) profiles. *Front. Microbiol.* **10**, 118.

Limberger, J., Boxem, T., Pluymaekers, M., Bruhn, D., Manzella, A., Calcagno, P., Beekman, F., Cloetingh, S., van Wees, J. D. (2018) Geothermal energy in deep aquifers: A global assessment of the resource base for direct heat utilization. *Renew. Sust. Energ. Rev.* **82** (1), 961–975.

Lin, X., Wakeham, S. G., Putnam, I. F., Astor, Y. M., Scranton, M. I., Chistoserdov, A. Y., Taylor, G. T. (2006) Comparison of vertical distributions of prokaryotic assemblages in the anoxic Cariaco Basin and Black Sea by use of fluorescence in situ hybridization. *Appl. Environ. Microbiol.* **72** (4), 2679–2690.

Lindivat, M., Larsen, A., Hess-Erga, O. K., Bratbak, G., Hoell, I. A. (2020) Bioorthogonal Non-canonical Amino Acid Tagging Combined with Flow Cytometry for Determination of Activity in Aquatic Microorganisms. *Front. Microbiol.* **11**, 1929.

Liu, Q., Huang, C., Chen, X., Wu, Y., Lv, S., Wang, A. (2020) Succession of functional bacteria in a denitrification desulphurisation system under mixotrophic conditions. *Environ. Res.* **188**, 109708.

Locey, K. J., Lennon, J. T. (2016) Scaling laws predict global microbial diversity. *Proc. Natl. Acad. Sci. U S A* **113** (21), 5970–5975.

López-López, O., Cerdán, M. E., González-Siso, M. I. (2013) Hot spring metagenomics. *Life* **3** (2), 308–320.

Louca, S., Doebeli, M., Parfrey, L.W. (2018) Correcting for 16S rRNA gene copy numbers in microbiome surveys remains an unsolved problem. *Microbiome* **6**, 41.

Ludwig, W., Schleifer, K. H. (1994) Bacterial phylogeny based on 16S and 23S rRNA sequence analysis. *FEMS Microbiol. Rev.* **15** (2-3), 155–173.

Ma, Y., Yates, J. R. (2018) Proteomics and pulse azidohomoalanine labeling of newly synthesized proteins: what are the potential applications? *Expert Rev Proteomics.* **15** (7), 545–554.

Mackenzie, R., Pedrós-Alió, C., Díez, B. (2013) Bacterial composition of microbial mats in hot springs in Northern Patagonia: Variations with seasons and temperature. *Extremophiles* **17** (1), 123–136.

Mahajan, G. B., Balachandran, L. (2017) Sources of antibiotics: Hot springs. *Biochem. Pharmacol.* **134**, 35–41.

Malygina, A., Balkin, A., Polyakova, E., Stefanov, S., Potekhin, A., Gogoleva, N. (2023) Taxonomic Diversity of the Microbial Biofilms Collected along the Thermal Streams on Kunashir Island *Ecologies* **4** (1), 106-123.

Manz, W., Amann, R., Ludwig, W., Wagner, M., Schleifer, K. H. (1992) Phylogenetic oligodeoxynucleotide probes for the major subclasses of proteobacteria: problems and solutions. *Syst. Appl. Microbiol.* **15** (4), 593-600.

Marić, S., Vraneš, J. (2007) Characteristics and significance of microbial biofilm formation. *Period. Biol.* **109**, 115–121.

Marković, T., Sladović, Ž., Domitrović, D., Karlović, I., Larva, O. (2022) Current utilization and hydrochemical characteristics of geothermal aquifers in the Bjelovar sub-depression. *Geol. Croat* **75**, 223–233.

Martinez, J. N., Nishihara, A., Lichtenberg, M., Trampe, E., Kawai, S., Tank, M., Kühl, M., Hanada, S., Thiel, V. (2019) Vertical distribution and diversity of phototrophic bacteria within a hot spring microbial mat (Nakabusa hot springs, Japan). *Microbes Environ.* **34** (4), 374–387.

McMurdie, P. J., Holmes, S. (2013) phyloseq: an R package for reproducible interactive analysis and graphics of microbiome census data. *PloS One* **8** (4), e61217.

Mehta, R., Singhal, P., Singh, H., Damle, D., Sharma, A. K. (2016) Insight into thermophiles and their wide-spectrum applications. *3 Biotech*. **6** (1), 81.

Mende, D. R., Sunagawa, S., Zeller, G., Bork, P. (2013) Accurate and universal delineation of prokaryotic species. *Nat. Methods.* **10** (9), 881–884.

Mitrović, M., Kostešić, E., Marković, T., Selak, L., Hausmann, B., Pjevac, P., Orlić, S. (2022) Microbial community composition and hydrochemistry of underexplored geothermal waters in Croatia. *Syst. Appl. Microbiol.* **45** (6), 126359.

Monis, P. T., Giglio, S. (2006) Nucleic acid amplification-based techniques for pathogen detection and identification. *Infect. Genet. Evol.* **6** (1), 2–12.

Mori, K., Suzuki, K. (2008) Thiofaba tepidiphila gen. nov., sp. nov., a novel obligately chemolithoautotrophic, sulfur-oxidizing bacterium of the Gammaproteobacteria isolated from a hot spring. *Int. J. Syst. Evol. Microbiol.* **58** (Pt 8), 1885–1891.

Morrissey, E. M., Mau, R. L., Schwartz, E., Caporaso, J. G., Dijkstra, P., van Gestel, N., Koch, B. J., Liu, C. M., Hayer, M., McHugh, T. A., Marks, J. C., Price, L. B., Hungate, B. A. (2016) Phylogenetic organization of bacterial activity. *ISME J* **10** (9), 2336–2340.

Møller, S., Sternberg, C., Andersen, J. B., Christensen, B. B., Ramos, J. L., Givskov, M., Molin, S. (1998) In situ gene expression in mixed-culture biofilms: evidence of metabolic interactions between community members. *Appl. Environ. Microbiol.* **64** (2), 721–732.

Msarah, M. J., Faiz, M., Yusoff, M., Nurema, S., Prabhakaran, P., Ibrahim, I., Aqma, W. S. (2018) Extreme environment: biofilms and microbial diversity. *Malays. J. Microbiol.* **14** (5), 435–443.

Murugapiran, S. K., Huntemann, M., Wei, C. L., Han, J., Detter, J. C., Han, C., Erkkila, T. H., Teshima, H., Chen, A., Kyrpides, N., Mavrommatis, K., Markowitz, V., Szeto, E., Ivanova, N., Pagani, I., Pati, A., Goodwin, L., Peters, L., Pitluck, S., Lam, J., McDonald, A. I., Dodsworth, J. A., Woyke, T., Hedlund, B. P. (2013) Thermus oshimai JL-2 and T. thermophilus JL-18 genome analysis illuminates pathways for carbon, nitrogen, and sulfur cycling. *Stand. Genomic Sci.* **7** (3), 449–468.

Musat, N., Musat, F., Weber, P. K., Pett-Ridge, J. (2016) Tracking microbial interactions with NanoSIMS. *Curr. Opin. Biotechnol.* **41**, 114–121.

Najar, I. N., Das, S., Kumar, S., Sharma, P., Mondal, K., Sherpa, M. T., Thakur, N. (2022) Coexistence of Heavy Metal Tolerance and Antibiotic Resistance in Thermophilic Bacteria Belonging to Genus *Geobacillus*. *Front. Microbiol.* **13**, 914037.

Nandagopal, P., Steven, A. N., Chan, L. W., Rahmat, Z., Jamaluddin, H., Mohd Noh, N. I. (2021) Bioactive Metabolites Produced by Cyanobacteria for Growth Adaptation and Their Pharmacological Properties. *Biology* **10** (10), 1061.

Narihiro, T., Sekiguchi, Y. (2007) Microbial communities in anaerobic digestion processes for waste and wastewater treatment: a microbiological update. *Curr. Opin. Biotechnol.* **18** (3), 273–278.

Nguyen, M. T., Le, T. T., Yoon, S. H. (2017) Optimal growth condition and pyruvate supplementation for biomass production by cyanobacteria Synechococcus elongatus PCC 7942. *App. Biol. Chem.* **60** (5), 517-524.

Nguyen, T. A. and Nguyen, X. C. (2022) Bacterial Cellulose-Based Biofilm Forming Agent Extracted from Vietnamese Nata-de-Coco Tree by Ultrasonic Vibration Method: Structure and Properties. *J. Chem.* **2022**, 7502796.

Nishida, A., Thiel, V., Nakagawa, M., Ayukawa, S., Yamamura, M. (2018) Effect of light wavelength on hot spring microbial mat biodiversity. *PloS One* **13** (1), e0191650.

Novak R. (1968) Osvrt na klasifikaciju termomineralnih voda [Review of classification of thermomineral waters]. *Rad Med Fak Zagrebu.* **16** (1), 63–70.

Nübel, U., Bateson, M. M., Vandieken, V., Wieland, A., Kühl, M., Ward, D. M. (2002) Microscopic examination of distribution and phenotypic properties of phylogenetically diverse Chloroflexaceae-related bacteria in hot spring microbial mats. *Appl. Environ. Microbiol.* **68** (9), 4593–4603.

Nuñez, J., Renslow, R., Cliff, J. B., Anderton, C. R. (2017) NanoSIMS for biological applications: Current practices and analyses. *Biointerphases* **13** (3), 03B301.

Nwe, K., Brechbiel, M. W. (2009) Growing applications of "click chemistry" for bioconjugation in contemporary biomedical research. *Cancer Biother. Radiopharm.* **24** (3), 289–302.

Ogg, C. D., Greene, A. C., Patel, B. K. C. (2010) Thermovenabulum gondwanense sp. nov., a thermophilic anaerobic Fe (III)-reducing bacterium isolated from microbial mats thriving in a Great Artesian Basin bore runoff channel. *Int. J. Syst. Evol. Microbiol.* **60** (Pt 5), 1079–1084.

Paerl, H. W., Pinckney, J. L. (1996) A mini review of microbial consortia: Their roles in aquatic production and biogeochemical cycling. *Microb. Ecol.* **31** (3), 225–247.

Paerl, H. W., Pinckney, J. L., Steppe, T. F. (2000) Cyanobacterial-bacterial mat consortia: Examining the functional unit of microbial survival and growth in extreme environments. *Environ. Microbiol.* **2** (1), 11–26.

Parada, A. E., Needham, D. M., Fuhrman, J. A. (2016) Every base matters: assessing small subunit rRNA primers for marine microbiomes with mock communities, time series and global field samples. *Environ. Microbiol.* **18** (5), 1403–1414.

Parks, D. H., Imelfort, M., Skennerton, C. T., Hugenholtz, P., Tyson, G. W. (2015) CheckM: assessing the quality of microbial genomes recovered from isolates, single cells, and metagenomes. *Genome Res.* **25** (7), 1043–1055.

Pin, L., Eiler, A., Fazi, S., Friberg, N. (2021) Two different approaches of microbial community structure characterization in riverine epilithic biofilms under multiple stressors conditions: Developing molecular indicators. *Mol. Ecol. Resour.* **21** (4), 1200–1215.

Pjevac, P., Hausmann, B., Schwarz, J., Kohl, G., Herbold, C. W., Loy, A., Berry, D. (2021) An Economical and Flexible Dual Barcoding, Two-Step PCR Approach for Highly Multiplexed Amplicon Sequencing. *Front. Microbiol.* **12**, 669776.

Podar, P. T., Yang, Z., Björnsdóttir, S. H., Podar, M. (2020) Comparative Analysis of Microbial Diversity Across Temperature Gradients in Hot Springs From Yellowstone and Iceland. *Front. Microbiol.* **11**, 1625.

Poddar, A., Das, S. K. (2018) Microbiological studies of hot springs in India: a review. *Arch. Microbiol.* **200** (1), 1–18.

Portillo, M. C., Sririn, V., Kanoksilapatham, W., Gonzalez, J. M. (2009) Differential microbial communities in hot spring mats from Western Thailand. *Extremophiles* **13** (2), 321–331.

Power, J. F., Carere, C. R., Lee, C. K., Wakerley, G. L. J., Evans, D. W., Button, M., White, D., Climo, M. D., Hinze, A. M., Morgan, X. C., McDonald, I. R., Cary, S. C., & Stott, M. B. (2018) Microbial biogeography of 925 geothermal springs in New Zealand. *Nat. Commun.* **9** (1), 2876.

Prieto-Barajas, C. M., Valencia-Cantero, E., Santoyo, G. (2018) Microbial mat ecosystems: structure types, functional diversity, and biotechnological application. *Electron. J. Biotechnol.* **31**, 48– 56.

Pruesse, E., Peplies, J., Glöckner, F. O. (2012) SINA: accurate high-throughput multiple sequence alignment of ribosomal RNA genes. *Bioinformatics* **28** (14), 1823–1829.

Purcell, D., Sompong, U., Yim, L. C., Barraclough, T. G., Peerapornpisal, Y., Pointing, S. B. (2007) The effects of temperature, pH and sulphide on the community structure of hyperthermophilic streamers in hot springs of northern Thailand. *FEMS Microbiol. Ecol.* **60** (3), 456–466.

Quince, C., Walker, A. W., Simpson, J. T., Loman, N. J., Segata, N. (2017) Shotgun metagenomics, from sampling to analysis. *Nat Biotechnol.* **35** (9), 833–844.

Rabbani, M., Bagherinejad, M. R., Sadeghi, H. M., Shariat, Z. S., Etemadifar, Z., Moazen, F., Rahbari, M., Mafakher, L., Zaghian, S. (2014) Isolation and characterization of novel thermophilic lipase-secreting bacteria *Braz. J. Microbiol*. **44** (4), 1113–1119.

Rai, M., Pandit, R., Gaikwad, S., Kövics, G. (2016) Antimicrobial peptides as natural bio-preservative to enhance the shelf-life of food. *J. Food Sci. Technol.* **53** (9), 3381–3394.

Ranawat, P., Rawat, S. (2018) Metal-tolerant thermophiles: metals as electron donors and acceptors, toxicity, tolerance and industrial applications. *Environ. Sci. Pollut. Res.* **25**, 4105-4133.

Ravot, G., Ollivier, B., Magot, M., Patel, B., Crolet, J., Fardeau, M., Garcia, J. (1995) Thiosulfate reduction, an important physiological feature shared by members of the order thermotogales. *Appl. Environ. Microbiol.* **61** (5), 2053–2055.

Rawlings, N. D., Barrett, A. J., Finn, R. (2016) Twenty years of the MEROPS database of proteolytic enzymes, their substrates and inhibitors. *Nucleic Acids Res.* **44** (D1), D343–D350.

Reichart, N. J., Jay, Z. J., Krukenberg, V., Parker, A. E., Spietz, R. L., Hatzenpichler, R. (2020) Activity-based cell sorting reveals responses of uncultured archaea and bacteria to substrate amendment. *The ISME J* **14** (11), 2851–2861.

Renslow, R. S., Lindemann, S. R., Cole, J. K., Zhu, Z., Anderton, C. R. (2016) Quantifying element incorporation in multispecies biofilms using nanoscale secondary ion mass spectrometry image analysis. *Biointerphases* **11** (2), 02A322.

Riesenfeld, C. S., Goodman, R. M., Handelsman, J. (2004) Uncultured soil bacteria are a reservoir of new antibiotic resistance genes. *Environ. Microbiol.* **6**, 981–989.

Rocha, R., Almeida, C., Azevedo, N. F. (2018) Influence of the fixation/permeabilization step on peptide nucleic acid fluorescence in situ hybridization (PNA-FISH) for the detection of bacteria. *PloS One* **13** (5), e0196522.

Rozanov, A. S., Bryanskaya, A. V., Ivanisenko, T. V., Malup, T. K., Peltek, S. E. (2017) Biodiversity of the microbial mat of the Garga hot spring. *BMC Evol Biol.* **17**, 254.

Sahay, H., Yadav, A. N., Singh, A. K., Singh, S., Kaushik, R., Saxena, A. K. (2017) Hot springs of Indian Himalayas: potential sources of microbial diversity and thermostable hydrolytic enzymes. *3 Biotech.* **7** (2), 118.

Sahoo, R. K., Kumar, M., Sukla, L. B., Subudhi, E. (2017) Bioprospecting hot spring metagenome: lipase for the production of biodiesel. *Environ. Sci. Pollut. Res. Int.* **24** (4), 3802–3809.

Sakoula, D., Smith, G. J., Frank, J., Mesman, R. J., Kop, L. F. M., Blom, P., Jetten, M. S. M., van Kessel, M. A. H. J., Lücker, S. (2022) Universal activity-based labeling method for ammonia- and alkane-oxidizing bacteria. *ISME J* **16** (4), 958–971.

Salas-Jara, M. J., Ilabaca, A., Vega, M., García, A. (2016) Biofilm Forming Lactobacillus: New Challenges for the Development of Probiotics. *Microorganisms* **4** (3), 35.

Saleh, A. M., Wilding, K. M., Calve, S., Bundy, B. C., Kinzer-Ursem, T. L. (2019) Non-canonical amino acid labeling in proteomics and biotechnology. *J. Biol. Eng.* **13**, 43.

Salim, T., Ratnawati, L., Agustina, W. (2015) Bioethanol Production from Glucose by Thermophilic Microbes from Ciater Hot Springs. *Procedia Chem.* **16**, 503-510.

Samo, T. J., Smriga, S., Malfatti, F., Sherwood, B. P., Azam, F. (2014) Broad distribution and high proportion of protein synthesis active marine bacteria revealed by click chemistry at the single cell level. *Front. Mar. Sci.* **1**, 48.

Santoro, C., Arbizzani, C., Erable, B., Ieropoulos, I. (2017) Microbial fuel cells: From fundamentals to applications. A review. *J. Power Sources* **356**, 225–244.

Schmidt, H., Eickhorst, T., Tippkötter, R. (2012) Evaluation of tyramide solutions for an improved detection and enumeration of single microbial cells in soil by CARD-FISH. *J. Microbiol. Methods.* **91** (3), 399–405.

Schmeisser, C., Stöckigt, C., Raasch, C., Wingender, J., Timmis, K. N., Wenderoth, D. F., Flemming, H. C., Liesegang, H., Schmitz, R. A., Jaeger, K. E., Streit, W. R. (2003) Metagenome survey of biofilms in drinking-water networks. *Appl. Environ. Microbiol.* **69** (12), 7298–7309.

Schmieder, R., Edwards, R. (2011) Quality control and preprocessing of metagenomic datasets. *Bioinformatics* **27** (6), 863-864.

Schubotz, F., Meyer-Dombard, D. R., Bradley, A. S., Fredricks, H. F., Hinrichs, K. U., Shock, E. L., Summons, R. E. (2013) Spatial and temporal variability of biomarkers and microbial diversity reveal metabolic and community flexibility in Streamer Biofilm Communities in the Lower Geyser Basin, Yellowstone National Park. *Geobiology* **11** (6), 549–569.

Schubotz, F., Hays, L. E., Meyer-Dombard, D. R., Gillespie, A., Shock, E. L., Summons, R. E. (2015) Stable isotope labeling confirms mixotrophic nature of streamer biofilm communities at alkaline hot springs. *Front. Microbiol.* **6,** 42.

Schuler, C. G., Havig, J. R., Hamilton, T. L. (2017) Hot spring microbial community composition, morphology, and carbon fixation: Implications for interpreting the ancient rock record. *Front. Earth. Sci.* **5**, 1–17.

Seenivasagan, R., Babalola, O. O. (2021) Utilization of Microbial Consortia as Biofertilizers and Biopesticides for the Production of Feasible Agricultural Product. *Biology* **10** (11), 1111.

Sekoai, P. T., Chunilall, V., Sithole, B., Habimana, O., Ndlovu, S., Ezeokoli, O. T., Sharma, P., Yoro, K. O. (2022) Elucidating the Role of Biofilm-Forming Microbial Communities in Fermentative Biohydrogen Process: An Overview. *Microorganisms* **10** (10), 1924.

Selengut, J. D., Haft, D. H., Davidsen, T., Ganapathy, A., Gwinn-Giglio, M., Nelson, W. C., Richter, A. R., White, O. (2007) TIGRFAMs and Genome Properties: tools for the assignment of molecular function and biological process in prokaryotic genomes. *Nucleic Acids Res.* **35**, D260–D264.

Serbulea, M., Payyappallimana, U. (2012) Onsen (hot springs) in Japan--transforming terrain into healing landscapes. *Health Place* **18** (6), 1366–1373.

Severin, I., Acinas, S. G., Stal, L. J. (2010) Diversity of nitrogen-fixing bacteria in cyanobacterial mats. *FEMS Microbiol. Ecol.* **73** (3), 514–525.

Shakoori, A. R. (2017) Fluorescence In Situ Hybridization (FISH) and Its Applications. *Chromosome Structure and Aberrations*, 343–367. <https://doi.org/10.1007/978-81-322-3673-3_16>. Accessed July 17, 2023.

Shukla, A. K., Singh, A. K. (2020) Exploitation of Potential Extremophiles for Bioremediation of Xenobiotics Compounds: A Biotechnological Approach. *Curr. Genomics* **21** (3), 161–167.

Siliakus, M. F., van der Oost, J., Kengen, S. W. M. (2017) Adaptations of archaeal and bacterial membranes to variations in temperature, pH and pressure. *Extremophiles* **21** (4), 651–670.

Singh, J., Behal, A., Singla, N., Joshi, A., Birbian, N., Singh, S., Bali, V., Batra, N. (2009) Metagenomics: Concept, methodology, ecological inference and recent advances. *Biotechnol J.* **4** (4), 480–494.

Singh, T., Kshirsagar, P. R., Das, A., Yadav, K., Mallik, S., Mascarenhas-Pereira, M. B. L., Thomas, T. R. A., Shivarmu, M. S., LokaBharathi, P. A., Khadge, N. H., Nagender Nath, B., Dhakephalkar, P. K., Iyer, S. D., Ray, D., Valsangkar, A. B., Garg, A., Babu, C. P., Waghole, R. J., Waghmare, S. S., Rajwade, J. M., Paknikar, K. M. (2019) Implications of microbial thiosulfate utilization in red clay sediments of the Central Indian Basin: The Martian analogy. *Geochem. Geophys. Geosyst.* **20**, 708–729.

Smith, R.H., Glendinning, L., Walker, A.W., Watson, M. (2022) Investigating the impact of database choice on the accuracy of metagenomic read classification for the rumen microbiome. *Anim. microbiome* **4**, 57.

Sompong, U., Hawkins, P. R., Besley, C., Peerapornpisal, Y. (2005) The distribution of cyanobacteria across physical and chemical gradients in hot springs in northern Thailand. *FEMS Microbiol. Ecol.* **52** (3), 365–376.

Sorokin, D. Y., Lysenko, A. M., Mityushina, L. L., Tourova, T. P., Jones, B. E., Rainey, F. A., Robertson, L. A., Kuenen, G. J. (2001) Thioalkalimicrobium aerophilum gen. nov., sp. nov. and Thioalkalimicrobium sibericum sp. nov., and Thioalkalivibrio versutus gen. nov., sp. nov., Thioalkalivibrio nitratis sp.nov., novel and Thioalkalivibrio denitrificancs sp. nov., novel obligately alkaliphilic and obligately chemolithoautotrophic sulfur-oxidizing bacteria from soda lakes. *Int. J. Syst. Evol. Microbiol.* **51** (Pt 2), 565–580.

Spear, J. R., Walker, J. J., Pace, N. R. (2006) Microbial Ecology and Energetics in Yellowstone Hot Springs. *Science* **14** (1), 17–24.

Srinivasan, R., Santhakumari, S., Poonguzhali, P., Geetha, M., Dyavaiah, M., Xiangmin, L. (2021) Bacterial biofilm inhibition: a focused review on recent therapeutic strategies for combating the biofilm mediated infections. *Front. Microbiol.* **12**, 676458.

Stahl, D. A., Lane, D. J., Olsen, G. J., Pace, N. R. (1985) Characterization of a Yellowstone hot spring microbial community by 5S rRNA sequences. *Appl. Environ. Microbiol.* **49** (6), 1379–1384.

Starke, R., Pylro, V. S., Morais, D. K. (2021) 16S rRNA Gene Copy Number Normalization Does Not Provide More Reliable Conclusions in Metataxonomic Surveys. *Microb. Ecol.* **81** (2), 535–539.

Stewart, P. S., Franklin, M. J. (2008) Physiological heterogeneity in biofilms. *Nat. Rev. Microbiol.* **6** (3), 199–210.

Stoddard, S. F., Smith, B. J., Hein, R., Roller, B. R., Schmidt, T. M. (2015) rrnDB: improved tools for interpreting rRNA gene abundance in bacteria and archaea and a new foundation for future development. *Nucleic Acids Res.* **43**, D593–D598.

Stoodley, P., Sauer, K., Davies, D. G., Costerton, J. W. (2002) Biofilms as complex differentiated communities. *Annu. Rev. Microbiol.* **56**, 187–209.

Swingley, W. D., Meyer-Dombard, D. R., Shock, E. L., Alsop, E. B., Falenski, H. D., Havig, J. R., Raymond, J. (2012) Coordinating Environmental Genomics and Geochemistry Reveals Metabolic Transitions in a Hot Spring Ecosystem. *PLoS One* **7** (6): e38108.

Tamburello, G., Chiodini, G., Ciotoli, G., Procesi, M., Rouwet, D., Sandri, L., Carbonara, N., Masciantonio, C. (2022) Global thermal spring distribution and relationship to endogenous and exogenous factors. *Nat. Commun.* **13** (1), 6378.

Tanner, K., Vilanova, C., Porcar, M. (2017) Bioprospecting challenges in unusual environments. *Microb. Biotechnol.* **10** (4), 671–673.

Thiel, K., Vuorio, E., Aro, E. M., Kallio, P. T. (2017) The effect of enhanced acetate influx on Synechocystis sp. PCC 6803 metabolism. *Microb Cell Fact.* **16** (1), 21.

Tirawongsaroj, P., Sriprang, R., Harnpicharnchai, P., Thongaram, T., Champreda, V., Tanapongpipat, S., Pootanakit, K., Eurwilaichitr, L. (2008) Novel thermophilic and thermostable lipolytic enzymes from a Thailand hot spring metagenomic library. *J Biotechnol.* **133** (1), 42–49.

Toshchakov, S. V., Izotova, A. O., Vinogradova, E. N., Kachmazov, G. S., Tuaeva, A. Y., Abaev, V. T., Evteeva, M. A., Gunitseva, N. M., Korzhenkov, A. A., Elcheninov, A. G., Patrushev, M. V., Kublanov, I. V. (2021) Culture-Independent Survey of Thermophilic Microbial Communities of the North Caucasus. *Biology* **10** (12), 1352.

Trexler, R. V., Van Goethem, M. W., Goudeau, D., Nath, N., Malmstrom, R. R., Northen, T. R., Couradeau, E. (2023) BONCAT-FACS-Seq reveals the active fraction of a biocrust community undergoing a wet-up event. *Front. Microbiol.* **14**, 1176751.

Tringe, S. G., von Mering, C., Kobayashi, A., Salamov, A. A., Chen, K., Chang, H. W., Podar, M., Short, J. M., Mathur, E. J., Detter, J. C., Bork, P., Hugenholtz, P., Rubin, E. M. (2005). Comparative metagenomics of microbial communities. *Science* **308** (5721), 554–557.

Tripathi, C., Mahato, N. K., Rani, P., Singh, Y., Kamra, K., Lal, R. (2016) Draft genome sequence of Lampropedia cohaerens strain CT6 (T) isolated from arsenic rich microbial mats of a Himalayan hot water spring. *Stand. Genomic Sci.* **11** (1), 64.

Truong, D. T., Franzosa, E. A., Tickle, T. L., Scholz, M., Weingart, G., Pasolli, E., Tett, A., Huttenhower, C., Segata, N. (2015) MetaPhlAn2 for enhanced metagenomic taxonomic profiling. *Nat. Methods* **12** (10), 902–903.

Tyson, G. W., Chapman, J., Hugenholtz, P., Allen, E. E., Ram, R. J., Richardson, P. M., Solovyev, V. V., Rubin, E. M., Rokhsar, D. S., Banfield, J. F. (2004) Community structure and metabolism through reconstruction of microbial genomes from the environment. *Nature* **428** (6978), 37–43.

Uchiyama, T., Abe, T., Ikemura, T., Watanabe, K. (2005) Substrate-induced gene-expression screening of environmental metagenome libraries for isolation of catabolic genes. *Nat. Biotechnol.* **23** (1), 88–93.

Urbieta, M. S., González-Toril, E., Bazán, Á. A., Giaveno, M. A., Donati, E. (2015) Comparison of the microbial communities of hot springs waters and the microbial biofilms in the acidic geothermal area of Copahue (Neuquén, Argentina). *Extremophiles* **19** (2), 437–450.

Uribe-Lorío, L., Brenes-Guillén, L., Hernández-Ascencio, W., Mora-Amador, R., González, G., Ramírez-Umaña, C. J., Díez, B., Pedrós-Alió, C. (2019) The influence of temperature and pH on bacterial community composition of microbial mats in hot springs from Costa Rica. *MicrobiologyOpen* **8** (10), e893.

Valeriani, F., Crognale, S., Protano, C., Gianfranceschi, G., Orsini, M., Vitali, M., Spica, V. R. (2018) Metagenomic analysis of bacterial community in a travertine depositing hot spring. *New Microbiol.* **41** (2), 126–135.

Vandamme, P., Pot, B., Gillis, M., de Vos, P., Kersters, K., Swings, J. (1996) Polyphasic taxonomy, a consensus approach to bacterial systematics. *Microbiol. Rev.* **60** (2), 407–438.

Vaser, R., Sović, I., Nagarajan, N., Šikić, M. (2017) Fast and accurate de novo genome assembly from long uncorrected reads. *Genome Res.* **27** (5), 737–746.

Venter, J. C., Remington, K., Heidelberg, J. F., Halpern, A. L., Rusch, D., Eisen, J. A., Wu, D., Paulsen, I., Nelson, K. E., Nelson, W., Fouts, D. E., Levy, S., Knap, A. H., Lomas, M. W., Nealson, K., White, O., Peterson, J., Hoffman, J., Parsons, R., Baden-Tillson, H., Pfannkoch, C., Rogers, Y. H., Smith, H. O. (2004) Environmental genome shotgun sequencing of the Sargasso Sea. *Science* **304** (5667), 66–74.

Venturi, S., Crognale, S., Di Benedetto, F., Montegrossi, G., Casentini, B., Amalfitano, S., Baroni, T., Rossetti, S., Tassi, F., Capecchiacci, F., Vaselli, O., Fazi, S. (2022) Interplay between abiotic and microbial biofilm-mediated processes for travertine formation: Insights from a thermal spring (Piscine Carletti, Viterbo, Italy). *Geobiology* **20** (6), 837–856.

Vermelho, A. B., Noronha, E. F., Filho, E. X. F., Ferrara, M. A., Bon, E. P. S. (2013) Diversity and Biotechnological Applications of Prokaryotic Enzymes. In: *The Prokaryotes* (Rosenberg, E., DeLong, E. F., Lory, S., Stackebrandt, E., Thompson, F. eds). Springer, Berlin, 213–240.

Vésteinsdóttir, H., Reynisdóttir, D. B., Örlygsson, J. (2011) Hydrogenophilus islandicus sp. nov., a thermophilic hydrogen-oxidizing bacterium isolated from an Icelandic hot spring. *Int. J. Syst. Evol. Microbiol.* **61** (Pt 2), 290-294.

Vieites, J. M., Guazzaroni, M. E., Beloqui, A., Golyshin, P. N., Ferrer, M. (2009) Metagenomics approaches in systems microbiology. *FEMS Microbiol. Rev.* **33** (1), 236–255.

Vishnivetskaya, T. A., Hamilton-Brehm, S. D., Podar, M., Mosher, J. J., Palumbo, A. V., Phelps, T. J., Keller, M., Elkins, J. G. (2015) Community Analysis of Plant Biomass-Degrading Microorganisms from Obsidian Pool, Yellowstone National Park. *Microb. Ecol.* **69** (2), 333–345.

Voget, S., Leggewie, C., Uesbeck, A., Raasch, C., Jaeger, K. E., Streit, W. R. (2003) Prospecting for novel biocatalysts in a soil metagenome. *Appl. Environ. Microbiol.* **69** (10), 6235–6242.

Vondra, M., Buzík, J., Horňák, D., Procházková, M., Miklas, V., Touš, M., Jegla, Z., Máša, V. (2023) Technology for Hot Spring Cooling and Geothermal Heat Utilization: A Case Study for Balneology Facility. *Energies* **16** (7), 2941.

Xia, Y., Wang, Y., Wang, Y., Chin, F. Y., Zhang, T. (2016) Cellular adhesiveness and cellulolytic capacity in Anaerolineae revealed by omics-based genome interpretation. *Biotechnol. Biofuels.* **9**, 111.

Xu, X. J., Chen, C., Wang, A. J., Yu, H., Zhou, X., Guo, H. L., Yuan, Y., Lee, D. J., Zhou, J., Ren, N. Q. (2014) Bioreactor performance and functional gene analysis of microbial community in a limited-oxygen fed bioreactor for co-reduction of sulfate and nitrate with high organic input. *J. Hazard. Mater.* **278**, 250–257.

Wagner M. (2009) Single-cell ecophysiology of microbes as revealed by Raman microspectroscopy or secondary ion mass spectrometry imaging. *Annu. Rev. Microbiol.* **63**, 411–429.

Wagner, M., Haider, S. (2012) New trends in fluorescence in situ hybridization for identification and functional analyses of microbes. *Curr Opin Biotechnol.* **23** (1), 96–102.

Wagner, M., Horn, M., Daims, H. (2003) Fluorescence in situ hybridisation for the identification and characterisation of prokaryotes. *Curr. Opin. Microbiol.* **6** (3), 302–309.

Wang, S., Hou, W., Dong, H., Jiang, H., Huang, L., Wu, G., Zhang, C., Song, Z., Zhang, Y., Ren, H., Zhang, J., Zhang, L. (2013) Control of temperature on microbial community structure in hot springs of the Tibetan Plateau. *PloS One* **8** (5), e62901.

Waoo, A. A., Singh, S., Pandey, A., Kant, G., Choure, K., Amesho, K. T. T., Srivastava, S. (2023) Microbial exopolysaccharides in the biomedical and pharmaceutical industries. *Heliyon* **9** (8), e18613.

Ward, D. M., Bateson, M. M., Weller, R., Ruff-Roberts, A. L. (1992) Ribosomal RNA analysis of microorganisms as they occur in nature. *Adv. Microb. Ecol.* **12**, 219–286.

Ward, D. M., Ferris, M. J., Nold, S. C., Bateson, M. M. (1998) A natural view of microbial biodiversity within hot spring cyanobacterial mat communities. *Microbiol. Mol. Biol. Rev.* **62** (4), 1353–1370.

Ward, D. M., Weller, R., Bateson, M. M. (1990) 16S rRNA sequences reveal numerous uncultured microorganisms in a natural community. *Nature* **345** (6270), 63–65.

Wasmund, K., Mußmann, M., Loy, A. (2017) The life sulfuric: microbial ecology of sulfur cycling in marine sediments. *Environ. Microbiol. Rep.* **9** (4), 323–344.

Weiland-Bräuer, N. (2021) Friends or Foes - Microbial Interactions in Nature. *Biology* **10** (6), 496.

Wheaton, G., Counts, J., Mukherjee, A., Kruh, J. Kelly, R. (2015) The Confluence of Heavy Metal Biooxidation and Heavy Metal Resistance: Implications for Bioleaching by Extreme Thermoacidophiles. *Minerals* **5** (3), 397–451.

Wickham, H. (2009) ggplot2: elegant graphics for data analysis. Springer-Verlag, New York. <https://doi.org/10.1007/978-0-387-98141-3> Accessed January 20, 2023.

Winkel, M., Pjevac, P., Kleiner, M., Littmann, S., Meyerdierks, A., Amann, R., Mußmann, M. (2014) Identification and activity of acetate-assimilating bacteria in diffuse fluids venting from two deep-sea hydrothermal systems. *FEMS Microbiol. Ecol.* **90** (3), 731–746.

Woebken, D., Burow, L. C., Behnam, F., Mayali, X., Schintlmeister, A., Fleming, E. D., Prufert-Bebout, L., Singer, S. W., Cortés, A. L., Hoehler, T. M., Pett-Ridge, J., Spormann, A. M., Wagner, M., Weber, P. K., Bebout, B. M. (2015) Revisiting N2 fixation in Guerrero Negro intertidal microbial mats with a functional single-cell approach. *ISME J* **9** (2), 485–496.

Woese, C. R. (1987) Bacterial evolution. *Microbiol. Rev.* **51** (2), 221–271.

Wu, B., Liu, F., Fang, W., Yang, T., Chen, G. H., He, Z., Wang, S. (2021) Microbial sulfur metabolism and environmental implications. *Sci. Total Environ.* **778**, 146085.

Yang, C., Chowdhury, D., Zhang, Z., Cheung, W. K., Lu, A., Bian, Z., Zhang, L. (2021) A review of computational tools for generating metagenome-assembled genomes from metagenomic sequencing data. *Comput. Struct. Biotechnol. J.* **19**, 6301–6314.

Yasir, M., Qureshi, A. K., Srinivasan, S., Ullah, R., Bibi, F., Rehan, M., Khan, S. B., Azhar, E. I. (2020) Domination of Filamentous Anoxygenic Phototrophic Bacteria and Prediction of

Metabolic Pathways in Microbial Mats from the Hot Springs of Al Aridhah. *Folia Biol.* **66** (1), 24–35.

Yong, D., Toleman, M. A., Giske, C. G., Cho, H. S., Sundman, K., Lee, K., Walsh, T. R. (2009) Characterization of a new metallo-β-lactamase gene, blaNDM-1, and a novel erythromycin esterase gene carried on a unique genetic structure in Klebsiella pneumoniae sequence type 14 from India. *Antimicrob. Agents Chemother.* **53** (12), 5046-5054.

Zebrowska, J., Witkowska, M., Struck, A., Laszuk, P. E., Raczuk, E., Ponikowska, M., Skowron, P. M., Zylicz-Stachula, A. (2022) Antimicrobial Potential of the Genera *Geobacillus* and *Parageobacillus*, as Well as Endolysins Biosynthesized by Their Bacteriophages. *Antibiotics* **11** (2), 242.

Zeller, M., Huson, D. H. (2022) Comparison of functional classification systems. *NAR Genom Bioinform.* **4** (4), lqac090.

Zhang, H., Yohe, T., Huang, L., Entwistle, S., Wu, P., Yang, Z., Busk, P. K., Xu, Y., Yin, Y. (2018) dbCAN2: a meta server for automated carbohydrate-active enzyme annotation. *Nucleic Acids Res.* **46** (W1), W95–W101.

Zhang, L., Chen, F., Zeng, Z., Xu, M., Sun, F., Yang, L., Bi, X., Lin, Y., Gao, Y., Hao, H., Yi, W., Li, M., Xie, Y. (2021) Advances in Metagenomics and Its Application in Environmental Microorganisms. *Front. Microbiol.* **12**, 766364.

Zhang, F., Liu, X., Dong, X. (2012) Thermosyntropha tengcongensis sp. nov., a thermophilic bacterium that degrades long-chain fatty acids syntrophically. *Int. J. Syst. Evol. Microbiol.* **62** (Pt 4), 759–763.

Zhang, Y., Sun, L., Zhou, J. (2019) Simultaneous biological and chemical removal of sulfate and Fe (II) EDTA-NO in anaerobic conditions and regulation of sulfate reduction products. *Minerals* **9** (6), 330.

Zheng, S., Bawazir, M., Dhall, A., Kim, H. E., He, L., Heo, J., Hwang, G. (2021) Implication of Surface Properties, Bacterial Motility, and Hydrodynamic Conditions on Bacterial Surface Sensing and Their Initial Adhesion. *Front. Bioeng. Biotechnol.* **9**, 643722.

Zhou, Z., Tran, P. Q., Breister, A. M., Liu, Y., Kieft, K., Cowley, E. S., Karaoz, U., Anantharaman, K. (2022) METABOLIC: high-throughput profiling of microbial genomes for

functional traits, metabolism, biogeochemistry, and community-scale functional networks. *Microbiome* **10** (1), 33.

Zhou, E. M., Xian, W. D., Jiao, J. Y., Liu, L., Li, M. M., Ding, Y. P., Yin, Y. R., Zhao, J., Nimaichand, S., Xiao, M., Li, W. J. (2018) Physiological and genomic properties of Thermus tenuipuniceus sp. nov., a novel slight reddish color member isolated from a terrestrial geothermal spring. *Syst. Appl. Microbiol.* **41** (6), 611–618.

Internet Sources

URL1: <https://sites.google.com/a/sps.nus.edu.sg/earthians/main/home> Accessed August 10, 2023.

URL 2: <https://www.hach.com/asset-get.download-en.jsa?id=7639983731> Accessed July 11, 2023.

URL 3: Laros JFJ, <https://www.github.com/jfjlaros/demultiplex> Accessed August 13, 2023.

URL 4: <https://www.bdbiosciences.com/content/dam/bdb/marketing-documents/FACSMelody-ug-ruo.pdf> Accessed August 10, 2023.

URL 5: <https://www.github.com/nanoporetech/medaka> Accessed June 20, 2023

URL 6: <https://github.com/AnantharamanLab/METABOLIC> Accessed March 15, 2023.

8. SUPPLEMENTARY MATERIALS

Appendix 1. Examples of sorting strategy for FACS with generated reports
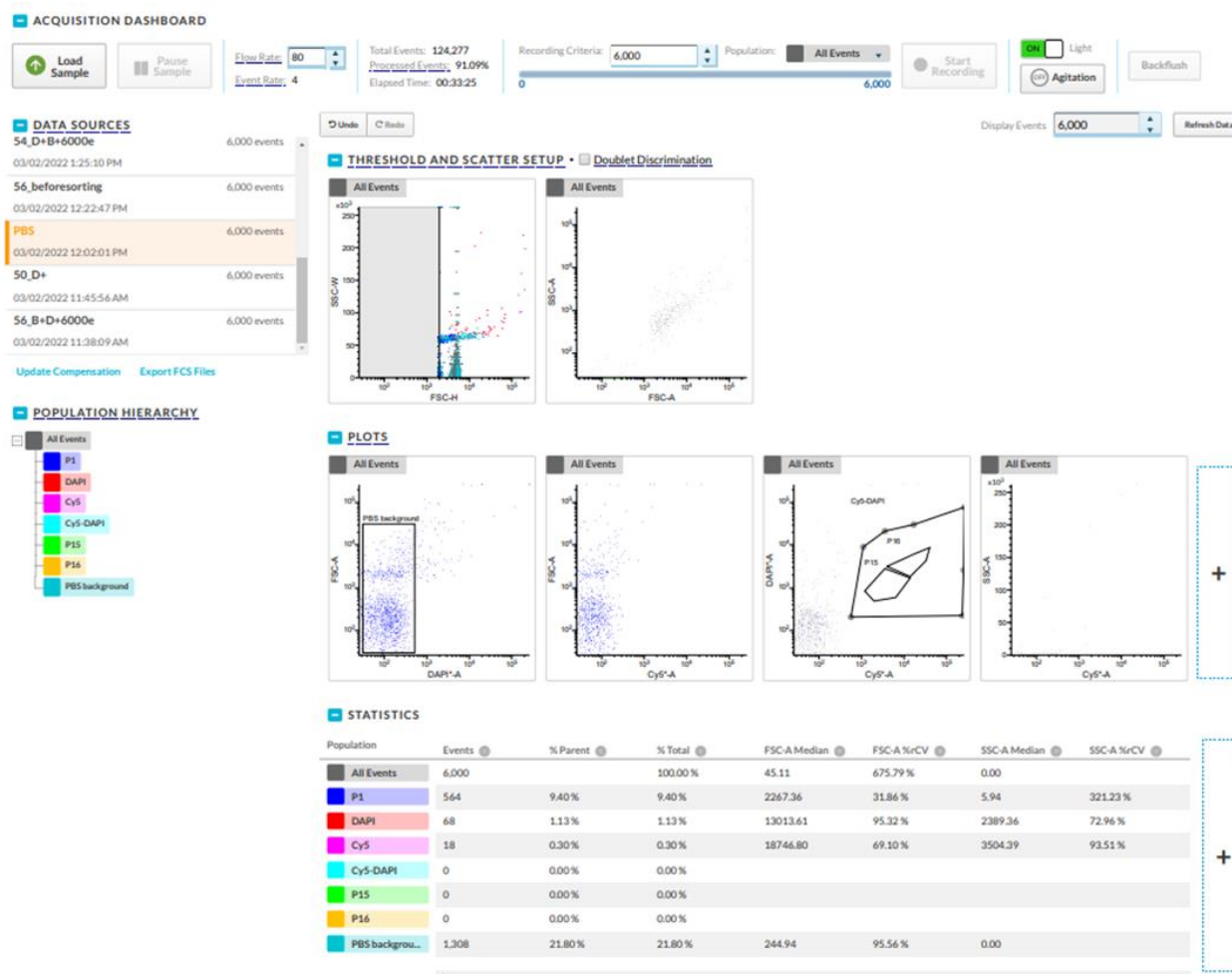
Figure S1. FACS report for PBS recording to identify background produced by PBS.

First, a sorting tube containing only PBS is recorded to remove potential background caused by salts and particles in the PBS. As shown in Figure S1, the sterile PBS used in the experiment produces an easily detectable background in an area that is not characteristic for other types of events. Then, a control sample stained only with DAPI is recorded to detect an area characteristic only of cells stained with DAPI. Next, a control sample stained with DAPI, and another dye not used for the experiment is recorded using same parameters to detect unbound dye, changes due to CLICK staining and autofluorescence in the sample. In this experiment, the Cy3 azide dye was used for the control incubations (Figure S2), and no signal was detected in the region characteristic for signal generated with Cy5 dye.

Figure S2. FACS report for control incubation recording stained with DAPI and Cy3.

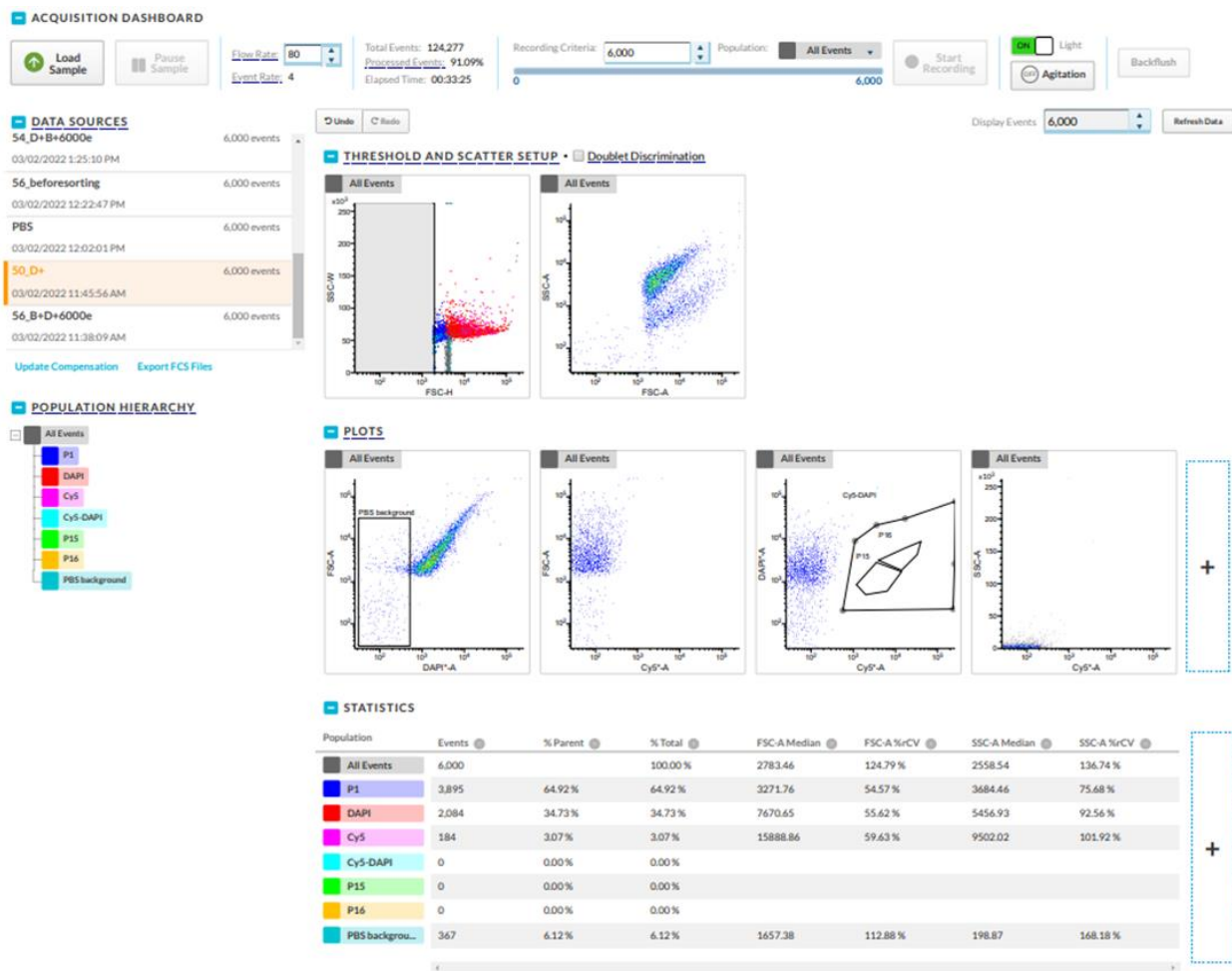Then, the same control sample stained with DAPI and Cy5 azide dye is recorded to detect area characteristic for Cy5 signal and to allow comparison between control samples and samples incubated with different substrate amendments. The control samples are not sorted.
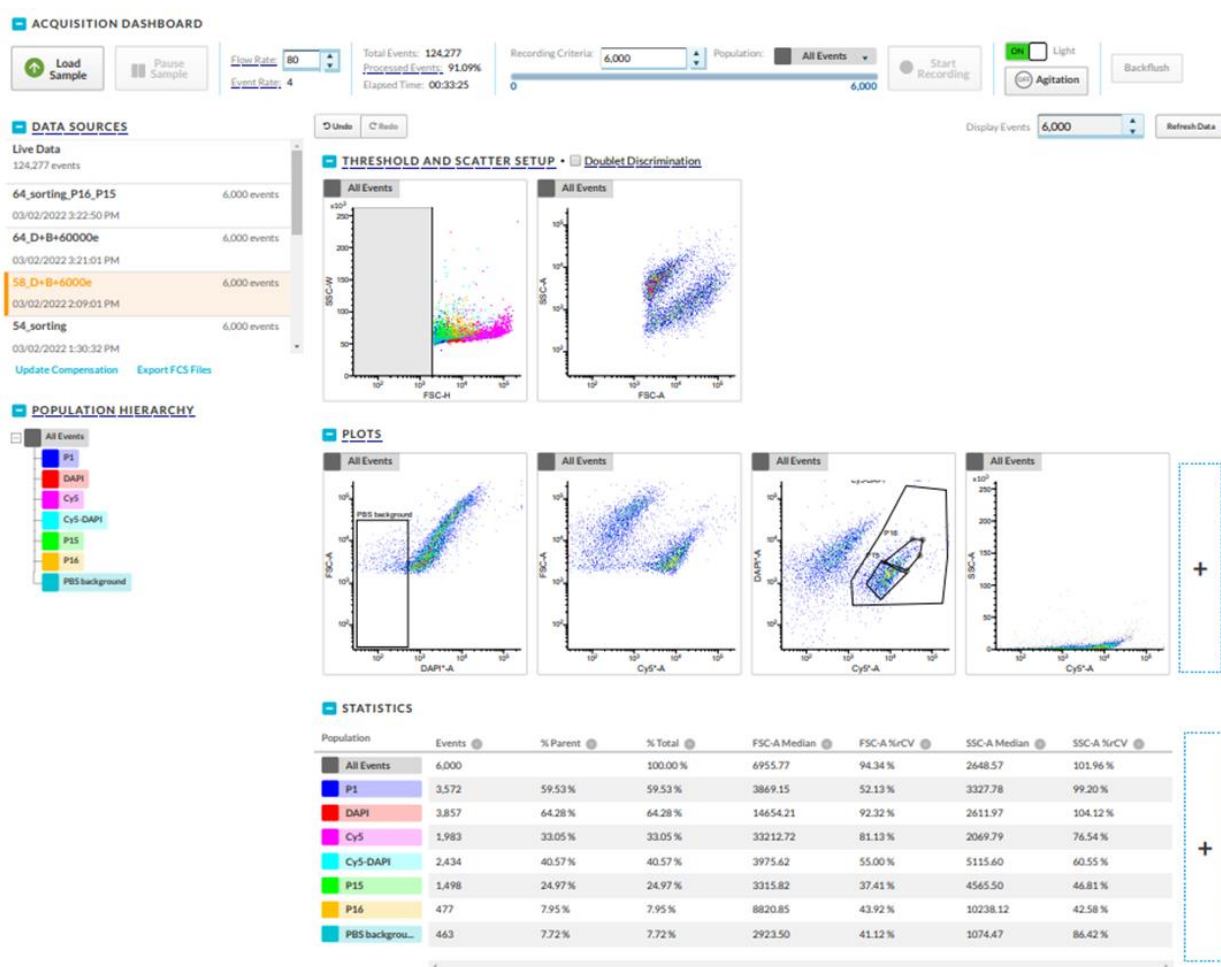
Figure S3. Report for of Bizovac sample in 48 h incubation amendment with thiosulfate stained with DAPI and Cy5 recording on FACS.

Finally, the sample incubated in substrate amendment, stained with DAPI and Cy5 azide dye is recorded (Figure S3). The sample shows the Bizovac biofilm incubated in a thiosulfate substrate for 48 h. In the region characteristic for double stained DAPI-Cy5 cells, the event density takes an exponential form, indicating reliable data obtained by the experiment. 60.6 % of all events are double DAPI-Cy5 stained. Considering the approximate size of the events, two groups are identified - P15 as smaller events and P16 as events with larger size, indicating flocs and cell aggregates. After setting the appropriate flow rate, desired number of sorted events, sorting mode, and necessary parameters for optimal sorting, both groups of events are sorted, after which 16S rRNA amplicon sequencing is performed.

Appendix 2. All results of image analysis acquired with daime software

Table S1. All results acquired through daime software for combination of BONCAT and CARD-FISH methods applied on biofilm samples collected in spring 2021.

Biofilm	Substrate	Time point	Probe	Histogram stretching	Segmentation	% biovolume	% congruence
Tuhelj	acetate	24	Gamm42a	30-200 (1x)	Isodata	11.4	29
Tuhelj	acetate	48	Gamm42a	50-200 (1x)	Custom:5-255	3.6	50
Tuhelj	glucose	24	Gamm42a	60-200 (1x)	Custom:5-255	26.2	54
Tuhelj	glucose	48	Gamm42a	40-200 (1x)	Custom:30-255	36.2	31
Tuhelj	pyruvate	24	Gamm42a	40-150 (1x)	Custom:90-255	25.4	29
Tuhelj	pyruvate	48	Gamm42a	30-150 (1x)	Custom:60-255	28.5	41
Tuhelj	thiosufate	24	Gamm42a	50-200 (1x)	Custom:30-255	24.4	44
Tuhelj	thiosufate	48	Gamm42a	30-200 (1x)	Custom:90-255	47.9	56
Tuhelj	HPG + Light	24	Gamm42a	50-200 (1x)	Custom:30-255	14.1	21
Tuhelj	HPG + Light	48	Gamm42a	50-200 (1x)	Custom:5-255	16.4	24
Tuhelj	HPG+Dark	24	Gamm42a	20-150 (2x)	Custom:5-255	9.7	37
Tuhelj	HPG+Dark	48	Gamm42a	20-150 (1x)	Isodata	9.9	46
Bizovac	acetate	24	Gamm42a	20-60 (1x)	Isodata	17.5	66
Bizovac	acetate	48	Gamm42a	50-200 (1x)	Custom:5-255	12.3	42
Bizovac	glucose	24	Gamm42a	20-150 (1x)	Isodata	43.3	83
Bizovac	glucose	48	Gamm42a	20-150 (1x)	Isodata	55.5	65
Bizovac	pyruvate	24	Gamm42a	10-150 (1x)	Isodata	32.7	82
Bizovac	pyruvate	48	Gamm42a	20-150 (2x)	Custom:5-255	36.9	69
Bizovac	thiosufate	24	Gamm42a	20-150 (1x)	Custom:90-255	37.4	98
Bizovac	thiosufate	48	Gamm42a	20-150 (1x)	Custom:5-255	61	71.5
Bizovac	HPG + Light	24	Gamm42a	20-150 (1x)	Custom:5-255	26	38
Bizovac	HPG + Light	48	Gamm42a	20-150 (1x)	Isodata	7.1	74
Bizovac	HPG+Dark	24	Gamm42a	20-150 (2x)	Custom:5-255	24.2	88
Bizovac	HPG+Dark	48	Gamm42a	30-150 (1x)	Custom:20-150 (1x)	24.9	48
Tuhelj	acetate	24	CFX1223	50-200 (1x)	Custom:5-255	10.8	50
Tuhelj	acetate	48	CFX1223	30-150 (1x)	Custom:60-255	9	57
Tuhelj	glucose	24	CFX1223	5-20 (1x)	Custom:5-255	24	88
Tuhelj	glucose	48	CFX1223	70-255 (1x)	Custom:90-255	47.1	46
Tuhelj	pyruvate	24	CFX1223	60-200 (1x)	Isodata	19.4	55
Tuhelj	pyruvate	48	CFX1223	60-200 (1x)	Custom:5-255	25.5	41
Tuhelj	thiosufate	24	CFX1223	50-200 (1x)	Custom:90-255	23.7	28
Tuhelj	thiosufate	48	CFX1223	30-150 (1x)	Custom:5-255	37.6	29
Tuhelj	HPG + Light	24	CFX1223	60-200 (1x)	Custom:30-255	14.2	26
Tuhelj	HPG + Light	48	CFX1223	50-200 (1x)	Custom:5-255	18.2	52

Tuhelj	HPG+Dark	24	CFX1223	50-200 (1x)	Custom:30-255	19.3	32
Tuhelj	HPG+Dark	48	CFX1223	0-10 (1x)	Custom:30-255	15.1	84
Bizovac	acetate	24	CFX1223	20-150 (1x)	Isodataa	15.1	52
Bizovac	acetate	48	CFX1223	20-150 (1x)	Isodata	20.7	96
Bizovac	glucose	24	CFX1223	0-40 (1x)	Custom:5-255	7.9	89
Bizovac	glucose	48	CFX1223	1-150 (1x)	Isodata	29.9	95
Bizovac	pyruvate	24	CFX1223	20-150 (1x)	Isodata	11.1	71
Bizovac	pyruvate	48	CFX1223	20-150 (1x)	Custom:5-255	20.1	44
Bizovac	thiosufate	24	CFX1223	100-255 (1x)	Custom:30-255	6.4	35
Bizovac	thiosufate	48	CFX1223	20-150 (1x)	Custom:5-255	28.9	40
Bizovac	HPG + Light	24	CFX1223	20-150 (1x)	Custom:20-150 (1x)	7.7	47
Bizovac	HPG + Light	48	CFX1223	20-150 (1x)	Custom:5-255	9.5	28
Bizovac	HPG+Dark	24	CFX1223	20-255 (1x)	Isodata	1.8	73
Bizovac	HPG+Dark	48	CFX1223	20-150 (2x)	Custom:5-255	8.9	11
Tuhelj	acetate	24	EUBI-III	70-200 (1x)	Custom:5-255	25.2	48
Tuhelj	acetate	48	EUBI-III	70-200 (1x)	Custom:5-255	40.1	33
Tuhelj	glucose	24	EUBI-III	20-150	Isodata	22.4	95
Tuhelj	glucose	48	EUBI-III	20-150	Isodata	46	95
Tuhelj	pyruvate	24	EUBI-III	30-150	Custom:5-255	34.3	25
Tuhelj	pyruvate	48	EUBI-III	30-200	Custom:5-255	48.3	29
Tuhelj	thiosufate	24	EUBI-III	50-200 (1x)	Custom:5-255	53.8	36
Tuhelj	thiosufate	48	EUBI-III	40-200 (1x)	Custom:5-255	62.5	43
Tuhelj	HPG + Light	24	EUBI-III	40-150 (1x)	Custom:5-255	36.5	27
Tuhelj	HPG + Light	48	EUBI-III	100-200 (1x)	Custom:5-255	42	19
Tuhelj	HPG+Dark	24	EUBI-III	30-200 (1x)	Custom:5-255	34.9	48
Tuhelj	HPG+Dark	48	EUBI-III	20-150 (1x)	Custom:30-255	36.7	23
Bizovac	acetate	24	EUBI-III	20-150 (1x)	Isodata	34.9	79
Bizovac	acetate	48	EUBI-III	20-150 (2x)	Isodata	48.8	60
Bizovac	glucose	24	EUBI-III	0-150	Custom:5-255	33.7	59
Bizovac	glucose	48	EUBI-III	50-200	Isodata	58.1	53
Bizovac	pyruvate	24	EUBI-III	20-150 (1x)	Custom:90-255	46.3	78
Bizovac	pyruvate	48	EUBI-III	20-150 (1x)	Isodata	40.5	80
Bizovac	thiosufate	24	EUBI-III	125-255 (1x)	Isodata	37.4	98
Bizovac	thiosufate	48	EUBI-III	20-190 (1x)	Isodata	52	99
Bizovac	HPG + Light	24	EUBI-III	20-150 (1x)	Isodata	32.2	96
Bizovac	HPG + Light	48	EUBI-III	20-190 (1x)	Isodata	34.8	97
Bizovac	HPG+Dark	24	EUBI-III	30-150 (1x)	Custom:30-255	33.2	40
Bizovac	HPG+Dark	48	EUBI-III	20-150 (1x)	Isodata	35.3	94

9. BIOGRAPHY

Ema Kostešić was born on December 24, 1993 in Pula. She graduated Chemical Technology at the Faculty of Chemistry and Technology at the University of Split in 2019 with a thesis entitled "Heterogeneous catalytic transesterification of waste vegetable oil using modified natural zeolite". In the same year, she enrolled in the post-graduate university (doctoral) study of Biotechnology and Bioprocess Engineering, Food Technology and Nutrition at the Faculty of Food and Biotechnology at the University of Zagreb. Since 2019, she has been employed as an assistant on the project "Multiphase approach for deciphering microbial ecology and biotechnological potential of geothermal sources in Croatia" at the Ruđer Bošković Institute in Zagreb. She spent 7 months at the Center for Microbial Ecology and Environmental System Sciences at the University of Vienna. She is a member of the Croatian Microbiological Society. She is the co-author of two scientific articles cited by Web of Science and nine abstracts in conference proceedings. Her main area of interest is the ecology of thermophiles and the methodology of working with biofilms.

Publications:

Kostešić, E., Mitrović, M., Kajan, K., Marković, T., Hausmann, B., Orlić, S., Pjevac, P. (2023) Microbial Diversity and Activity of Biofilms from Geothermal Springs in Croatia. *Microb. Ecol.* 10.1007/s00248-023-02239-1. **O**nline publication <https://doi.org/10.1007/s00248-023-02239-1>**.** Accessed October 02, 2023.

Mitrović, M., Kostešić, E., Marković, T., Selak, L., Hausmann, B., Pjevac, P., Orlić, S. (2022) Microbial community composition and hydrochemistry of underexplored geothermal waters in Croatia. *Syst. Appl. Microbiol.* **45** (6), 126359.